Cdx2 is essential for embryonic axial growth and identity of the adult intestinal stem cells

Salvatore Simmini

Utrecht 2015

Cdx2 is essential for embryonic axial growth and identity of the adult intestinal stem cells

Cdx2 is onmisbaar voor embryonale axiale groei en
identiteit van de volwassen intestinale stamcellen
(met een samenvatting in het Nederlands)

Proefschrift

ter verkrijging van de graad van doctor aan de Universiteit Utrecht op gezag
van derectormagnificus, prof.dr. G.J. van der Zwaan, ingevolge het besluit
van hetcollege voor promotiesin het openbaar te verdedigen op
dinsdag 20 januari 2015 des ochtends te 10.30 uur

door
Salvatore Simmini

geboren op 2 februari 1985
te Copertino (Lecce), Italië

Index

Summary

During mouse development, progenitor cells, located along the primitive streak and in the tailbud, lay down descendants that generate all primordia of the trunk and tail tissues of the embryo. A pool of these progenitor cells, with stem cell-like properties, contributes to the neuroectoderm and mesoderm during axial elongation of the trunk and tail. These so called, long-term bipotent Neuro-Mesodermal axial progenitors, together with the caudal lateral epiblast flanking the primitive streak, form the embryonic posterior growth zone. This is described in the Introduction (Chapter 1).

The three mouse Cdx genes encode transcription factors involved in elongation and patterning of the embryonic axial structures. They are expressed in the posterior growth zone. In order to reveal the extent of the role played by these genes in the laying down of the embryonic trunk and tail tissues we generated and characterized the triple Cdx^{null} mutant embryos (Chapter 2). These mutants lose activity of their posterior growth zone and fail to generate any axial tissue posterior to occipital primordia. Our data indicate that Cdx genes are crucial for trunk and posterior tissue generation by regulating downstream Fgf and Wnt signaling in the growth zone.

Comparison of Cdx mutant phenotypes made it clear that *Cdx2* is, among the three Cdx genes, the main contributor to the axial elongation. Another transcription factor, *T Brachyury,* is expressed in the growth zone and is crucial for posterior axial extension. Cdx2 and T Brachyury support this process by positively regulating the Fgf and Wnt pathways. However, whether they interact in another way it is still unclear. To better investigate the role played by *Cdx2* and *T Brachyury* during axial elongation we generated $Cdx2^{null}$/*T Brachyury*^{null} mutant embryos (Chapter 3). We show that the simultaneous loss of function of these two genes disrupts axial elongation much more severely than each single mutation. We discuss whether *Cdx2* and *T Brachyury* cooperate in regulating parallel pathways during mouse development and how these pathways would interact during the generation of the trunk and tail.

The epithelia of the gastric pylorus and of the small intestine carry functional units called stomach glands and intestinal crypts/villi, respectively.

They harbor actively cycling Lgr5-expressing stem cells that are responsible for the renewal of both epithelia throughout life. Isolated Lgr5-positive intestinal and stomach stem cells can generate 3D structures *in vitro*, made of epithelium that recapitulates the epithelium of their organ of origin. This is described in the Introduction (Chapter 1). Taking advantage of this organoid culture system, we show that the expression of *Cdx2* is absolutely required for maintaining the identity of the adult intestinal stem cells (Chapter 4). *Cdx2^{null}* intestinal stem cells exhibit a stomach instead of an intestinal gene expression signature and give rise to organoids that resemble stomach organoids and express markers of the gastric pylorus. Our data indicate that *Cdx2* is cell autonomously required in the adult intestinal stem cells to keep them self-renewing and to maintain their intestinal differentiation program. We provide evidence of the plasticity of adult stem cells in which the intestinal commitment can be converted into a gastric one upon inactivation of the single transcription factor Cdx2.

Chapter 5 contains a general discussion of our findings.

Chapter 1
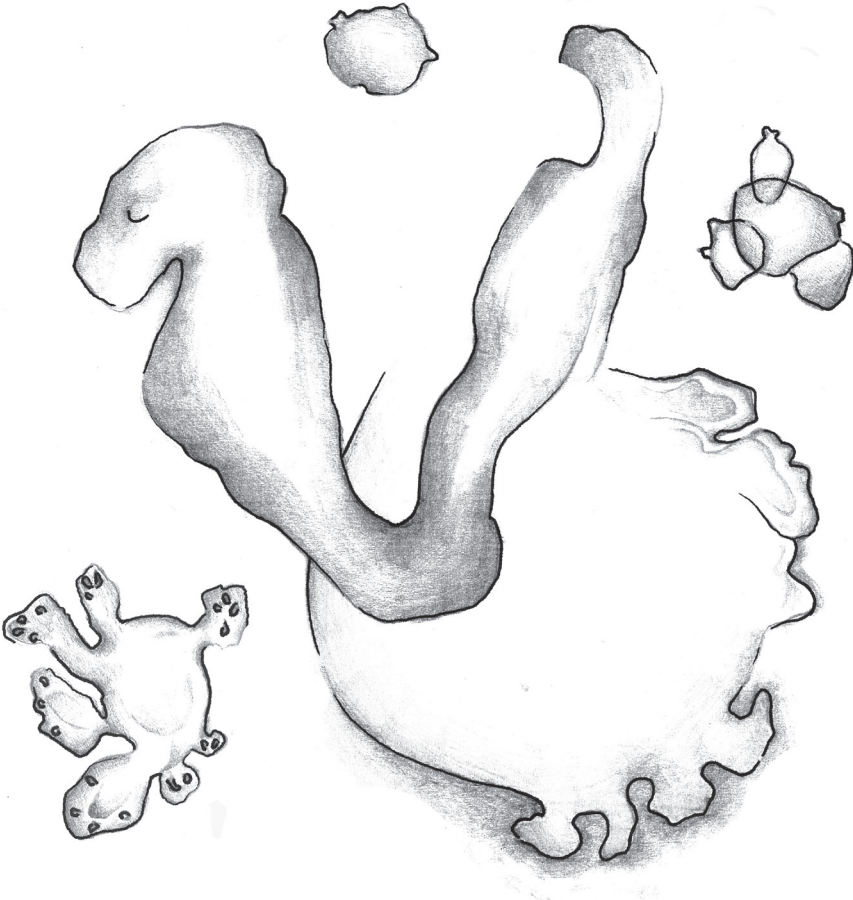
Introduction: stem cell populations in embryos and adult mice

1

1. Mouse embryonic development

1.1. From fertilization to gastrulation

Pre-implantation development of the mouse conceptus culminates with the formation of the blastocyst. It consists of an outer layer of trophectoderm (TE) enclosing a fluid filled space cavity (blastocoele), and the inner cell mass (ICM), a group of cells sequestred at one pole of this cavity [reviewed by (Pfister et al., 2007)]. At embryonic day (E) 4.5 implantation occurs and a group of ICM cells, in contact with the blastocoele, differentiate into the primitive endoderm. Descendants of these cells will differentiate into the Visceral Endoderm (VE) and the Parietal Endoderm. The rest of the ICM cells rapidly grows and expands inside the yolk sac (Snell, 1966; Snow, 1977) forming, at E5.5, a cup-shaped columnar epithelium, called epiblast, that surrounds the pro-amniotic cavity [reviewed by (Rivera-Perez and Hadjantonakis, 2014)]. At this stage the conceptus has a cylindrical shape and is called egg cylinder. It is connected to the uterine tissue by the ectoplacental cone that defines the proximal pole of the transient proximo-distal axis [reviewed by (Pereira et al., 2011)].

1.2. Primitive streak formation and gastrulation

Gastrulation is the fundamental process that leads to the formation of the three germ layers (ectoderm, mesoderm and endoderm) from which all the fetal tissues will develop.

Before the onset of gastrulation, an antero-posterior (AP) polarity is established in the epiblast. It has been shown that the polarity of the pregastrulating embryo results from reciprocal cell-cell interactions between the epiblast and two extra-embryonic tissues: the Extraembryonic Ectoderm (ExE) and the VE (Brennan et al., 2001). The TGFβ family member, Nodal, plays an initial role in polarization of the epiblast. At E5.5, uncleaved Nodal precursor, uniformly expressed in the epiblast, activates the transcription in the ExE of *Furin* and *Pcsk6*, which encode convertase enzymes. These convertases, secreted by the ExE, produce the active form of Nodal. This generates a proximo-distal gradient of signaling activity into the epiblast that, together with Gdf3 and Cripto, induces the patterning of the overlying VE

1

(Tam and Loebel, 2007). Patterning of the VE leads to the definition of the Distal Visceral Endoderm (DVE), a subpopulation of VE cells located at the distal tip of the egg cylinder (Tam and Loebel, 2007). At the same time, at the border between the ExE and the epiblast, Nodal induces the expression of *Bmp4* that directly activates *Wnt3* in the posterior epiblast (Rivera-Perez and Magnuson, 2005). At E5.75, the resulting unbalanced gene expression induces the migration of the DVE proximally to become Anterior Visceral Endoderm (AVE). By continuously expressing antagonists of both Wnt and Nodal, the AVE restricts the activity of these two signaling molecules to the posterior part of the epiblast (Kimura et al., 2000). This event finally specifies the posterior side of the embryo, preceeding primitive streak appearance and the beginning of gastrulation (Mesnard et al., 2004; Perea-Gomez et al., 2004).

Genetic studies demonstrated that Wnt3 (Barrow et al., 2007; Liu et al., 1999) and Nodal (Arnold and Robertson, 2009; Lowe et al., 2001) are essential signaling molecules for the initiation of the AP axis and for the induction of the primitive streak. At E6.0 *T Brachyury* expression is induced by Wnt3 in the posterior region of the epiblast where gastrulation and mesoderm formation take place. From E6.2 onwards, epiblast cells ingress through the primitive streak forming a layer of mesoderm, and generating definitive endoderm that will intercalate into the primitive endoderm (Kwon et al., 2008). The ectoderm, the germ layer that gives rise to the nervous system and epidermis, is contributed to by epiblast cells that do not ingress through the streak. By E7.5, the primordia of head and anterior tissues have been formed in the mouse embryo. From this moment on, the primitive streak area and its continuation in the posterior part of the embryo will progressively generate the nascent trunk and tail tissues.

1

2. Axial elongation

2.1. Axial progenitor cells

During gastrulation, progenitor cells, allocated along the primitive streak, lay down descendants that contribute to the generation of all primordia of the trunk and tail tissues of the embryo.

After E6.2 the primitive streak elongates toward the distal part of the embryo. During this process distinct populations of mesodermal progenitors are ingressing through the streak according to their position along the streak (Lawson, 1999). Fate mapping studies have attempted to understand how the mesodermal progenitors are regionalized along the primitive streak (Kinder et al., 1999; Tam and Beddington, 1992). These studies made clear that axial mesoderm (notochord) is generated from the anterior-most part of the primitive streak. From the next more anterior region of the primitive streak the paraxial mesoderm is generated, giving rise to the somites and therefrom the vertebral column, skeletal muscles, tendons and dermis. The lateral plate mesoderm is formed from the next more anterior region of the streak and gives rise to the circulatory system, the limb buds, the gut wall and other organs and structures. At the posterior-most part of the streak the extraembryonic mesoderm is formed that generates the allantois, the yolk sac vasculature and the primitive blood (Fig. 1).

Formed mesoderm leaves the primitive streak region immediately after ingression. However, recent experimental evidence has documented the existence of a pool of long term paraxial mesodermal progenitors residing in the anteriormost part of the streak, at the border with the node, during the axial elongation process (Cambray and Wilson, 2002, 2007) (Fig. 1).

The first studies supporting the existence of stem cell progenitors in the node and primitive streak region were performed in chick. Selleck and colleagues, by using a fluorescent dye, labeled single cells in the primitive streak and node, and observed the appearance of less heavily labeled cells more anteriorly located in the notochord while label remained in the node. This suggested the existence of stem cells residing in the node whose daughter cells contribute to the elongation of the notochord (Selleck and Stern, 1991; Stern et al., 1992). Subsequent time-lapse imaging experiments in early somite chick embryos, indicated the presence of a stem cell-like population

1

in the posterior epiblast, contributing descendants to the elongating neural axis (Mathis et al., 2001). Cell lineage analysis upon HRP labeling of single epiblast cells was performed in early mouse embryos subsequently cultured *in vitro*. It allowed the identification of cells in the anterior part of the primitive streak and node, the descendants of which were found at more anterior positions as well as in the node region (Forlani et al., 2003; Lawson et al., 1991). Some of these progenitors, just posterior to the node were found to give descendants in both neurectoderm and mesoderm (Forlani et al., 2003). Subsequent experiments using serial grafting in early somite mouse and chick embryos reinforced the evidence for the existence of potential stem cell-like progenitors residing at the node-streak border (NSB) area, in the anterior part of the streak (and caudo-lateral epiblast, CLE), and in the tailbud (chordo-neural hinge, CNH) at later stages of development (Cambray and Wilson, 2002, 2007; McGrew et al., 2008) (Fig. 2a). Daughter cells produced by these progenitors were found to contribute to neural tube and mesoderm of the elongating trunk. Retrospective clonal studies, performed in mouse embryos, confirmed once more the existence of axial stem cell-like progenitors and inferred some of their properties.

These studies took advantage of a strategy permitting to analyze the descendants of single cell events after long periods of time. For this purpose the *LacZ* reporter gene was modified (termed *LaacZ*) with a duplication in the coding region that resulted in a truncated and inactive form of β-Galactosidase. Rare reversion events, that led to produce a functional *LacZ* form, could randomly occur and X-gal staining could label the single revertant cells and their descendants allowing retrospective clonal analysis. The use of this reporter system under control of the *Rosa26* ubiquitous promoter confirmed the existence of stem cell progenitors that could contribute both to neuroectoderm and mesoderm during the whole axial elongation. For this reason this population has been defined as "long term bipotent Neuro-Mesodermal (NM) axial progenitors" (Tzouanacou et al., 2009). According to the evidence provided by Cambray and colleagues, this cell population is most probably located at the NSB at E8.5 (Fig. 1 and Fig. 2a) and then in the CNH in the tail bud at E10.5 (Cambray and Wilson, 2002, 2007) (Fig. 1 and Fig. 2a).
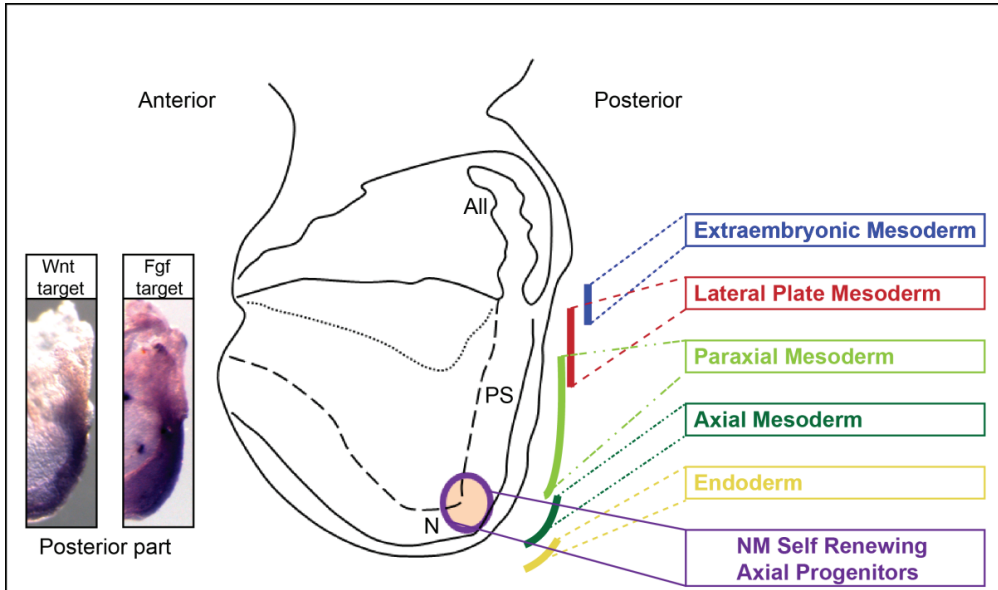
1

Figure 1. Tissue progenitors along the primitive streak of the mouse embryo. Schematic representation of a mouse embryo at E8.0 (side view, anterior is on the left). On the right, regionalized location of tissue progenitors in the primitive streak at this stage of axial elongation. At the posterior-most level of the streak the extraembryonic mesoderm is formed and generates the allantois, the yolk sac vasculature and the primitive blood; the lateral plate mesoderm is formed from the next more anterior region of the streak and gives rise to the circulatory system, the limb buds, the gut wall and other organs and structures; from the next more anterior region of the primitive streak the paraxial mesoderm is generated, giving rise to the somites and therefrom the vertebral column, skeletal muscles, tendons and dermis; the axial mesoderm (notochord) and the endoderm are generated from the anterior-most part of the primitive streak. Neuroectoderm is generated from the non-ingressing epiblast flanking the node anteriorly. Neuromesodermal (NM) self-renewing axial progenitors localize at the anterior part of the primitive streak. On the left side of the scheme expression of Wnt and Fgf target genes, *Axin2* and *Spry4* respectively, along the primitive streak visualized by in situ hybridization on E8.0 mouse embryos. All, Allantois; PS, Primitive Streak; N, Node. References in the text.

In addition, data from Tzouanacou and colleagues suggested the presence of distinct classes of clones descending from NM progenitors indicating a possible change in the composition of the axial stem cell progenitors with time and axial position during trunk and tail formation (Tzouanacou et al., 2009). This observation, together with the hypothesis that the properties of this stem cell population were conferred by a specific embryonic environment rather than being inherent to the cells (Cambray and Wilson, 2002, 2007; McGrew et al., 2008), suggested that the potential of the axial stem cells could be modulated by genes regionally active during trunk and tail formation.

The residence area of the long term NM progenitors, NSB and CNH, together with the caudal lateral epiblast (CLE) flanking the anterior primitive streak constitutes the posterior zone from which tissues are generated to

construct the trunk and tail, and are referred to hereafter as the embryonic posterior growth zone.

2.2. Regulation of axial elongation:

Signaling pathways and transcription factors

Several signaling pathways and transcription factors control specification and patterning of the emerging tissues during development. Among these, the Wnt and Fgf pathways play an important role in regulating genes involved in appropriate AP axial elongation of the trunk, such as Cdx and *T Brachyury*.

2.2.1. Wnt signaling

Wingless-Type (Wnt) genes encode secreted signaling glycoproteins, many of which are expressed since early stages of development (Fig. 2a). The first *Wnt -Wnt3-* expression can be detected in the posterior VE of the egg-cylinder, earlier than gastrulation onset at E5.5; some hours later, at about E5.75, *Wnt3* expression is also present in the posterior epiblast (Rivera-Perez and Magnuson, 2005). Generation of knock out mutants indicated that *Wnt3* is essential for primitive streak induction, node definition and mesoderm formation (Barrow et al., 2007; Liu et al., 1999). Although *Wnt3* mutant embryos did undergo AP polarization, they did not elongate, mainly because initiation of the mesoderm was impaired (no induction of *T Brachyury* expression) (Rivera-Perez and Magnuson, 2005). Because of Wnt3 dual expression in the posterior VE and in the epiblast, the critical role of this gene during AP axis formation could not be assigned to either tissue in standard knock out experiments. Moreover, the fact that development of the mutant embryos does not proceed through gastrulation did not give the possibility to study the molecular events downstream of *Wnt3* at later stages (Tortelote et al., 2013). For these reasons, studies using a tissue specific conditional *Wnt3* allele have been conducted. Embryos lacking *Wnt3* expression exclusively in the epiblast, obtained by crossing *Wnt3⁻ᐟᶠˡ* mice with Sox2Cre recombinase-positive mice, showed primitive streak appearance and gastrulation initiation. However they were delayed in development and died in utero at E9.5. These results indicated that *Wnt3* is necessary for

1

maintenance but not for initiation of gastrulation (Tortelote et al., 2013). Unlike previous studies in which standard *Wnt3* knock out embryos were analyzed (Barrow et al., 2007; Liu et al., 1999), Tortelote and colleagues detected expression of the primitive streak marker *T Brachyury* and *Wnt3* itself in their *Wnt3* conditional epiblast mutants. This indicated that Wnt3 signaling provided by the posterior VE, in contact with the epiblast, is sufficient to initiate gastrulation. It controls the expression of primitive streak specific markers and it is required for its own induction in the epiblast. Establishment of a Wnt3 positive feedback loop between the epiblast and the posterior VE is then essential for its expression throughout gastrulation (Tortelote et al., 2013).

Soon after mesoderm initiation by induction of *T Brachyury* expression in the primitive streak, *Wnt3a* takes over the function of *Wnt3* in stimulating the embryonic growth from the caudal region (Fig. 2a). *Wnt3a^{null}* embryos show a severe truncation of the axis. The embryos do not present defects in allantois development and can develop to term (Takada et al., 1994). In *Wnt3a^{null}* mutants ectopic neural tissues appear at posterior axial levels as a consequence of the impairment of paraxial mesoderm differentiation. In absence of Wnt3a signaling, essential for maintaining *T Brachyury* expression in the primitive streak (Yamaguchi et al., 1999), paraxial mesodermal specification is impaired favoring neural fate choice (Yoshikawa et al., 1997) (Fig. 2b).

Other mutations affecting effectors of the Wnt pathway also cause axial elongation deficiencies. *Lef1^{null}/Tcf1^{null}* compound mutants show a very comparable phenotype with that of *Wnt3a^{null}* mutants but, additionally, have defects in placental formation due to impaired allantoic growth (Galceran et al., 1999). β-catenin^{null} mutants die before gastrulation (Haegel et al., 1995), but conditional deletion of β-catenin, using a TCre recombinase, results in loss of primitive streak and posterior mesoderm at E8.5. The embryos show severe axial truncation with almost no expression of *Fgf8* (Dunty et al., 2008). The expression of *Fgf8* was also found to be affected in the epiblast specific *Wnt3* conditional knock out embryos (Tortelote et al., 2013).
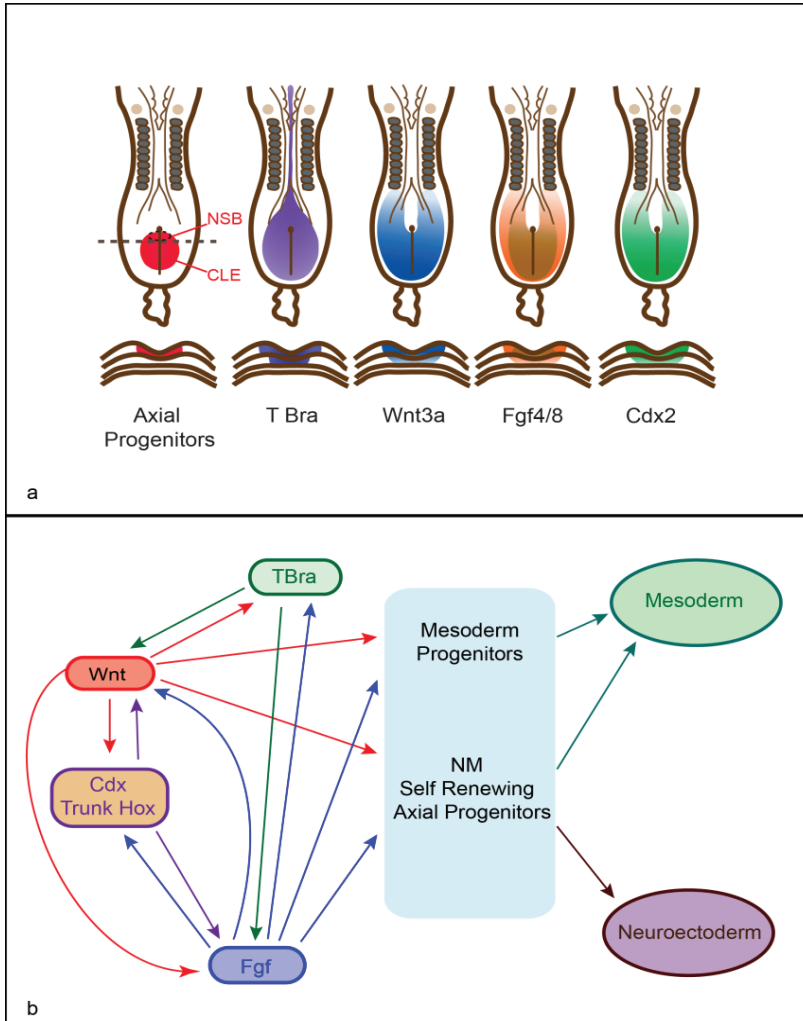
Figure 2. Localization of axial progenitors, and expression and interaction of molecular players in posterior growth during elongation of the embryonic trunk. a. Schematic representation of the posterior region of mouse embryo at E8.5 (10-somites) (dorsal view, anterior is up). The primitive streak is represented by a vertical black line, with a black dot at its anterior end, representing the node. From left to right: the red colored area specifies the epiblast cells contributing to the stem cell-like population eventually releasing descendants in mesoderm and neurectoderm of the growing axis (NM axial progenitors); the anterior-most part of the domain corresponds to the "node-streak border" (NSB), and the rest to the caudolateral epiblast (CLE) (Cambray and Wilson, 2007; Wilson et al., 2009); purple indicates transcription of *T Bra* (Kispert and Herrmann, 1994) and dark blue to the expression of *Wnt3a* (Nowotschin et al., 2012; Yoshikawa et al., 1997); orange with brown sub-domain stands for expression of *Fgf8* (orange) and *Fgf4* (brown) (Molotkova et al., 2005; Naiche et al., 2011); *Cdx2* expression is shown in green (Young et al., 2009). The lower set of schemes shows the localization of progenitors, gene expression and signals in cross sections of the embryos shown above at the level of the anterior primitive streak (dashed line). The three germ layers are shown, of which the upper layer is epiblast, and the middle layer mesoderm. Below is the primitive endoderm. Adapted from Neijts R. et al, 2014 (Neijts et al., 2014). **b.** Representation of interactions between Wnt and Fgf signaling and the genes encoding T Brachyury (TBra) and Cdx/Trunk Hox transcription factors in the primitive streak. This interaction leads to maintenance of the mesoderm and NM self-renewing axial progenitors. On the right, the production of mesoderm and neuroectoderm.

1

2.2.2. Fgf signaling

Fibroblast growth factors (Fgfs) are secreted polypeptides with a key role in many morphogenetic processes including posterior body formation (Fig. 2). *Fgf4* and *Fgf8* play key roles at different stages of development. *Fgf4null* mutant embryos die after implantation due to impaired proliferation of the ICM (Feldman et al., 1995). *Fgf8null* mutant embryos show defects in mesoderm formation: epiblast cells ingress through the primitive streak, undergo epithelial-mesenchymal transition (EMT), but fail to move away from the streak (Sun et al., 1999). These cells accumulate in the streak region because they are not able to down regulate E-cadherin, a prerequisite for cell migration. Loss of Fgfr1, the main receptor for Fgf8 expressed throughout the epiblast, causes death of the embryo during gastrulation. Also in *Fgfr1null* mutants, accumulation of ingressed cells beneath the streak is observed with a resulting severe impairment of the paraxial mesoderm (Deng et al., 1994; Yamaguchi et al., 1994).

Generation of conditional alleles for components of the Fgf pathway allowed further studies of their function at later stages during embryonic trunk and tail formation. *Fgf4/Fgf8* conditional double knock out mutant embryos, induced by a TCre recombinase, are truncated at the level of the forelimb buds. In addition, they show severe problems in somite formation and patterning (Naiche et al., 2011). The conditional loss of *Fgfr1* induced by the same TCre has also been described and shown to lead to a similar but milder phenotype (Wahl et al., 2007).

Similarly to what has been described in the *Wnt3anull* mutants, both the *Fgf4/Fgf8* conditional double knock out mutant embryos and the *Fgfr1null* mutants show a severe loss of *T Brachyury* expression (Ciruna and Rossant, 2001; Yamaguchi et al., 1999).

Fgf signaling, via *Fgf4* and *Fgf8*, as well as Wnt signaling are required for generating *T Brachyury*-expressing mesodermal cells at the primitive streak (Fig. 2b). Overall, the phenotypic similarities of mutants in the Fgf and Wnt pathways and their complex regulatory relationship suggest that these two pathways act together, in promoting elongation of the body axis while maintaining active stem cells in the posterior epiblast (Boulet and Capecchi, 2012).

2.2.3. *T Brachyury*

T Brachyury (*T Bra*) deficient mice were the very first genetic mutant mouse model generated by mutagenesis in the early 1900s (Dobrovolskaia-Zavadskaia, 1927). Null mutation in the *T Brachyury* locus is semi-dominant: heterozygous mice exhibit a shorter tail or sometimes no tail at all. The tail phenotype manifested in the *T Brachyury*[het] mutant mice indicates defects in developing a correct number of vertebral elements. Homozygous mutant embryos cannot survive longer than E10.5: they fail to grow an allantois and, consequently, to generate the chorio-allantoic placenta. Already before this embryonic stage, mutants embryos show severe problems: a maximum of 7 somites are formed (Dobrovolskaia-Zavadskaia, 1927; Naiche et al., 2005), the neural tube is severely kinked (H., 1958; P., 1935), there are defects in left-right patterning (Yanagisawa et al., 1981) and morphological abnormalities in heart development (Herrmann and Kispert, 1994; King et al., 1998). Cloning of the *T Brachyury* gene allowed to investigate its key role during embryo development (Herrmann et al., 1990). Its first expression occurs in the posterior region of the egg-cylinder, just before gastrulation onset (E6.0). During gastrulation, it marks the primitive streak region. Later in development, *T Brachyury* is expressed in the node and the notochord and remains expressed in the remnants of the primitive streak in the tail bud throughout the whole body axis extension process (Satoh and Jeffery, 1995) (Fig. 2a).

Studies at the cellular level revealed that *T Brachyury*[null] epiblast cells accumulate in the primitive streak region because they are incapable of migrating rostrally (Wilson et al., 1995). This causes a severe impairment of paraxial mesoderm formation and the appearance of an enlarged posterior growth region similar to the one observed in *Fgfr1*[null] mutants (Deng et al., 1994; Yamaguchi et al., 1994). In addition, it has been shown that *T Brachyury* has an important function in modulating fate decision of the NM axial progenitors at the NSB and later at the CNH (Gentsch et al., 2013) (Fig. 2a).

The essential function of *T Brachyury*, a T-box protein encoding gene, for embryonic development is in agreement with his evolutionary conservation. Recent studies have showed that the T-box transcription factors have a long pre-metazoan evolutionary history, being present in several non-metazoan

1

unicellular taxa. Specifically a gene homolog of *T Brachyury* has been found in the ameba *Capsaspora owczarzaki*, identifying *T* as the founder of the T-box transcription factors family (Papaioannou, 2014; Sebe-Pedros et al., 2013).

Recent ChIP-Sequencing (ChIP-Seq) experiments applied on mouse embryonic stem (ES) cells forced to differentiate into "primitive streak" *in vitro* revealed that at the molecular level *T Brachyury* controls many genes involved in mesoderm formation and migration, and endoderm development (Lolas et al., 2014). Expression studies confirmed that T Brachyury directly interacts with the Wnt and Fgf pathways: it binds the proximal promoter of *Wnt3a* and *Fgf8* that were found downregulated in *T Brachyury* mutant embryos (Evans et al., 2012) (Fig. 2b). These data reinforced even more what the past genetic analyses have already suggested. *T Brachyury* establishes positive feedback loops with Wnt and Fgf for maintaining the posterior mesodermal progenitors active during axial elongation (Ciruna and Rossant, 2001; Dunty et al., 2008; Martin and Kimelman, 2010; Yamaguchi et al., 1999) (Fig. 2b). They also support the T-mediated expression of *Cyp26a1* gene throughout the axial extension period in order to clear the stem cells area from retinoic acid (RA), a differentiation signal present more anteriorly in the somite region (Martin and Kimelman, 2010).

T Brachyury, and the Fgf and Wnt pathways cooperate to ensure correct signaling in the posterior growth zone, thereby creating a suitable microenvironment for the axial progenitors (Fig. 2). Besides T Brachyury and its downstream signaling, the genes encoding Cdx transcription factors belonging to the para-Hox family are required for posterior development of the mouse embryo and for its AP patterning, in a way resembling T Brachyury requirement (Fig. 2).

2.2.4. Cdx

The Cdx genes encode transcription factors, orthologs of *Drosphila* Caudal. In vertebrates, they play an important role in generating and patterning the trunk and tail tissues. The mouse genome expresses three *Caudal*-related homeobox genes which are: *Cdx1*, *Cdx2* and, the X-linked, *Cdx4*.

1

The earliest Cdx gene expressed is *Cdx2* in the trophectoderm of the blastocyst (Beck et al., 1995; Rayon et al., 2014). At this developmental stage *Cdx2* is essential for the implantation of the embryo: *Cdx2^null* mutants do not implant (Chawengsaksophak et al., 1997).

Cdx2 is also expressed in the embryo (Fig. 2a), together with *Cdx1* and *Cdx4*, during the elongation of the axis. The three genes, are expressed during gastrulation in the ectoderm and mesoderm of the primitive streak and at the base of the allantois. They remain expressed in the tailbud until the end of the axial elongation process (E12.5). Although the three Cdx genes are expressed in the posterior region of the embryo, they have different anterior expression boundaries: *Cdx1* is the most anteriorly expressed, whereas *Cdx4* is the less rostrally. Expression of these genes also varies in time: *Cdx4* is down regulated around E10, whereas the decrease in expression of *Cdx1* and *Cdx2* begins at the trunk/tail transition (E10.5) to reach complete downregulation in the mesoderm and neurectoderm around E12.5. After that stage *Cdx1* and *Cdx2* transcripts remain present in the tailbud and in the endoderm where they play an essential role in patterning this germ layer (Guo et al., 2004; Sherwood et al., 2009) (see below).

In order to study the function of *Cdx2* in the embryo proper, initially, aggregation of tetraploid wild-type morulas with *Cdx2^null* ES cells has been performed (Chawengsaksophak et al., 2004). Later on, the generation of a *Cdx2* conditional allele (Savory et al., 2009; Young et al., 2009), together with the use of Sox2Cre recombinase (Hayashi et al., 2002), allowed the ablation of this transcription factor in the early epiblast, after the implantation stages. *Cdx2^null* mutant embryos show a severe axial truncation phenotype. They form at the maximum 17 pairs of somites the last of which lies close to the posterior tip of the embryo. No unsegmented paraxial mesoderm remains caudally to the last somite and allantois development is severely compromised (Chawengsaksophak et al., 2004). Consequently, the embryos die in utero around E10.5 due to the lack of a placental labyrinth, the most crucial functional component of the placenta.

Cdx genes belong to the para-Hox gene family and, when mutated, can cause vertebral homeotic transformations similarly to the Hox genes. *Cdx1^null* and *Cdx4^null* single or double mutant mice are viable and fertile but they exhibit homeotic transformations that involve vertebral elements at

1

different levels of the AP axis (Subramanian et al., 1995; van den Akker et al., 2002; van Nes et al., 2006). *Cdx2het* mice show anterior transformation of vertebrae and a very mild axial truncation with occasionally a shorter and kinky tail (Chawengsaksophak et al., 1997; van den Akker et al., 2002). This posterior truncation phenotype of the tail is more severe in compound mutants that constitute an allelic series of increasingly severe phenotype: *Cdx2het* (Chawengsaksophak et al., 1997), *Cdx1het/Cdx2het* (van den Akker et al., 2002), *Cdx1null/Cdx2het* (van den Akker et al., 2002), *Cdx2het/Cdx4null* (van de Ven et al., 2011; van Nes et al., 2006; Young et al., 2009), *Cdx2null* (Chawengsaksophak et al., 2004; Savory et al., 2009), *Cdx2null/Cdx4null* and *Cdx1null/Cdx2null* (Savory et al., 2011). These results indicate that all three Cdx genes participate in controlling axial elongation, and that they do so in a dosage dependent manner. Comparison between phenotypes of all Cdx compound mutants made it clear that *Cdx2* is, among the three Cdx genes, the main contributor to the axial extension. In Chapter 2 we further investigate how the complete loss of Cdx function affects the mouse embryonic trunk and tail formation.

Similarly to *T Brachyury*, Cdx genes are dependent on Wnt (Gaunt et al., 2003; Ikeya and Takada, 2001; Pilon et al., 2006; Shimizu et al., 2005) and Fgf (Bel-Vialar et al., 2002; Pownall et al., 1998) for their expression (Fig. 2b). In addition, a *Lef1* gain of function can rescue the Cdx truncation defects suggesting that Cdx establishes a positive feedback loop on the Wnt pathway during axial elongation. This role exerted by Cdx on Wnt is reminiscent of the relationship between *T Brachyury* and *Wnt3a* (Martin and Kimelman, 2010; Yamaguchi et al., 1999) (Fig. 2b). Given all the similarities between the involvement of *Cdx* and *T Brachyury* in embryogenesis, we investigate, in Chapter 3**,** the relationship between their mode of action.

3. Endoderm and gastrointestinal tract development

The gastrointestinal (GI) tract is the primary site for digestion of food, absorption of nutrients, and excretion of solid waste. It extends from the mouth to the anus and includes the tubular gut (i.e., esophagus, stomach, small intestine, and colon) and the accessory digestive organs (i.e., pancreas and liver) (Fig. 3c). The tubular gut is composed by two tissue layers, the epithelium and the mesenchyme, which are derived from endoderm and mesoderm,

respectively. The epithelium surrounds the lumen of the gut tube and it is the tissue where all the digestive functions take place. The mesenchyme covers the epithelium, to which it provides structural and vascular support, in addition to delivering signals. Gut motility, essential for the flux of nutrients, is partly controlled by innervations within the mesenchyme from the enteric nervous system, which has an ectodermal origin.

In the following section, the signaling pathways and transcription factors driving GI tract development will be described.

3.1. Endoderm development and patterning

3.1.1. From endoderm specification to primitive gut formation

Around E6.2, the mouse embryo undergoes gastrulation and epiblast cells ingressing through the anterior part of the primitive streak generate endoderm descendants. The endodermal cells, the definitive endoderm (DE), migrate on the ventral surface of the embryo and intercalate into the primitive endoderm (Kwon et al., 2008). Subsequently, the endoderm elongates (Fig. 3a) together with the other germ layers and at E9.5, by coordinated morphogenic movements, it folds and closes forming the primitive gut tube surrounded by the closely associated mesoderm.

AP patterning of the gut, is already initiated well before gut tube formation (Sherwood et al., 2009) (Fig. 3b). This process involves precise spatio-temporal control of signaling pathway activity and expression of transcription factors (Fig. 3a, b).

3.2. Signaling pathways

The interaction between several signaling pathways is essential for specification and patterning of the endoderm and for directing organogenesis within the GI tract. An essential pathway for both early endoderm and mesoderm generation is that of Nodal (Brennan et al., 2001; Conlon et al., 1994; Zhou et al., 1993) (Fig. 3a, b). Null mutations in *Nodal* cause arrest of development at the gastrulation stage (Conlon et al., 1994; Iannaccone et al., 1992; Zhou et al., 1993), while hypomorphic mutations, with lower levels

1

of Nodal signaling, result in a loss of endoderm, but not of mesoderm (Lowe et al., 2001; Vincent et al., 2003). Conversely, targeted inactivation of Nodal antagonists, such as *Drap1* or *Lefty2*, results into an expanded primitive streak and defective mesoderm migration with an excess of endoderm formation (Iratni et al., 2002; Meno et al., 1999). *Nodal* gene function, therefore, is required for directing anterior streak epiblast differentiation toward an endodermal rather than a mesodermal fate.

Nodal initiates a cascade of gene expression leading to Wnt and Fgf accumulation in the caudal part of the embryo (Fig. 3a). In the early gut tube, gradients of expression of Wnt and Fgf, as well as retinoic acid (RA), establish the patterning of the endodermal primordia along the AP axis (Zorn and Wells, 2009) (Fig. 3b). Wnt and Fgf pathways induce differentiation of the hindgut, while RA signaling, which restricts the Wnt and Fgf anterior expression domain, directs differentiation of the foregut (Zorn and Wells, 2009) (Fig. 3b).

3.3. Transcription factors

At early stages of development, the transcription factors Gata4 (Jacobsen et al., 2002; Soudais et al., 1995), and Gata6 (Koutsourakis et al., 1999; Morrisey et al., 1998) are essential for VE and DE formation.

Later in development, a number of transcription factors are expressed along the primitive gut endoderm and mesoderm. The interaction between these two germ layers specifies the identity of the different endoderm regions. Hox genes have been found to play a regulatory role in the mesoderm to endoderm signaling (Kondo et al., 1996; Roberts et al., 1998). Hox genes are expressed in specific AP patterns in the mesoderm of the gut tube (Roberts et al., 1995; Yokouchi et al., 1995). Their combinatorial expression, has been proposed to constitute a "Hox code" that delineates gut subregions (i.e., fore-, mid- and hindgut), later organ territories (i.e., stomach, small intestine and colon) and transitions between adjacent organs (Kawazoe et al., 2002; Sekimoto et al., 1998). This organ-specific patterning involves the interaction between Hox and para-Hox factors like Pdx1 and Cdx with signaling molecules such as Fgf, Wnt and RA (Grapin-Botton, 2005; Kawazoe et al., 2002; Shimizu et al., 2006; Zacchetti et al., 2007) (Fig. 3b).
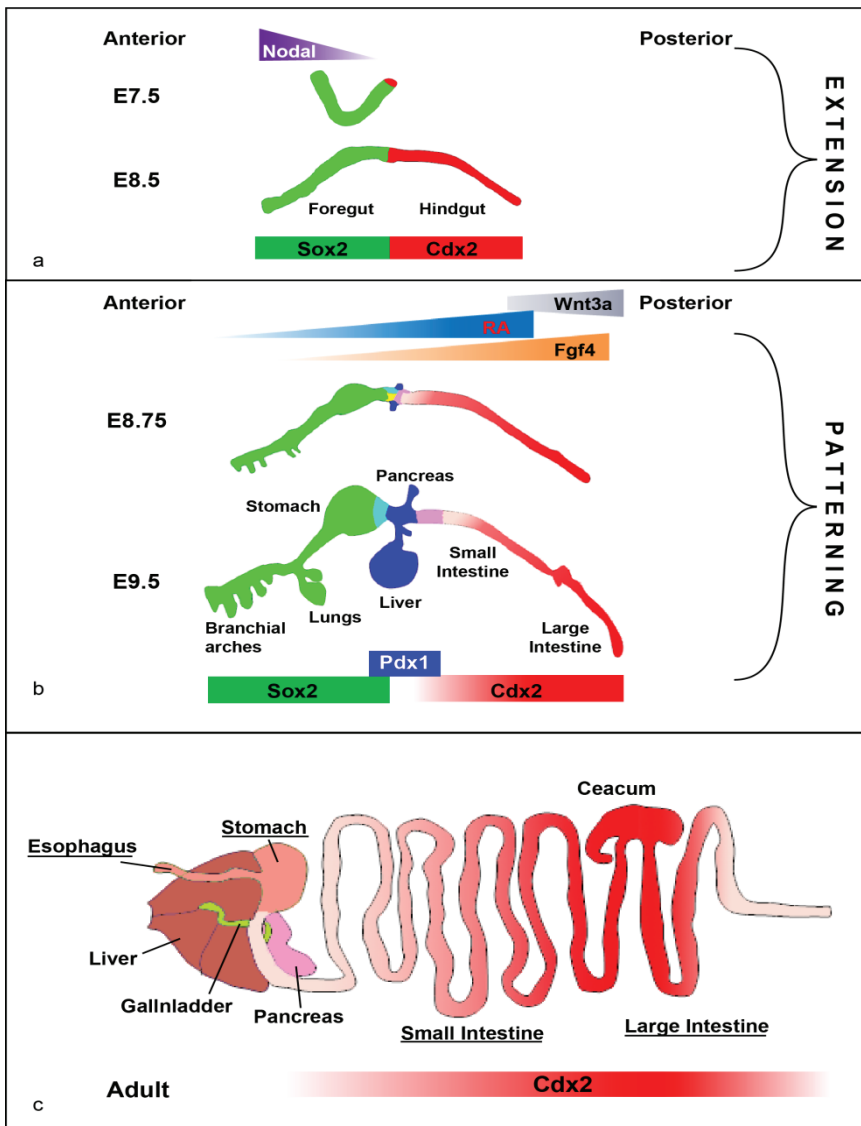
Figure 3. Endoderm development and patterning by the expression of transcription factor Cdx2. a. Schematic representation of the embryonic endoderm in extension at E7.5 and E8.5. Anterior expression of Nodal signaling induces *Sox2* expression in the anterior endoderm-foregut (green domain)- whereas *Cdx2* is expressed in the posterior endoderm–hindgut (red domain). **b.** Schematic representation of mouse embryonic endoderm tissue patterning at E8.75 and E9.5. The *Sox2/Cdx2* boundary is established and *Sox2* is expressed in the foregut (green domain) and *Cdx2* according to a gradient in the hindgut (red domain). At the *Sox2/Cdx2* boundary *Pdx1* starts to be expressed at E8.75 and specifies liver and pancreas development (accessory organs of the GI tract). Posterior to anterior expression gradients of Wnt3a, RA and Fgf4 signaling molecules are essential for endoderm patterning along the AP axis. E9.5 scheme of the endoderm, adapted from Aaron M. Zorn and James M. Wells, 2010 (Zorn and Wells, 2009). Graded expression of signaling pathways, after Grapin-Botton, 2008 (Grapin-Botton, 2008). **c.** Schematic representation of the gastrointestinal tract of the adult mouse where the *Cdx2* domain is shown in red. Maximal expression is at the level of the boundary between the small and the large intestine (cecum).

1

At E7.75 a differential AP pattern of transcription factors along the endoderm is already manifest. *FoxA2* (Ang et al., 1993; Dufort et al., 1998; Lolas et al., 2014; Sasaki and Hogan, 1993; Weinstein et al., 1994) and *Sox2* (Sherwood et al., 2009) are expressed broadly in foregut endoderm, while *Cdx2* (Sherwood et al., 2009) and *Sox17* (Kanai-Azuma et al., 2002) expression marks midgut and hindgut endoderm (Zorn and Wells, 2009), respectively. Between E8.5 and E9.5, *Sox2* and *Cdx2* are expressed on opposite sides of an expression boundary defining the border between the foregut and the mid-hindgut (Sherwood et al., 2009) (Fig. 3a, b). These mutually exclusive expression domains established early in development remain constant thereafter, not only until birth, but also in the adult animal. At the boundary between the Sox2 and Cdx2 domains, the expression of *Pdx1* marks the region that later will give rise to the three accessory digestive organs (liver, gall bladder, and pancreas) (Fig. 3b). The Pdx1-positive area of the tubular gut also gives rise to the pylorus as well as the surrounding distal antrum and proximal duodenum (Grapin-Botton, 2008).

This thesis work focuses on the function of Cdx2 in defining and maintaining the identity of the adult small intestinal stem cells residing in the intestinal crypts (see Chapter 4).

4. Adult GI tract, stem cells and organoids

The adult GI tract is subdivided into several anatomical parts: esophagus, stomach, small intestine and large intestine (Fig. 3c). Digestion of the food mainly takes place in the stomach where nutrients are chemically broken into small parts, releasing molecules that are subsequently absorbed across the epithelium of the small intestine to finally enter the circulation.

4.1. The adult gastrointestinal tract

4.1.1. Stomach

The stomach is a glandular organ that can be anatomically divided into two parts: corpus, which constitutes the main body of the stomach and secretes hydrochloric acid and zymogens responsible for food digestion, and pylorus/antrum, which represents the smaller region located close to the intestine and producing mucous and hormones. The stomach epithelium

carries many tubular-shaped functional units called gastric glands (Fig. 4a).

The structure of the gastric units differs between corpus and pylorus. Corpus glands comprise pit cells, which are mucous releasing cells located on the surface, parietal cells or acid secreting cells, chief cells, which contain zymogen granules and secrete the enzyme pepsinogen, and endocrine cells that secrete hormones such as Somatostatin, Histamine and Leptin (Karam and Leblond, 1993). Pyloric/antral glands, instead, are mainly composed of mucous cells secreting protective gastric mucin (Muc5AC), enteroendocrine cells that secrete Gastrin and Somatostatin, and occasionally parietal cells (Lee and Leblond, 1985) (Fig. 4a).

4.1.2. Intestine

The gut epithelium regulates nutrients absorption and water and ion fluxes, and represents the first defensive barrier against toxins and enteric pathogens (Catalioto et al., 2011).

The gut is anatomically and functionally divided into small intestine, which mainly absorbs nutrients, and large intestine, or colon, which functions more in reabsorbing water.

The small intestine comprises three anatomically distinct parts: duodenum, jejunum, and ileum. Their epithelium is organized into small pits called crypts (Fig. 4a) and finger-like structures called villi that, protruding into the lumen, maximize the exchange surface.

Five differentiated cell types form the crypt/villus functional unit of the small intestine. They are enterocytes, goblet cells, enteroendocrine cells, M-cells and Paneth cells (Fig. 4a). Enterocytes are polarized cells with an apical brush border that is responsible for the absorption and transportation of the nutrients across the epithelium. Goblet cells secrete protective mucins and trefoil proteins that are required for the movement of the gut contents and provide protection against chemical damage. Enteroendocrine cells secrete specific peptide hormones important for modulating and coordinating organ functions and for maintaining homeostasis. M-cells transport antigens, by endocytosis, from the gut lumen to the immune cells, such as intraepithelial macrophages and lymphocytes, thereby stimulating the mucosal immune response. Paneth cells play also a rule of innate immunity. They produce

1

secretory granules containing specific proteins such as lysozymes, antimicrobials and defensins (van der Flier and Clevers, 2009) (Fig. 4a).
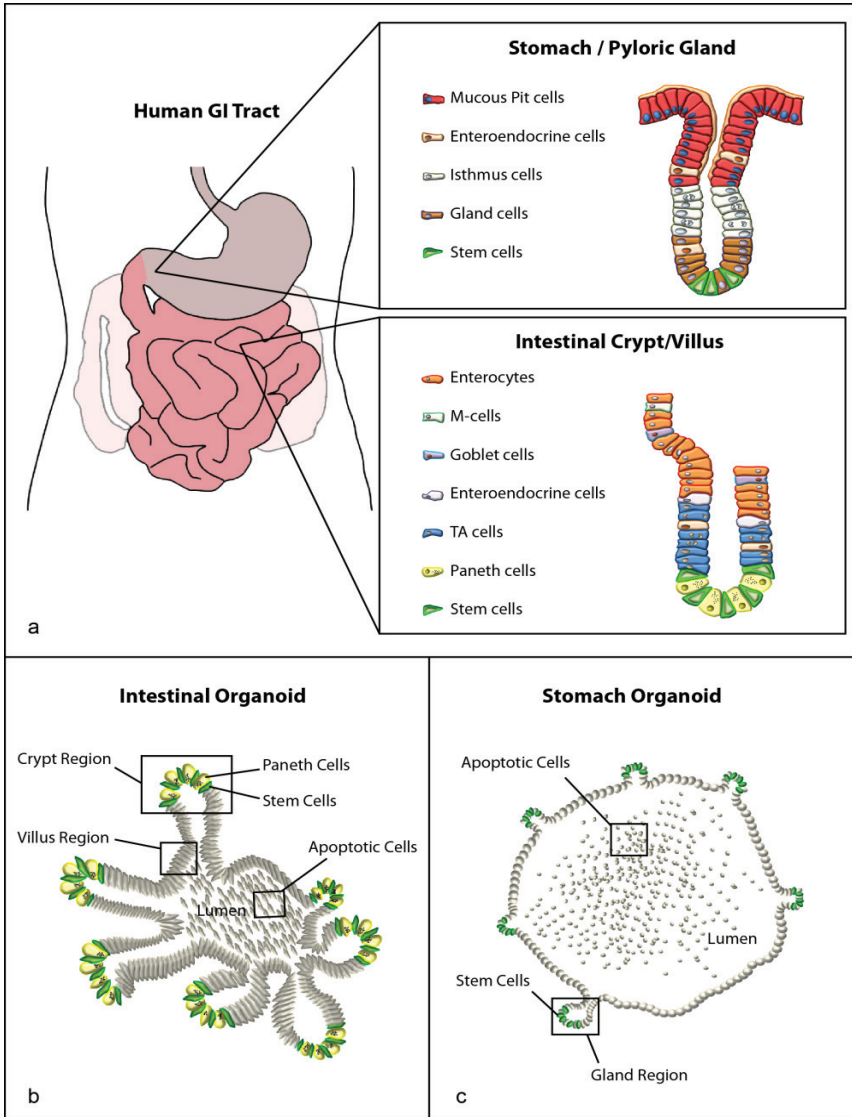

Figure 4. Stomach glands and intestinal crypts harbor stem cells that give rise to organoids *in vitro*. a. Left side, representation of human gastrointestinal (GI) tract (adapted from Ashley Jones, 2009). Right side, schematic representations of functional units: stomach/pyloric gland (top panel), and intestinal crypt/villus (panel down). They both harbor stem cells (green triangular cells) at the bottom. Adapted from Schuijers J. and Clevers H, 2012 (Schuijers and Clevers, 2012). **b.** Schematic representation of an intestinal organoid grown from a single intestinal stem cell. These organoids recapitulate *in vitro* the intestinal epithelium organization, forming crypt regions where stem cells (in green) and paneth cells (in yellow) reside and villus regions that face the lumen where apoptotic cells accumulate. **c.** Schematic representation of a stomach organoid grown from a single stomach stem cell. These organoids recapitulate *in vitro* the stomach epithelium organization, forming gland regions where stem cells (in green) reside and the rest of the epithelium that faces the lumen where apoptotic cells accumulate.

1

The intestinal epithelium is the most rapidly renewing tissue of the body: the whole epithelium is continuously renewed every 5 days (Heath, 1996). Self-renewal is supported by stem cells residing at the bottom of the crypts. They produce proliferative daughter cells, called transient amplifying (TA) cells that rapidly divide while migrating upwards (Fig. 4a). When they reach the villus region, they differentiate into all previously described distinct cell types essential for the intestinal functions. The differentiated cells keep migrating upwards until they undergo apoptosis at the tip of the villus. The Paneth cells are the only ones to escape this upward migration but instead descend to the crypt base where they live for up to 6 weeks in intimate contact with the stem cells (Fig. 4a).

The colon presents the same kind of tissue organization as the small intestine except for the absence of Paneth cells.

4.2. Stem cells and organoids

4.2.1. Small intestinal stem cells and organoids

Already 40 years ago, Cheng and Leblond speculated that all the cell types present in the intestinal epithelium originate from the same precursors, the crypt-base columnar cells (CBC), residing at the bottom of the crypts, interspersed between the Paneth cells (Cheng and Leblond, 1974). Recently, it has been demonstrated by lineage tracing studies that cycling, long lived, multipotent stem cells reside at the bottom of the crypt contributing to the daily maintenance and renewal of the intestinal epithelium (Barker and Clevers, 2007) (Fig. 4a). These studies made use of the expression of an intestinal stem cell-specific marker, Lgr5 (GPR49) (Barker and Clevers, 2007; Barker et al., 2008). Other intestinal stem cell markers have also been characterized (Asai et al., 2005; Holmberg et al., 2006; May et al., 2009; Sangiorgi and Capecchi, 2008; Yuqi et al., 2008), but Lgr5 (*GPR49*) has been the most studied one (Barker and Clevers, 2007; Barker et al., 2008; Haegebarth and Clevers, 2009). *Lgr5* codes for a G-protein coupled receptor, closely related to the thyroid-stimulating hormone receptor, and is regulated by the canonical Wnt pathway (Barker and Clevers, 2007; Barker et al., 2008; Haegebarth and Clevers, 2009; van der Flier and Clevers, 2009). Lgr5^{high} single stem cells, sorted from the intestinal crypts of adult mice, were able to generate 3D intestinal organoids in a matrigel based *in vitro* culture system (Sato et al., 2009) (Fig. 4b). These, so defined "mini-guts" grow in the presence of the

1

Epidermal growth factor (EGF), Noggin, an inhibitor of the Bmp signaling, and Rspondin1, an agonist of the Wnt pathway (ENR culture conditions). Single intestinal stem cells, with a plating efficiency of 1-2% or stem cells-Paneth cells doublets, with a 50% plating efficiency, give rise to spherically shaped organoids with an inner luminal structure, villus domains and outward projecting crypt-like structures containing Lgr5-positive stem cells (Sato et al., 2009) (Fig. 4b). In ENR culture conditions the organoids produces all the differentiated intestinal cell types, such as goblet cells, Paneth cells (in close contact with the stem cells in the crypt-like structures) (Fig. 4b) and enteroendocrine cells. They can be passaged weekly for long periods of time without changes in phenotype or karyotype (Sato and Clevers, 2013; Sato et al., 2009).

4.2.2. Stomach stem cells and organoids

For a long time it has been thought that the stem cell zone of the stomach glands was located into the isthmus area. Self-renewing cells were exclusively identified in this area (Stevens and Leblond, 1953). They produced daughter cells migrating bidirectionally toward the pit and the base regions where they differentiated (Karam and Leblond, 1993; Lee and Leblond, 1985).

Lineage tracing studies have confirmed the presence of two distinct stem cell populations in the gland. A rare population of dormant stem cells was identified below the isthmus region of the pyloric gland, by using VillinCre recombinase (Qiao et al., 2007). Normally in a quiescent state, these cells re-enter the cell cycle only after damage and they, then, differentiate into all the cell types that constitute the gastric unit (Qiao et al., 2007). More recently, the existence of another population of actively self-renewing stem cells residing at the bottom of the gland has been demonstrated (Fig. 4a). It was found that these cells express the adult stem cell marker Lgr5 and actively contribute to the daily renewal of the gastric epithelium (Barker et al., 2010). Lineage tracing studies using Lgr5Cre recombinase in the antrum revealed that the Villin-positive quiescent stem cells described by Qiao and colleagues (Qiao et al., 2007) were descendants of the Lgr5-positive stem cells (Barker et al., 2010). The quiescent stem cells, once differentiated, lose *Lgr5* expression which can be reactivated upon damage in order to immediately restore the

normal functionality and structure of the stomach epithelium (Vries et al., 2010).

Barker and colleagues compared the expression profile of the Lgr5^{high} versus the Lgr5^{low} daughter cells. Similarly to the situation with the intestinal stem cells (Sato et al., 2009), they found an enrichment of Wnt target gene expression in the Lgr5^{high} cell population of the stomach. These cells exclusively could give rise to gastric organoids in a matrigel-based *in vitro* system (Barker et al., 2010) (Fig. 4c).

The stomach organoids exhibit a cystic structure with small buds around the cyst surface where the stem cell compartment resides (Fig. 4c). They can be cultured in conditions very similar to those required by the intestinal organoids (Sato et al., 2009), but they have an additional dependence on Wnt3a and Gastrin for growth and on FGF10 for budding. Under these culture conditions (ENRWfg), the gastric organoids can be passaged for long periods of time without genetic or phenotypic alterations and they generate all the differentiated gastric epithelial cell types except pit and enteroendocrine cells, which are only observed after reducing the Wnt3a concentration in the medium (differentiation conditions) (Barker et al., 2010).

The fact that intestinal and stomach organoids could be derived from single Lgr5-expressing cells from the respective organs demonstrates the extraordinary potential of the corresponding adult stem cells to contribute to all known intestinal and pyloric epithelial cells, respectively. Moreover it is impressive how well both intestinal and stomach organoids recapitulate the complete stem cell differentiation program and the functional units of their organ of origin.

Nowadays all the standard techniques used for cell lines have been implemented for the organoid culture system. Protocols for storage by freezing, infection with recombinant retro- and lentiviruses (Koo et al., 2013; Koo et al., 2012) as well as molecular expression analysis are available. Application of the inducible CreERT2 recombinase system (Koo et al., 2013; Koo et al., 2012) and ultimately development of genome editing systems including the CRISPR/Cas9 (Schwank et al., 2013) allow gene manipulations in organoids, the effects of which can be followed in real time (Sato and Clevers, 2013). This provides excellent tools for cell fate determination studies (see Chapter 4) that were not possible before.

5. Cdx and the intestinal fate

Cdx1 and *Cdx2* are the only Cdx genes expressed in the endoderm of the primitive gut after E12.5. They are expressed antero-posteriorly in overlapping patterns in embryos and, after birth, this expression is maintained in adults (Silberg et al., 2000). In the adult intestine the expression pattern of the two Cdx genes, while still overlapping, exhibits some differences. *Cdx1* expression increases posteriorly along the intestine to reach its highest expression levels in the colon. Instead, the expression of *Cdx2* progressively increases from the duodenum to the distal small intestine while decreasing posteriorly, thus showing the highest expression levels in the cecum (at the junction between ileum and colon) (Beck et al., 1995; James et al., 1994; Silberg et al., 1997; Silberg et al., 2000) (Fig. 3c). Differences in expression are also evident along the crypt/villus axis. *Cdx1* is expressed at higher levels in the crypt than in the villus (Silberg et al., 1997; Silberg et al., 2000), whereas *Cdx2* is uniformly expressed in both, but is differently phosphorilated along the intestinal unit suggesting that its activity is post-transcriptionally regulated (Houde et al., 2001; Rings et al., 2001).

Mouse mutants have been generated for these two homeobox transcription factors. *Cdx1[null]* mice have no abnormal gut phenotype (Subramanian et al., 1995; van den Akker et al., 2002), whereas *Cdx2[het]* mutant mice show adenomatous polyps formation in the intestinal mucosa, particularly in the proximal colon (Chawengsaksophak et al., 1997). The latter study of Chawengsaksophak and colleagues (Chawengsaksophak et al., 1997), as well as the more recent study of Hryniuk and colleagues (Hryniuk et al., 2014), suggested that *Cdx2* functions in the colon as tumor suppressor. Further studies in *Cdx2[het]* mutant mice led to the discovery of gastric metaplastia in the coecal area (Beck et al., 1999). Ectopic expression of *Cdx2* in the stomach causes intestinal metaplasia, pre-carcinogenic transformation of the stomach epithelium (Mutoh et al., 2002; Mutoh et al., 2004; Silberg et al., 2002). These results already suggested a role of *Cdx2* in driving the intestinal program. This notion was strengthened by experiments in which specific ablation of *Cdx2* expression was performed in the endoderm at different embryonic stages. *Cdx2* inactivation at E9.5 (Gao et al., 2009) and E13.5 (Grainger et al., 2010), resulted in a dramatic conversion of the intestinal epithelium into esophagus and stomach epithelium, respectively. Knock out of *Cdx2* specifically in the adult intestinal stem cell population, using

an *Lgr5CreER^{T2}* allele, led to a partial transformation of the intestinal into stomach epithelium, with the formation of submucosal empty cysts expressing stomach markers (Hryniuk et al., 2012; Stringer et al., 2012). In both Verzi's and Stringer's studies, *Cdx1* ablation in addition to *Cdx2* loss resulted in an acceleration but not in aggravation of the intestinal transformation, resulting in a more rapid death of the mice due to loss of enterocytes in a different time course (Stringer et al., 2012; Verzi et al., 2010). These results suggested a partial functional redundancy between these two factors in the intestine, and indicated Cdx2 as the main factor determining the intestinal identity. In Chapter 4 we further investigate the effect of *Cdx2* loss on the adult intestinal stem cells commitment.

1

1

Outline of the thesis

Cdx are Hox-related evolutionary conserved genes involved in controlling the elongation and patterning of the embryonic AP axis. Generation of mouse mutants in which the normal Cdx dosage has been progressively diminished indicated that the three Cdx genes control the axial elongation process in a dosage dependent manner. In the work described in Chapter 2 we completed the allelic series of Cdx loss of function mutants by generating *Cdx^{null}* embryos. This enabled us to define the full extent of Cdx activity during axial growth. We found that axial extension in these embryos stops at the boundary between occipital and trunk levels.

Axial extension also depends on the integrity of the transcription factor T Brachyury. Mouse mutants in *Cdx2* and *T Brachyury* exhibit severe axial truncation phenotypes and an overlapping spectrum of defects. *Cdx2* and *T Brachyury* both establish positive feedback loops with the Wnt and Fgf growth signaling pathways that are directly involved in controlling the laying down of trunk and tail tissues. Despite these similarities, the functional relationship between *Cdx2* and *T Brachyury* during axial extension has remained elusive. In Chapter 3 we investigated whether and how these two genes genetically interact during mouse embryonic trunk and tail formation.

Renewal of the small intestinal and stomach epithelia throughout life depends on actively cycling stem cells. *Cdx2* specifies the intestinal commitment of the gut epithelium both in embryos and in adults. In Chapter 4, we use organoid cultures *in vitro* to demonstrate the absolute requirement of Cdx2 for the identity and functions of the adult intestinal stem cells. We also show that the loss of this single transcription factor converts intestinal stem cells into stem cells with a different identity: that of the gastric pylorus.

Chapter 5 is a general discussion.

1

References

Ang, S.L., Wierda, A., Wong, D., Stevens, K.A., Cascio, S., Rossant, J., and Zaret, K.S. (1993). The formation and maintenance of the definitive endoderm lineage in the mouse: involvement of HNF3/forkhead proteins. Development *119*, 1301-1315.

Arnold, S.J., and Robertson, E.J. (2009). Making a commitment: cell lineage allocation and axis patterning in the early mouse embryo. Nature reviews Molecular cell biology *10*, 91-103.

Asai, R., Okano, H., and Yasugi, S. (2005). Correlation between Musashi-1 and c-hairy-1 expression and cell proliferation activity in the developing intestine and stomach of both chicken and mouse. Development, growth & differentiation *47*, 501-510.

Barker, N., and Clevers, H. (2007). Tracking down the stem cells of the intestine: strategies to identify adult stem cells. Gastroenterology *133*, 1755-1760.

Barker, N., Huch, M., Kujala, P., van de Wetering, M., Snippert, H.J., van Es, J.H., Sato, T., Stange, D.E., Begthel, H., van den Born, M.*, et al.* (2010). Lgr5(+ve) stem cells drive self-renewal in the stomach and build long-lived gastric units in vitro. Cell stem cell *6*, 25-36.

Barker, N., van de Wetering, M., and Clevers, H. (2008). The intestinal stem cell. Genes & development *22*, 1856-1864.

Barrow, J.R., Howell, W.D., Rule, M., Hayashi, S., Thomas, K.R., Capecchi, M.R., and McMahon, A.P. (2007). Wnt3 signaling in the epiblast is required for proper orientation of the anteroposterior axis. Developmental biology *312*, 312-320.

Beck, F., Chawengsaksophak, K., Waring, P., Playford, R.J., and Furness, J.B. (1999). Reprogramming of intestinal differentiation and intercalary regeneration in Cdx2 mutant mice. Proceedings of the National Academy of Sciences of the United States of America *96*, 7318-7323.

Beck, F., Erler, T., Russell, A., and James, R. (1995). Expression of Cdx-2

1

in the mouse embryo and placenta: possible role in patterning of the extra-embryonic membranes. Developmental dynamics : an official publication of the American Association of Anatomists *204*, 219-227.

Bel-Vialar, S., Itasaki, N., and Krumlauf, R. (2002). Initiating Hox gene expression: in the early chick neural tube differential sensitivity to FGF and RA signaling subdivides the HoxB genes in two distinct groups. Development *129*, 5103-5115.

Boulet, A.M., and Capecchi, M.R. (2012). Signaling by FGF4 and FGF8 is required for axial elongation of the mouse embryo. Developmental biology *371*, 235-245.

Brennan, J., Lu, C.C., Norris, D.P., Rodriguez, T.A., Beddington, R.S., and Robertson, E.J. (2001). Nodal signalling in the epiblast patterns the early mouse embryo. Nature *411*, 965-969.

Cambray, N., and Wilson, V. (2002). Axial progenitors with extensive potency are localised to the mouse chordoneural hinge. Development *129*, 4855-4866.

Cambray, N., and Wilson, V. (2007). Two distinct sources for a population of maturing axial progenitors. Development *134*, 2829-2840.

Catalioto, R.M., Maggi, C.A., and Giuliani, S. (2011). Intestinal epithelial barrier dysfunction in disease and possible therapeutical interventions. Current medicinal chemistry *18*, 398-426.

Chawengsaksophak, K., de Graaff, W., Rossant, J., Deschamps, J., and Beck, F. (2004). Cdx2 is essential for axial elongation in mouse development. Proceedings of the National Academy of Sciences of the United States of America *101*, 7641-7645.

Chawengsaksophak, K., James, R., Hammond, V.E., Kontgen, F., and Beck, F. (1997). Homeosis and intestinal tumours in Cdx2 mutant mice. Nature *386*, 84-87.

Cheng, H., and Leblond, C.P. (1974). Origin, differentiation and renewal of the four main epithelial cell types in the mouse small intestine. I. Columnar cell. The American journal of anatomy *141*, 461-479.

1

Ciruna, B., and Rossant, J. (2001). FGF signaling regulates mesoderm cell fate specification and morphogenetic movement at the primitive streak. Developmental cell *1*, 37-49.

Conlon, F.L., Lyons, K.M., Takaesu, N., Barth, K.S., Kispert, A., Herrmann, B., and Robertson, E.J. (1994). A primary requirement for nodal in the formation and maintenance of the primitive streak in the mouse. Development *120*, 1919-1928.

Deng, C.X., Wynshaw-Boris, A., Shen, M.M., Daugherty, C., Ornitz, D.M., and Leder, P. (1994). Murine FGFR-1 is required for early postimplantation growth and axial organization. Genes & development *8*, 3045-3057.

Dobrovolskaia-Zavadskaia, N. (1927). Sur la mortification spontanee de la queue chez la souris nouveau-nee et sur l'existence d'un caractere hereditaire "non viable". C R Hebd Soc Biol, 114-116.

Dufort, D., Schwartz, L., Harpal, K., and Rossant, J. (1998). The transcription factor HNF3beta is required in visceral endoderm for normal primitive streak morphogenesis. Development *125*, 3015-3025.

Dunty, W.C., Jr., Biris, K.K., Chalamalasetty, R.B., Taketo, M.M., Lewandoski, M., and Yamaguchi, T.P. (2008). Wnt3a/beta-catenin signaling controls posterior body development by coordinating mesoderm formation and segmentation. Development *135*, 85-94.

Evans, A.L., Faial, T., Gilchrist, M.J., Down, T., Vallier, L., Pedersen, R.A., Wardle, F.C., and Smith, J.C. (2012). Genomic targets of Brachyury (T) in differentiating mouse embryonic stem cells. PloS one *7*, e33346.

Feldman, B., Poueymirou, W., Papaioannou, V.E., DeChiara, T.M., and Goldfarb, M. (1995). Requirement of FGF-4 for postimplantation mouse development. Science *267*, 246-249.

Forlani, S., Lawson, K.A., and Deschamps, J. (2003). Acquisition of Hox codes during gastrulation and axial elongation in the mouse embryo. Development *130*, 3807-3819.

Galceran, J., Farinas, I., Depew, M.J., Clevers, H., and Grosschedl, R. (1999). Wnt3a-/--like phenotype and limb deficiency in Lef1(-/-)Tcf1(-/-) mice.

Genes & development *13*, 709-717.

Gao, N., White, P., and Kaestner, K.H. (2009). Establishment of intestinal identity and epithelial-mesenchymal signaling by Cdx2. Developmental cell *16*, 588-599.

Gaunt, S.J., Drage, D., and Cockley, A. (2003). Vertebrate caudal gene expression gradients investigated by use of chick cdx-A/lacZ and mouse cdx-1/lacZ reporters in transgenic mouse embryos: evidence for an intron enhancer. Mechanisms of development *120*, 573-586.

Gentsch, G.E., Owens, N.D., Martin, S.R., Piccinelli, P., Faial, T., Trotter, M.W., Gilchrist, M.J., and Smith, J.C. (2013). In vivo T-box transcription factor profiling reveals joint regulation of embryonic neuromesodermal bipotency. Cell reports *4*, 1185-1196.

Grainger, S., Savory, J.G., and Lohnes, D. (2010). Cdx2 regulates patterning of the intestinal epithelium. Developmental biology *339*, 155-165.

Grapin-Botton, A. (2005). Antero-posterior patterning of the vertebrate digestive tract: 40 years after Nicole Le Douarin's PhD thesis. The International journal of developmental biology *49*, 335-347.

Grapin-Botton, A. (2008). Endoderm specification. In StemBook (Cambridge (MA)).

Guo, R.J., Suh, E.R., and Lynch, J.P. (2004). The role of Cdx proteins in intestinal development and cancer. Cancer biology & therapy *3*, 593-601.

H., G. (1958). Genetical studies on the skeleton of the mouse. XXIII. The development of brachyury and anury. J Embryol Exp Morphol *6*, 424-443.

Haegebarth, A., and Clevers, H. (2009). Wnt signaling, lgr5, and stem cells in the intestine and skin. The American journal of pathology *174*, 715-721.

Haegel, H., Larue, L., Ohsugi, M., Fedorov, L., Herrenknecht, K., and Kemler, R. (1995). Lack of beta-catenin affects mouse development at gastrulation. Development *121*, 3529-3537.

Hayashi, S., Lewis, P., Pevny, L., and McMahon, A.P. (2002). Efficient gene

modulation in mouse epiblast using a Sox2Cre transgenic mouse strain. Mechanisms of development *119 Suppl 1*, S97-S101.

Heath, J.P. (1996). Epithelial cell migration in the intestine. Cell biology international *20*, 139-146.

Herrmann, B.G., and Kispert, A. (1994). The T genes in embryogenesis. Trends in genetics : TIG *10*, 280-286.

Herrmann, B.G., Labeit, S., Poustka, A., King, T.R., and Lehrach, H. (1990). Cloning of the T gene required in mesoderm formation in the mouse. Nature *343*, 617-622.

Holmberg, J., Genander, M., Halford, M.M., Anneren, C., Sondell, M., Chumley, M.J., Silvany, R.E., Henkemeyer, M., and Frisen, J. (2006). EphB receptors coordinate migration and proliferation in the intestinal stem cell niche. Cell *125*, 1151-1163.

Houde, M., Laprise, P., Jean, D., Blais, M., Asselin, C., and Rivard, N. (2001). Intestinal epithelial cell differentiation involves activation of p38 mitogen-activated protein kinase that regulates the homeobox transcription factor CDX2. The Journal of biological chemistry *276*, 21885-21894.

Hryniuk, A., Grainger, S., Savory, J.G., and Lohnes, D. (2012). Cdx function is required for maintenance of intestinal identity in the adult. Developmental biology *363*, 426-437.

Hryniuk, A., Grainger, S., Savory, J.G., and Lohnes, D. (2014). Cdx1 and Cdx2 Function as Tumor Suppressors. The Journal of biological chemistry.

Iannaccone, P.M., Zhou, X., Khokha, M., Boucher, D., and Kuehn, M.R. (1992). Insertional mutation of a gene involved in growth regulation of the early mouse embryo. Developmental dynamics : an official publication of the American Association of Anatomists *194*, 198-208.

Ikeya, M., and Takada, S. (2001). Wnt-3a is required for somite specification along the anteroposterior axis of the mouse embryo and for regulation of cdx-1 expression. Mechanisms of development *103*, 27-33.

Iratni, R., Yan, Y.T., Chen, C., Ding, J., Zhang, Y., Price, S.M., Reinberg, D.,

1

and Shen, M.M. (2002). Inhibition of excess nodal signaling during mouse gastrulation by the transcriptional corepressor DRAP1. Science *298*, 1996-1999.

Jacobsen, C.M., Narita, N., Bielinska, M., Syder, A.J., Gordon, J.I., and Wilson, D.B. (2002). Genetic mosaic analysis reveals that GATA-4 is required for proper differentiation of mouse gastric epithelium. Developmental biology *241*, 34-46.

James, R., Erler, T., and Kazenwadel, J. (1994). Structure of the murine homeobox gene cdx-2. Expression in embryonic and adult intestinal epithelium. The Journal of biological chemistry *269*, 15229-15237.

Kanai-Azuma, M., Kanai, Y., Gad, J.M., Tajima, Y., Taya, C., Kurohmaru, M., Sanai, Y., Yonekawa, H., Yazaki, K., Tam, P.P.*, et al.* (2002). Depletion of definitive gut endoderm in Sox17-null mutant mice. Development *129*, 2367-2379.

Karam, S.M., and Leblond, C.P. (1993). Dynamics of epithelial cells in the corpus of the mouse stomach. V. Behavior of entero-endocrine and caveolated cells: general conclusions on cell kinetics in the oxyntic epithelium. The Anatomical record *236*, 333-340.

Kawazoe, Y., Sekimoto, T., Araki, M., Takagi, K., Araki, K., and Yamamura, K. (2002). Region-specific gastrointestinal Hox code during murine embryonal gut development. Development, growth & differentiation *44*, 77-84.

Kimura, C., Yoshinaga, K., Tian, E., Suzuki, M., Aizawa, S., and Matsuo, I. (2000). Visceral endoderm mediates forebrain development by suppressing posteriorizing signals. Developmental biology *225*, 304-321.

Kinder, S.J., Tsang, T.E., Quinlan, G.A., Hadjantonakis, A.K., Nagy, A., and Tam, P.P. (1999). The orderly allocation of mesodermal cells to the extraembryonic structures and the anteroposterior axis during gastrulation of the mouse embryo. Development *126*, 4691-4701.

King, T., Beddington, R.S., and Brown, N.A. (1998). The role of the brachyury gene in heart development and left-right specification in the mouse. Mechanisms of development *79*, 29-37.

Kispert, A., and Herrmann, B.G. (1994). Immunohistochemical analysis of the Brachyury protein in wild-type and mutant mouse embryos. Developmental biology *161*, 179-193.

Kondo, T., Dolle, P., Zakany, J., and Duboule, D. (1996). Function of posterior HoxD genes in the morphogenesis of the anal sphincter. Development *122*, 2651-2659.

Koo, B.K., Sasselli, V., and Clevers, H. (2013). Retroviral gene expression control in primary organoid cultures. Current protocols in stem cell biology *27*, Unit 5A 6.

Koo, B.K., Stange, D.E., Sato, T., Karthaus, W., Farin, H.F., Huch, M., van Es, J.H., and Clevers, H. (2012). Controlled gene expression in primary Lgr5 organoid cultures. Nature methods *9*, 81-83.

Koutsourakis, M., Langeveld, A., Patient, R., Beddington, R., and Grosveld, F. (1999). The transcription factor GATA6 is essential for early extraembryonic development. Development *126*, 723-732.

Kwon, G.S., Viotti, M., and Hadjantonakis, A.K. (2008). The endoderm of the mouse embryo arises by dynamic widespread intercalation of embryonic and extraembryonic lineages. Developmental cell *15*, 509-520.

Lawson, K.A. (1999). Fate mapping the mouse embryo. The International journal of developmental biology *43*, 773-775.

Lawson, K.A., Meneses, J.J., and Pedersen, R.A. (1991). Clonal analysis of epiblast fate during germ layer formation in the mouse embryo. Development *113*, 891-911.

Lee, E.R., and Leblond, C.P. (1985). Dynamic histology of the antral epithelium in the mouse stomach: IV. Ultrastructure and renewal of gland cells. The American journal of anatomy *172*, 241-259.

Liu, P., Wakamiya, M., Shea, M.J., Albrecht, U., Behringer, R.R., and Bradley, A. (1999). Requirement for Wnt3 in vertebrate axis formation. Nature genetics *22*, 361-365.

Lolas, M., Valenzuela, P.D., Tjian, R., and Liu, Z. (2014). Charting Brachyury-

1

mediated developmental pathways during early mouse embryogenesis. Proceedings of the National Academy of Sciences of the United States of America *111*, 4478-4483.

Lowe, L.A., Yamada, S., and Kuehn, M.R. (2001). Genetic dissection of nodal function in patterning the mouse embryo. Development *128*, 1831-1843.

Martin, B.L., and Kimelman, D. (2010). Brachyury establishes the embryonic mesodermal progenitor niche. Genes & development *24*, 2778-2783.

Mathis, L., Kulesa, P.M., and Fraser, S.E. (2001). FGF receptor signalling is required to maintain neural progenitors during Hensen's node progression. Nature cell biology *3*, 559-566.

May, R., Sureban, S.M., Hoang, N., Riehl, T.E., Lightfoot, S.A., Ramanujam, R., Wyche, J.H., Anant, S., and Houchen, C.W. (2009). Doublecortin and CaM kinase-like-1 and leucine-rich-repeat-containing G-protein-coupled receptor mark quiescent and cycling intestinal stem cells, respectively. Stem Cells *27*, 2571-2579.

McGrew, M.J., Sherman, A., Lillico, S.G., Ellard, F.M., Radcliffe, P.A., Gilhooley, H.J., Mitrophanous, K.A., Cambray, N., Wilson, V., and Sang, H. (2008). Localised axial progenitor cell populations in the avian tail bud are not committed to a posterior Hox identity. Development *135*, 2289-2299.

Meno, C., Gritsman, K., Ohishi, S., Ohfuji, Y., Heckscher, E., Mochida, K., Shimono, A., Kondoh, H., Talbot, W.S., Robertson, E.J*., et al.* (1999). Mouse Lefty2 and zebrafish antivin are feedback inhibitors of nodal signaling during vertebrate gastrulation. Molecular cell *4*, 287-298.

Mesnard, D., Filipe, M., Belo, J.A., and Zernicka-Goetz, M. (2004). The anterior-posterior axis emerges respecting the morphology of the mouse embryo that changes and aligns with the uterus before gastrulation. Current biology : CB *14*, 184-196.

Molotkova, N., Molotkov, A., Sirbu, I.O., and Duester, G. (2005). Requirement of mesodermal retinoic acid generated by Raldh2 for posterior neural transformation. Mechanisms of development *122*, 145-155.

Morrisey, E.E., Tang, Z., Sigrist, K., Lu, M.M., Jiang, F., Ip, H.S., and Parmacek,

1

M.S. (1998). GATA6 regulates HNF4 and is required for differentiation of visceral endoderm in the mouse embryo. Genes & development *12*, 3579-3590.

Mutoh, H., Hakamata, Y., Sato, K., Eda, A., Yanaka, I., Honda, S., Osawa, H., Kaneko, Y., and Sugano, K. (2002). Conversion of gastric mucosa to intestinal metaplasia in Cdx2-expressing transgenic mice. Biochemical and biophysical research communications *294*, 470-479.

Mutoh, H., Sakurai, S., Satoh, K., Osawa, H., Hakamata, Y., Takeuchi, T., and Sugano, K. (2004). Cdx1 induced intestinal metaplasia in the transgenic mouse stomach: comparative study with Cdx2 transgenic mice. Gut *53*, 1416-1423.

Naiche, L.A., Harrelson, Z., Kelly, R.G., and Papaioannou, V.E. (2005). T-box genes in vertebrate development. Annual review of genetics *39*, 219-239.

Naiche, L.A., Holder, N., and Lewandoski, M. (2011). FGF4 and FGF8 comprise the wavefront activity that controls somitogenesis. Proceedings of the National Academy of Sciences of the United States of America *108*, 4018-4023.

Neijts, R., Simmini, S., Giuliani, F., van Rooijen, C., and Deschamps, J. (2014). Region-specific regulation of posterior axial elongation during vertebrate embryogenesis. Developmental dynamics : an official publication of the American Association of Anatomists *243*, 88-98.

Nowotschin, S., Ferrer-Vaquer, A., Concepcion, D., Papaioannou, V.E., and Hadjantonakis, A.K. (2012). Interaction of Wnt3a, Msgn1 and Tbx6 in neural versus paraxial mesoderm lineage commitment and paraxial mesoderm differentiation in the mouse embryo. Developmental biology *367*, 1-14.

P., C. (1935). Development of the short-tailed mutant in the house mouse. Journal of Experimental Zoology *70*, 429-459.

Papaioannou, V.E. (2014). The T-box gene family: emerging roles in development, stem cells and cancer. Development *141*, 3819-3833.

Perea-Gomez, A., Camus, A., Moreau, A., Grieve, K., Moneron, G., Dubois, A., Cibert, C., and Collignon, J. (2004). Initiation of gastrulation in the mouse

1

embryo is preceded by an apparent shift in the orientation of the anterior-posterior axis. Current biology : CB *14*, 197-207.

Pereira, P.N., Dobreva, M.P., Graham, L., Huylebroeck, D., Lawson, K.A., and Zwijsen, A.N. (2011). Amnion formation in the mouse embryo: the single amniochorionic fold model. BMC developmental biology *11*, 48.

Pfister, S., Steiner, K.A., and Tam, P.P. (2007). Gene expression pattern and progression of embryogenesis in the immediate post-implantation period of mouse development. Gene expression patterns : GEP *7*, 558-573.

Pilon, N., Oh, K., Sylvestre, J.R., Bouchard, N., Savory, J., and Lohnes, D. (2006). Cdx4 is a direct target of the canonical Wnt pathway. Developmental biology *289*, 55-63.

Pownall, M.E., Isaacs, H.V., and Slack, J.M. (1998). Two phases of Hox gene regulation during early Xenopus development. Current biology : CB *8*, 673-676.

Qiao, X.T., Ziel, J.W., McKimpson, W., Madison, B.B., Todisco, A., Merchant, J.L., Samuelson, L.C., and Gumucio, D.L. (2007). Prospective identification of a multilineage progenitor in murine stomach epithelium. Gastroenterology *133*, 1989-1998.

Rayon, T., Menchero, S., Nieto, A., Xenopoulos, P., Crespo, M., Cockburn, K., Canon, S., Sasaki, H., Hadjantonakis, A.K., de la Pompa, J.L.*, et al.* (2014). Notch and hippo converge on Cdx2 to specify the trophectoderm lineage in the mouse blastocyst. Developmental cell *30*, 410-422.

Rings, E.H., Boudreau, F., Taylor, J.K., Moffett, J., Suh, E.R., and Traber, P.G. (2001). Phosphorylation of the serine 60 residue within the Cdx2 activation domain mediates its transactivation capacity. Gastroenterology *121*, 1437-1450.

Rivera-Perez, J.A., and Hadjantonakis, A.K. (2014). The Dynamics of Morphogenesis in the Early Mouse Embryo. Cold Spring Harbor perspectives in biology.

Rivera-Perez, J.A., and Magnuson, T. (2005). Primitive streak formation in mice is preceded by localized activation of Brachyury and Wnt3.

1

Developmental biology *288*, 363-371.

Roberts, D.J., Johnson, R.L., Burke, A.C., Nelson, C.E., Morgan, B.A., and Tabin, C. (1995). Sonic hedgehog is an endodermal signal inducing Bmp-4 and Hox genes during induction and regionalization of the chick hindgut. Development *121*, 3163-3174.

Roberts, D.J., Smith, D.M., Goff, D.J., and Tabin, C.J. (1998). Epithelial-mesenchymal signaling during the regionalization of the chick gut. Development *125*, 2791-2801.

Sangiorgi, E., and Capecchi, M.R. (2008). Bmi1 is expressed in vivo in intestinal stem cells. Nature genetics *40*, 915-920.

Sasaki, H., and Hogan, B.L. (1993). Differential expression of multiple fork head related genes during gastrulation and axial pattern formation in the mouse embryo. Development *118*, 47-59.

Sato, T., and Clevers, H. (2013). Growing self-organizing mini-guts from a single intestinal stem cell: mechanism and applications. Science *340*, 1190-1194.

Sato, T., Vries, R.G., Snippert, H.J., van de Wetering, M., Barker, N., Stange, D.E., van Es, J.H., Abo, A., Kujala, P., Peters, P.J*., et al.* (2009). Single Lgr5 stem cells build crypt-villus structures in vitro without a mesenchymal niche. Nature *459*, 262-265.

Satoh, N., and Jeffery, W.R. (1995). Chasing tails in ascidians: developmental insights into the origin and evolution of chordates. Trends in genetics : TIG *11*, 354-359.

Savory, J.G., Bouchard, N., Pierre, V., Rijli, F.M., De Repentigny, Y., Kothary, R., and Lohnes, D. (2009). Cdx2 regulation of posterior development through non-Hox targets. Development *136*, 4099-4110.

Savory, J.G., Mansfield, M., Rijli, F.M., and Lohnes, D. (2011). Cdx mediates neural tube closure through transcriptional regulation of the planar cell polarity gene Ptk7. Development *138*, 1361-1370.

Schuijers, J., and Clevers, H. (2012). Adult mammalian stem cells: the role of

1

Wnt, Lgr5 and R-spondins. The EMBO journal *31*, 2685-2696.

Schwank, G., Koo, B.K., Sasselli, V., Dekkers, J.F., Heo, I., Demircan, T., Sasaki, N., Boymans, S., Cuppen, E., van der Ent, C.K.*, et al.* (2013). Functional repair of CFTR by CRISPR/Cas9 in intestinal stem cell organoids of cystic fibrosis patients. Cell stem cell *13*, 653-658.

Sebe-Pedros, A., Ariza-Cosano, A., Weirauch, M.T., Leininger, S., Yang, A., Torruella, G., Adamski, M., Adamska, M., Hughes, T.R., Gomez-Skarmeta, J.L.*, et al.* (2013). Early evolution of the T-box transcription factor family. Proceedings of the National Academy of Sciences of the United States of America *110*, 16050-16055.

Sekimoto, T., Yoshinobu, K., Yoshida, M., Kuratani, S., Fujimoto, S., Araki, M., Tajima, N., Araki, K., and Yamamura, K. (1998). Region-specific expression of murine Hox genes implies the Hox code-mediated patterning of the digestive tract. Genes to cells : devoted to molecular & cellular mechanisms *3*, 51-64.

Selleck, M.A., and Stern, C.D. (1991). Fate mapping and cell lineage analysis of Hensen's node in the chick embryo. Development *112*, 615-626.

Sherwood, R.I., Chen, T.Y., and Melton, D.A. (2009). Transcriptional dynamics of endodermal organ formation. Developmental dynamics : an official publication of the American Association of Anatomists *238*, 29-42.

Shimizu, T., Bae, Y.K., and Hibi, M. (2006). Cdx-Hox code controls competence for responding to Fgfs and retinoic acid in zebrafish neural tissue. Development *133*, 4709-4719.

Shimizu, T., Bae, Y.K., Muraoka, O., and Hibi, M. (2005). Interaction of Wnt and caudal-related genes in zebrafish posterior body formation. Developmental biology *279*, 125-141.

Silberg, D.G., Furth, E.E., Taylor, J.K., Schuck, T., Chiou, T., and Traber, P.G. (1997). CDX1 protein expression in normal, metaplastic, and neoplastic human alimentary tract epithelium. Gastroenterology *113*, 478-486.

Silberg, D.G., Sullivan, J., Kang, E., Swain, G.P., Moffett, J., Sund, N.J., Sackett, S.D., and Kaestner, K.H. (2002). Cdx2 ectopic expression induces gastric intestinal metaplasia in transgenic mice. Gastroenterology *122*, 689-

696.

Silberg, D.G., Swain, G.P., Suh, E.R., and Traber, P.G. (2000). Cdx1 and cdx2 expression during intestinal development. Gastroenterology *119*, 961-971.

Snell, G.D.a.S.L.C. (1966). Early embryology. In "Biology of the Laboratory Mouse". EL Green ed, 205-245.

Snow, M.H.L. (1977). Gastrulation in the mouse: Growth and regionalization of the epiblast. J Embryol Exp Morphol *42*, 293-303.

Soudais, C., Bielinska, M., Heikinheimo, M., MacArthur, C.A., Narita, N., Saffitz, J.E., Simon, M.C., Leiden, J.M., and Wilson, D.B. (1995). Targeted mutagenesis of the transcription factor GATA-4 gene in mouse embryonic stem cells disrupts visceral endoderm differentiation in vitro. Development *121*, 3877-3888.

Stern, C.D., Hatada, Y., Selleck, M.A., and Storey, K.G. (1992). Relationships between mesoderm induction and the embryonic axes in chick and frog embryos. Dev Suppl, 151-156.

Stevens, C.E., and Leblond, C.P. (1953). Renewal of the mucous cells in the gastric mucosa of the rat. The Anatomical record *115*, 231-245.

Stringer, E.J., Duluc, I., Saandi, T., Davidson, I., Bialecka, M., Sato, T., Barker, N., Clevers, H., Pritchard, C.A., Winton, D.J.*, et al.* (2012). Cdx2 determines the fate of postnatal intestinal endoderm. Development *139*, 465-474.

Subramanian, V., Meyer, B.I., and Gruss, P. (1995). Disruption of the murine homeobox gene Cdx1 affects axial skeletal identities by altering the mesodermal expression domains of Hox genes. Cell *83*, 641-653.

Sun, X., Meyers, E.N., Lewandoski, M., and Martin, G.R. (1999). Targeted disruption of Fgf8 causes failure of cell migration in the gastrulating mouse embryo. Genes & development *13*, 1834-1846.

Takada, S., Stark, K.L., Shea, M.J., Vassileva, G., McMahon, J.A., and McMahon, A.P. (1994). Wnt-3a regulates somite and tailbud formation in the mouse embryo. Genes & development *8*, 174-189.

1

Tam, P.P., and Beddington, R.S. (1992). Establishment and organization of germ layers in the gastrulating mouse embryo. Ciba Foundation symposium *165*, 27-41; discussion 42-29.

Tam, P.P., and Loebel, D.A. (2007). Gene function in mouse embryogenesis: get set for gastrulation. Nature reviews Genetics *8*, 368-381.

Tortelote, G.G., Hernandez-Hernandez, J.M., Quaresma, A.J., Nickerson, J.A., Imbalzano, A.N., and Rivera-Perez, J.A. (2013). Wnt3 function in the epiblast is required for the maintenance but not the initiation of gastrulation in mice. Developmental biology *374*, 164-173.

Tzouanacou, E., Wegener, A., Wymeersch, F.J., Wilson, V., and Nicolas, J.F. (2009). Redefining the progression of lineage segregations during mammalian embryogenesis by clonal analysis. Developmental cell *17*, 365-376.

van de Ven, C., Bialecka, M., Neijts, R., Young, T., Rowland, J.E., Stringer, E.J., Van Rooijen, C., Meijlink, F., Novoa, A., Freund, J.N.*, et al.* (2011). Concerted involvement of Cdx/Hox genes and Wnt signaling in morphogenesis of the caudal neural tube and cloacal derivatives from the posterior growth zone. Development *138*, 3451-3462.

van den Akker, E., Forlani, S., Chawengsaksophak, K., de Graaff, W., Beck, F., Meyer, B.I., and Deschamps, J. (2002). Cdx1 and Cdx2 have overlapping functions in anteroposterior patterning and posterior axis elongation. Development *129*, 2181-2193.

van der Flier, L.G., and Clevers, H. (2009). Stem cells, self-renewal, and differentiation in the intestinal epithelium. Annual review of physiology *71*, 241-260.

van Nes, J., de Graaff, W., Lebrin, F., Gerhard, M., Beck, F., and Deschamps, J. (2006). The Cdx4 mutation affects axial development and reveals an essential role of Cdx genes in the ontogenesis of the placental labyrinth in mice. Development *133*, 419-428.

Verzi, M.P., Shin, H., He, H.H., Sulahian, R., Meyer, C.A., Montgomery, R.K., Fleet, J.C., Brown, M., Liu, X.S., and Shivdasani, R.A. (2010). Differentiation-

specific histone modifications reveal dynamic chromatin interactions and partners for the intestinal transcription factor CDX2. Developmental cell *19*, 713-726.

Vincent, S.D., Dunn, N.R., Hayashi, S., Norris, D.P., and Robertson, E.J. (2003). Cell fate decisions within the mouse organizer are governed by graded Nodal signals. Genes & development *17*, 1646-1662.

Vries, R.G., Huch, M., and Clevers, H. (2010). Stem cells and cancer of the stomach and intestine. Molecular oncology *4*, 373-384.

Wahl, M.B., Deng, C., Lewandoski, M., and Pourquie, O. (2007). FGF signaling acts upstream of the NOTCH and WNT signaling pathways to control segmentation clock oscillations in mouse somitogenesis. Development *134*, 4033-4041.

Weinstein, D.C., Ruiz i Altaba, A., Chen, W.S., Hoodless, P., Prezioso, V.R., Jessell, T.M., and Darnell, J.E., Jr. (1994). The winged-helix transcription factor HNF-3 beta is required for notochord development in the mouse embryo. Cell *78*, 575-588.

Wilson, V., Manson, L., Skarnes, W.C., and Beddington, R.S. (1995). The T gene is necessary for normal mesodermal morphogenetic cell movements during gastrulation. Development *121*, 877-886.

Wilson, V., Olivera-Martinez, I., and Storey, K.G. (2009). Stem cells, signals and vertebrate body axis extension. Development *136*, 1591-1604.

Yamaguchi, T.P., Harpal, K., Henkemeyer, M., and Rossant, J. (1994). fgfr-1 is required for embryonic growth and mesodermal patterning during mouse gastrulation. Genes & development *8*, 3032-3044.

Yamaguchi, T.P., Takada, S., Yoshikawa, Y., Wu, N., and McMahon, A.P. (1999). T (Brachyury) is a direct target of Wnt3a during paraxial mesoderm specification. Genes & development *13*, 3185-3190.

Yanagisawa, K.O., Fujimoto, H., and Urushihara, H. (1981). Effects of the brachyury (T) mutation on morphogenetic movement in the mouse embryo. Developmental biology *87*, 242-248.

1

Yokouchi, Y., Sakiyama, J., and Kuroiwa, A. (1995). Coordinated expression of Abd-B subfamily genes of the HoxA cluster in the developing digestive tract of chick embryo. Developmental biology *169*, 76-89.

Yoshikawa, Y., Fujimori, T., McMahon, A.P., and Takada, S. (1997). Evidence that absence of Wnt-3a signaling promotes neuralization instead of paraxial mesoderm development in the mouse. Developmental biology *183*, 234-242.

Young, T., Rowland, J.E., van de Ven, C., Bialecka, M., Novoa, A., Carapuco, M., van Nes, J., de Graaff, W., Duluc, I., Freund, J.N*., et al.* (2009). Cdx and Hox genes differentially regulate posterior axial growth in mammalian embryos. Developmental cell *17*, 516-526.

Yuqi, L., Chengtang, W., Ying, W., Shangtong, L., and Kangxiong, L. (2008). The expression of Msi-1 and its significance in small intestinal mucosa severely damaged by high-dose 5-FU. Digestive diseases and sciences *53*, 2436-2442.

Zacchetti, G., Duboule, D., and Zakany, J. (2007). Hox gene function in vertebrate gut morphogenesis: the case of the caecum. Development *134*, 3967-3973.

Zhou, X., Sasaki, H., Lowe, L., Hogan, B.L., and Kuehn, M.R. (1993). Nodal is a novel TGF-beta-like gene expressed in the mouse node during gastrulation. Nature *361*, 543-547.

Zorn, A.M., and Wells, J.M. (2009). Vertebrate endoderm development and organ formation. Annual review of cell and developmental biology *25*, 221-251.

1

Chapter 2
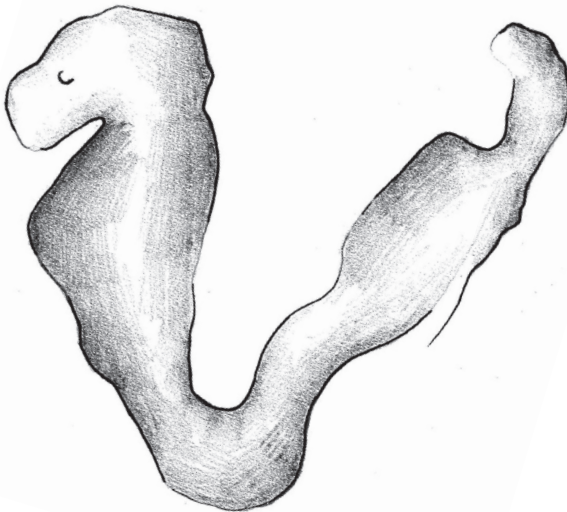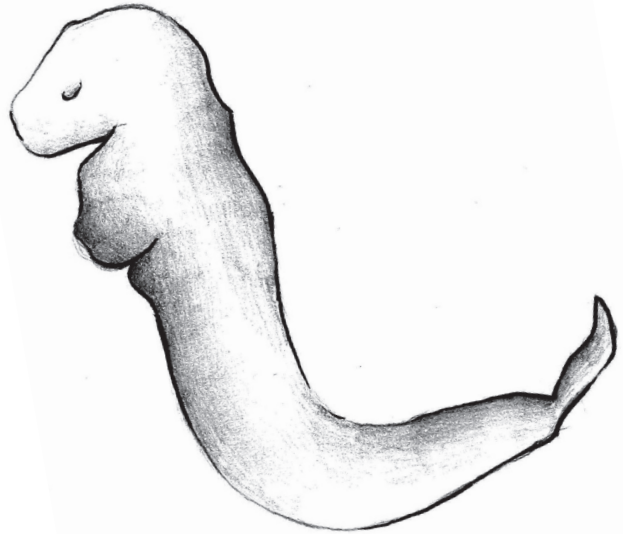
Evolutionarily conserved requirement of Cdx for post-occipital tissue emergence

Carina van Rooijen, Salvatore Simmini[*], Monika Bialecka[*], Roel Neijts[*], Cesca van de Ven, Felix Beck[2] and Jacqueline Deschamps

Hubrecht Institute, Developmental Biology and Stem cell Research, Uppsalalaan 8, 3584 CT Utrecht, and University Medical Center Utrecht, 3584 CX Utrecht, The Netherlands.

[2]Biochemistry Department, University of Leicester, Leicester, LE1 9HN, UK

*These authors contributed equally to this work

[*] Corresponding author: j.deschamps@hubrecht.eu

Abstract

Mouse Cdx genes are involved in axial patterning and partial Cdx mutants exhibit posterior embryonic defects. We found that mouse embryos in which all three Cdx genes are inactivated fail to generate any axial tissue beyond the cephalic and occipital primordia. Anterior axial tissues are laid down and well patterned in *Cdx^null* embryos, and a 3'Hox gene is initially transcribed and expressed in the hindbrain normally. Axial elongation stops abruptly at the post-occipital level in the absence of Cdx, as the posterior growth zone loses its progenitor activity. Exogenous Fgf8 rescues the posterior truncation of Cdx mutants, and the spectrum of defects of *Cdx^null* embryos matches that resulting from loss of posterior Fgfr1 signaling. Our data argue for a main function of Cdx in enforcing trunk emergence beyond the Cdx-independent cephalo-occipital region, and for a downstream role of Fgfr1 signaling in this function. Cdx requirement for the post-head section of the axis is ancestral as it takes place in arthropods as well.

Introduction

During gastrulation of the mouse embryo, progenitors for trunk and tail tissues are found in an ordered position in the epiblast flanking the primitive streak, from its more posterior extension to its rostral-most limit abutting the node (Kinder et al., 1999; Lawson et al., 1991; Tam and Beddington, 1987). Whereas the progenitors along the posterior and middle streak levels are transiently delivering descendants to extra-embryonic and embryonic mesoderm and do not leave residing cells after they have ingressed in the streak, the anterior-most level of the primitive streak harbors a self-renewing, stem cell-like population of progenitors that go on contributing cells to the elongating axial tissues until the end of axial growth by tissue addition (Cambray and Wilson, 2002, 2007; Wilson et al., 2009). Clonal analysis during embryogenesis provided evidence that bipotent long-term neuromesodermal (LT NM) progenitors contribute descendants to extended axial domains (Tzouanacou et al., 2009). These progenitors are likely to correspond to the stem cell-like axial progenitors shown by Cambray and Wilson to be present in the node-streak border and along the anterolateral primitive streak at embryonic day (E) 8.5, and in the chordo-neural hinge later on (Cambray and Wilson, 2002, 2007).

The mouse has three Cdx transcription factor encoding genes, *Cdx1*, *Cdx2* and *Cdx4*, homologs of *Drosophila caudal*. Cdx loss of function was first discovered to impair axial elongation when *Cdx2* was inactivated (Chawengsaksophak et al., 1997). Null mutants for *Cdx1* and *Cdx4* are not compromised in their axis extension but they fail to complete their axial development when missing an active allele of *Cdx2* (Savory et al., 2009; van den Akker et al., 2002; van Nes et al., 2006; Young et al., 2009). *Cdx4*[null] mutants heterozygote for *Cdx2* (hereafter termed *Cdx2/4* mutants) also suffer from limited allantoic vessel invasion in the chorionic ectoderm, and the allantois of *Cdx2*[null] mutants fails to grow out, preventing placental labyrinth ontogenesis and survival of the embryo beyond E10.5 (Chawengsaksophak et al., 2004; van de Ven et al., 2011; van Nes et al., 2006). Compound mutants for the different Cdx genes revealed redundancy between them in allowing embryonic tissues from the three germ layers to expand as development proceeds (Savory et al., 2009; Savory et al., 2011; van de Ven et al., 2011; van den Akker et al., 2002; Young et al., 2009). Histological and gene expression analyses combined with the fate-mapping information

on the progenitors of axial tissues in the mouse embryo (Cambray and Wilson, 2002, 2007; Tzouanacou et al., 2009) led to the conclusion that the Cdx mutations in *Cdx2/4* compound mutants affect tissue generation from progenitors residing along the primitive streak and its continuation in the tail bud without causing apoptosis (van de Ven et al., 2011; Young et al., 2009). Genetic analysis revealed that the axial extension defects of these mutants could be rescued by either a gain-of-function of Hox genes belonging to the middle part of the Hox clusters, or by expressing an activated form of the Wnt signaling effector Lef1 in the spatiotemporal window of Cdx expression (Young et al., 2009). The latter information and subsequent grafting experiments of the region harboring stem cell-like axial progenitors for trunk and tail tissues from *Cdx2/4* mutants into wild-type recipients revealed that the Cdx mutations disable the surrounding niche of these progenitors rather than the progenitors themselves (Bialecka et al., 2010). So far, the impact of ablating all three Cdx genes had not been tested. Cdx genes start to be transcribed at E7.2 in the posterior primitive streak. In order to study embryogenesis in the total absence of Cdx activity from early on in the epiblast, we generated mouse embryos totally deprived of Cdx expression using *Cdx1^{null}* and *Cdx4^{null}* alleles (Subramanian et al., 1995; van Nes et al., 2006), and a *Cdx2* conditional allele (Stringer et al., 2012), in combination with the epiblast-specific *Sox2Cre*. We show here, using mouse embryos in which the three Cdx genes are inactivated, that the realm of action of Cdx encompasses and is restricted to the entire trunk and tail sections of the axis. Ablation of all three Cdx genes causes agenesis of the axial domain posterior to the occipital region, involving the three germ layers. The key role of Fgf signaling in axial elongation was demonstrated by the observation that Fgf restores tissue emergence and gene expression in the embryonic growth zone of Cdx mutants in whole embryo cultures.

Results

Absence of Cdx prevents the generation of trunk and tail tissues during embryogenesis. Cdx triple null mutants were generated with mice carrying null alleles for *Cdx1*, *Cdx2* and *Cdx4*, and a conditional allele of *Cdx2* (Stringer et al., 2012) (T. Young, PhD thesis, Utrecht University, 2009), in combination with a *Sox2Cre* transgene (Hayashi et al., 2002) allowing *Cdx2* inactivation in the inner cell mass-derived embryonic tissues. Following this strategy, the epiblast of the triple mutant is totally deprived of Cdx activity from the earliest stage on, and the embryo proper is absolutely *Cdx^{null}*. Triple Cdx mutant embryos were recovered at the expected Mendelian frequency, but their generation required intensive efforts because of low breeding performance of *Cdx1^{-/-} Cdx2^{+/-} Sox2Cre* males used in the final cross (see Methods). We analyzed 52 *Cdx^{null}* triple embryos, 21 embryos with a genotype *Cdx1^{-/-} Cdx2^{-/-} Cd4^{+/-}* (indistinguishable from the *Cdx^{null}* triple mutants) and a larger number of *Cdx2^{null}* mutants and wild-type controls.

Cdx triple mutant (referred to as *Cdx^{null}* from here on) embryos at E7.5 are indistinguishable from wild-type embryos (Fig. S1A,B), except for the fact that their allantois fails to grow, as is the case in *Cdx2^{null}* embryos (Chawengsaksophak et al., 2004; van de Ven et al., 2011). Therefore, they do not survive beyond E10.5 because they never establish a placental labyrinth. Development seems to have arrested earlier than E10.5, as they are growth retarded at this stage in comparison with controls (Fig. S1E,F). *Cdx^{null}* mutants were severely posteriorly truncated, and the axial level of the last tissues generated was anterior to the forelimb buds (Fig. S1C-F). In addition, they exhibited an open neural tube, a condition that was also observed in the absence of *Cdx1* and *Cdx2* (Savory et al., 2011). The *Cdx^{null}* embryos generate a maximum of five somites. At E8.5, 25 out of 25 mutants had five somites instead of the eight to ten generated by control E8.5 littermates. At E9.5, seven out of eight mutants had five somites whereas age-matched controls had 22 to 25 somites (one mutant generating a small sixth somite). *Mox1* (*Meox1* – Mouse Genome Informatics), a marker of differentiated somites, was expressed in the paraxial mesoderm and confirmed the presence of five somites in the *Cdx^{null}* embryos (Fig. 1A,B). These somites were correctly patterned along their anteroposterior (A-P) axis, as revealed by *UncX4.1* (*Uncx* – Mouse Genome Informatics) expression, which identifies the posterior somitic compartments (Mansouri et al., 1997) in both

2

mutants and controls (Fig. 1C-F). *Mesp2*, which normally marks the anterior presomitic mesoderm (PSM), was not expressed in the mutant embryos (Fig. S1G,H). We conclude that *Cdx^{null}* mutants arrest their axial elongation after the occipital somites have been generated.
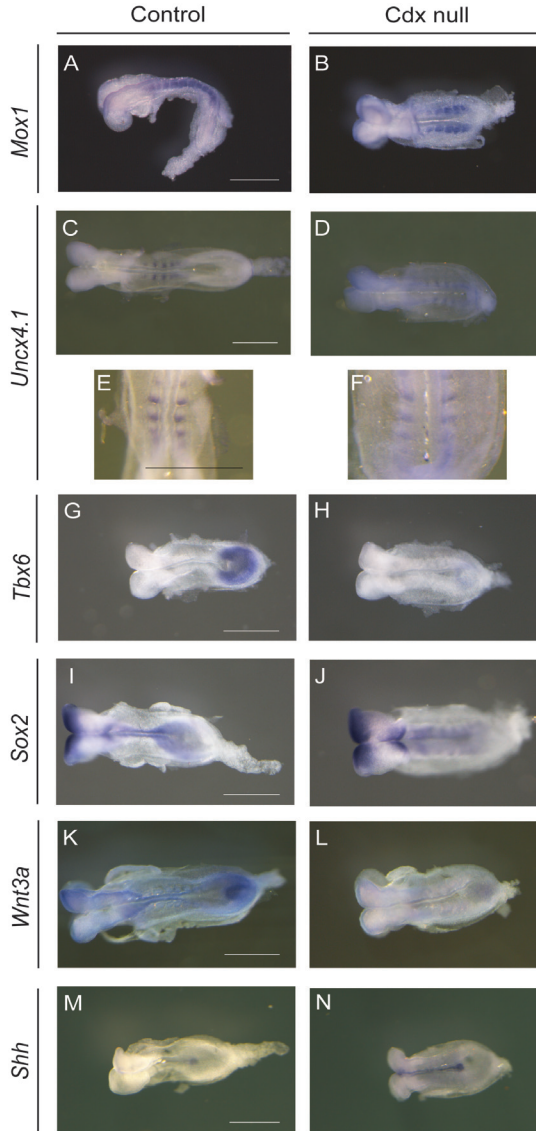

Figure 1. *Cdx^{null}* mutants make occipital somites and neural tissues but fail to generate more posterior tissues. (A-N) Expression of different markers in E8.5 *Cdx^{null}* embryos. (A,B) *Mox1* in a control (A) and a *Cdx^{null}* (B) embryo. (C-F) *UncX4.1* in a wild-type (C and E, 7 somites) and *Cdx^{null}* mutant (D and F, 5 somites). E and F are close ups of C and D. (G,H) *Tbx6* in a control (G, 6 somites) and *Cdx^{null}* mutant (H, 5-somites). (I,J) *Sox2* in a control (I, 6 somites) and *Cdx^{null}* mutant (J, 5 somites). (K,L) *Wnt3a* in a control (K, 9 somites) and *Cdx^{null}* mutant (L, 5/6 somites). (M,N) *Shh* in a wild-type (M, 5 somites) and *Cdx^{null}* mutant (N, 4 somites). Anterior is to the left in A-D and G-N, and to the top in E,F. Scale bars: 0.5 mm. See also Fig. S1.

Anterior tissues are generated in early gastrulating *Cdx^null* embryos but progenitor cells for trunk and tail fail to be maintained. E8.5 *Cdx^null* embryos and age-matched controls were subjected to in situ hybridization to detect the expression of genes marking recent mesoderm and neurectoderm generated from the posterior growth zone. *Tbx6*, a marker of the PSM, was hardly expressed in the posterior part of *Cdx^null* embryos, whereas transcripts were present in the most recently generated paraxial mesoderm in the controls (Fig. 1G,H), suggesting an arrest of mesoderm generation in the mutant. Posterior expression of *Sox2*, marking the neurectoderm, was lower in *Cdx^null* embryos than in controls (Fig. 1I,J). The posterior growth zone of *Cdx^null* mutants thus severely loses its activity in generating nascent mesoderm and neurectoderm. *Wnt3a* expression is also considerably lower in the growth zone of *Cdx^null* mutants versus controls (Fig. 1K,L).

The notochord of *Cdx^null* mutants expressed *Shh* (Fig. 1M,N) and *T Brachyury* (Fig. 2E,F). The posterior end of the notochord revealed by these two markers had a widened appearance, recognized as tubular by examination of transverse sections, stained for RNA and protein detection of *T Brachyury* (Fig. 2F,L,N compared with 2E,K,M). The notochord never expresses Cdx genes and should not be directly affected by the loss of Cdx expression. The tubular end of the notochord is reminiscent of the same feature in some mammalian embryos that develop as flat disks (C. Viebahn, personal communication) (Haldiman and Gier, 1981), and might thus result from the fact that the *Cdx^null* embryos are much flatter than their controls owing to their severe posterior truncation. The notochord of *Cdx^null* mutants at more anterior levels does not show this tubular feature (Fig. 2P) being comparable to the control (Fig. 2O). A striking feature in *Cdx^null* mutants is the absence of *T* expression in the primitive streak region posterior to the notochord end at E8.5, whereas the gene is strongly expressed in the streak and in adjacent tissues in age-matched controls (Fig. 2F compared with 2E). Investigations in earlier, head fold stage (E7.5) embryos revealed that their primitive streak region expresses *T* and is indistinguishable from that in age-matched controls (Fig. 2A-D). These observations strongly suggest that the progenitors for embryonic axial tissues along the primitive streak at E7.5 normally generate anterior mesoderm in *Cdx^null* mutants, whereas they fail to do so after five somites have been generated. Serial transverse sections through E8.5 embryos hybridized with a *T* probe show that whereas *T*-positive nascent mesoderm is emerging from the *T*-positive primitive streak in

the control, this is not the case in the mutant (Fig. 2H,J versus 2G,I). This suggests that no new mesoderm has emerged from the inactive primitive streak at E8.5 (Fig. 2H,J).
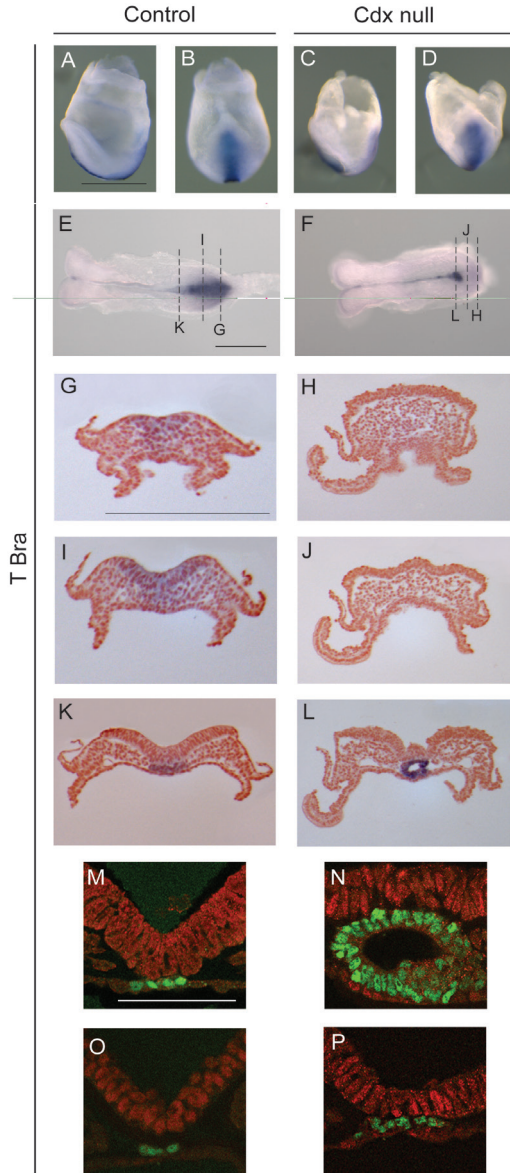

Figure 2. Early generation of nascent mesoderm takes place but ends at 5-somite stage because of loss of primitive streak activity. (A-L) Expression of *T* in E7.5 wild-types (A,B, lateral and posterior views) and *Cdx^null* mutant (C, D, lateral and posterior view), and in E8.5 wild-type (E, dorsal view, 4 somites) and *Cdx^null* mutant (F, dorsal view, 4 somites). (G-L), transversal sections of E and F. (M-P). Immunofluorescent staining of transversal sections of a E8.5 embryos wild-type (M,O) and *Cdx^null* (N,P) at the level of the posteriormost notochord (M,N) and at more anterior levels (O,P). N and P are from the same embryo, whereas M and O are from 2 different control embryos. Anterior is to the left in A,C,E,F; dorsal is up in G-P. Scale bars: 0.5 mm.

2

Anterior Hox genes are well induced in the primitive streak and correctly expressed in anterior tissues whereas more posterior Hox genes are not expressed. The expression of anterior Hox genes was similarly initiated in *Cdx^{null}* mutants and controls. Hox genes are initially transcriptionally induced in the posterior primitive streak at the late mid-streak stage (E7.0-7.2), and their expression domains spread anteriorwards along the streak and adjacent tissues, in a way that is temporally collinear with the position of the genes in their cluster (Deschamps and Wijgerde, 1993; Forlani et al., 2003; Gaunt et al., 1986; Iimura and Pourquie, 2006). These expression domains then extend further anteriorly in embryonic tissues, eventually reaching gene-specific rostral boundaries. *Hoxb1* is first expressed in the posterior streak at E7.2 and its expression domain has reached the anterior part of the streak by the head fold stage (E7.5) (Forlani et al., 2003) in *Cdx^{null}* mutants and in controls (Fig. 3A,B). At somite stages, the anterior expression pattern of *Hoxb1* in the mutant and control is the same, as shown by the restricted expression domain at the level of rhombomere (r) 4 (Fig. 3C,D).

However, a reduction of the expression level of this gene in posterior tissues was observed in the mutant, in the primitive streak area reported above to be losing its activity (Fig. 3D). The expression of more posterior Hox genes was analyzed in *Cdx^{null}* embryos and controls. *Hoxb4*, the rostral expression domain of which normally reaches the posterior hindbrain and somite 5/6 in the mesoderm (Gould et al., 1998), had an expression boundary caudal to the level of the fifth somite in *Cdx^{null}* embryos, and its expression decayed posteriorly (Fig. 3E,F). E8.5 *Cdx^{null}* embryos did not express *Hoxa5* and *Hoxb8*, normally expressed in trunk tissues (rostral limits in posterior hindbrain and somite 6/7 for *Hoxa5*, and below somite 5 in the neural tube and somite 11 in the paraxial mesoderm for *Hoxb8*) (Larochelle et al., 1999; van den Akker et al., 2002; Young et al., 2009) (Fig. 3G,H; Fig. S2). The same holds true for *Hoxa9* and for *Hoxb9*, two more 5' and later-initiated Hox genes that are expressed at trunk levels (Fig. 3I-L; Fig. S2). We conclude that the initial transcription of the first Hox gene of the cluster takes place correctly in the primitive streak of *Cdx^{null}* embryos at early stages. The transcription domain of this 3', early Hox gene normally expands anteriorly together with the emerging tissue that will form the rhombencephalic and occipital structures. The posterior part of the expression of these 3' genes later on fades away as the growth zone becomes inactive at the 5-somite stage, and more 5' (posterior) Hox genes are not expressed.
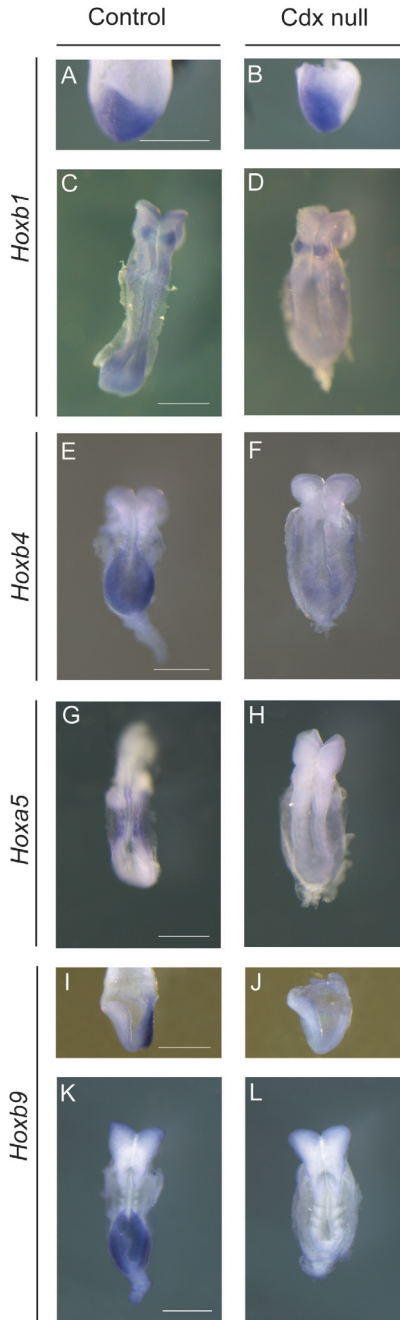
2

Control   Cdx null

Figure 3. Expression of Hox genes in control and *Cdxnull* embryos. (A-D) Whole mount in situ hybridization with a probe for *Hoxb1* on control (A, C) and *Cdxnull* (B, D) embryos at E7.5 (headfold stage, posterior view, A,B) and at E8.5 (C, 10 somites, and D, 5 somites). (E,F) Expression of *Hoxb4* in E8.5 control (E, 5 somites) and *Cdxnull* embryo (F, 5 somites). (G, H) expression of *Hoxa5* in E8.5 control (G, 9 somites) and *Cdxnull* mutant (H, 5 somites). (I –L) Expression of *Hoxb9* in 1- somite stage control (I) and *Cdxnull* embryos (J), and in E8.5 control (K, 7 somites) and *Cdxnull* embryos (L, 5 somites). Scale bars: 0.5 mm. See also Fig. S2.

Fgf is key to Cdx-dependent tissue generation from axial progenitors and rescues the posterior truncation in *Cdx2^null* mutants. Cdx factors have been suggested to regulate the gene encoding the retinoic acid (RA)-degrading enzyme *Cyp26a1* directly and positively (Forlani et al., 2003; Savory et al., 2009; Young et al., 2009). *Cyp26a1* was not transcribed at all in early somite *Cdx^null* mutants (Fig. 4A,B), at a stage when this gene is normally expressed posteriorly and allows the growth zone to clear the RA diffusing from the somites. E8.5 *Cdx^null* embryos have stopped generating PSM tissue beyond the last formed somite, and they express the RA-synthesizing enzyme Raldh2 (Aldh1a2 – Mouse Genome Informatics) at high level down to the growth zone, whereas *Raldh2* expression in wild-type is restricted to the somites and anterior PSM (Delfini et al., 2005), at a distance from the anterior streak (Fig. 4C-H). *Cdx^null* mutants, thus, unlike controls, synthesize RA within their growth zone at E8.5. Given the balanced antagonism between the RA and Fgf pathways during posterior embryonic morphogenesis (Diez del Corral and Storey, 2004; Ribes et al., 2009), we set out to test the involvement of the Fgf signaling pathway in causing the posterior axial truncations of *Cdx^null* mutants. Fgf signaling activity, revealed by *Spry4* expression (Naiche et al., 2011), was completely lost in the posterior part of E8.5 *Cdx^null* mouse embryos (Fig. 4I,J).

We designed whole embryo culture experiments to challenge the crucial involvement of Fgf loss in the posterior truncation phenotype of Cdx mutants. Envisaging rescue attempts on early embryos from the crosses used to generate *Cdx^null* embryos was unrealistic given the extremely low yield of these mutants, which cannot be genotyped before the culture. We therefore turned to Cdx mutants of the allelic series that are less severely impaired in their development, and easier to generate. *Cdx2^null* embryos arrest their development at E10.5 and never have more than 17 somites, regardless of whether they are analyzed at E9.5 or E10.5 (Chawengsaksophak et al., 2004; Chawengsaksophak et al., 1997; van de Ven et al., 2011), whereas controls typically have about 25 somites at E9.5, and 35 somites at E10.5 (average of many experiments) (Kaufman, 1995). We cultured whole E7.5 (presomite)/E8.0 (early somite) *Cdx2^null* mutant and control embryos for the same period of two days *in vitro*, in the presence or in the absence of added recombinant Fgf8 (Fgf8 isoform b). We scored the somite number that these embryos generated during the culture period. Fgf8 exposure was found to rescue the deficit in axial tissue growth of the mutants significantly
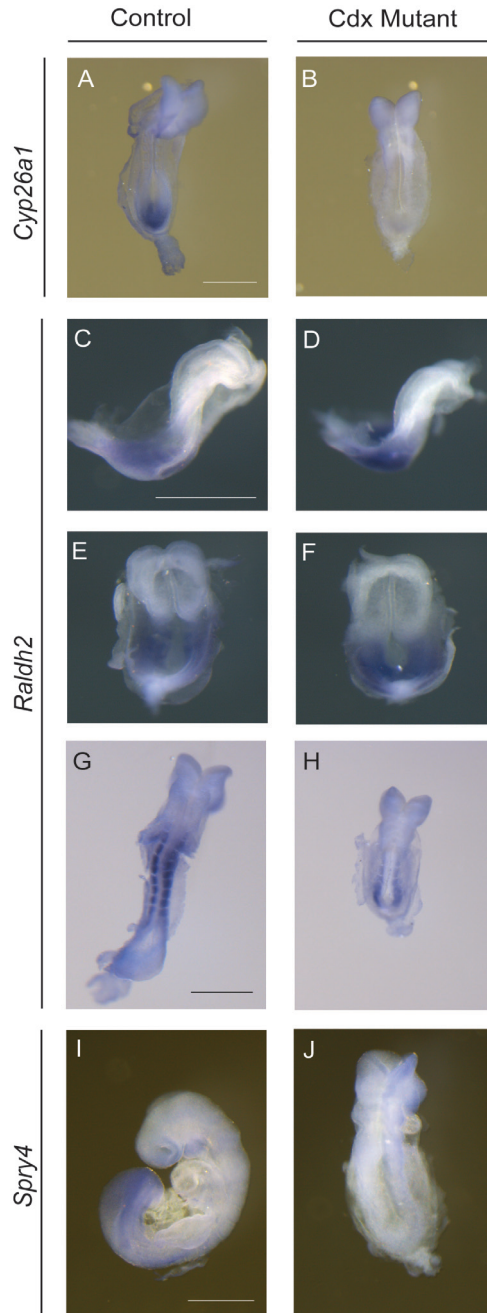
2

2

Figure 4. Fgf signaling is lost in the posterior growth zone of *Cdx^null* mutants. (A, B) Expression of *Cyp26a1* in E8.5 wild-type (A, 8 somites) and *Cdx^null* mutant embryos (B, 5 somites). (C,F) Expression of *Raldh2* in 2-somite embryos wild-type (C,E, lateral and dorsal views, respectively) and *Cdx^null* mutant (D,F, lateral and dorsal views, respectively). (G,H) *Raldh2* expression in E8.5 control (G, 10 somite) and *Cdx^null* (H, 4 somite). (I,J) Expression of the Fgf signaling target *Spry4* in E8.5 wild-type (I, 11 somites) and absence of expression in *Cdx^null* mutant (J, 5 somite). Anterior is to the top in A,B,E,F, and G-J, and to the right in C,D. Scale bars: 0.5 mm.

(Fig. 5F compared with 5D). *Cdx2* mutant embryos cultured with Fgf8 (n=7) made on average 23 somites during the culture, whereas they only made 16 somites without supplemented Fgf8 (n=5) (Fig. 5K). The rescue of the posterior truncation of *Cdx2null* embryos by Fgf8 was not complete as the PSM remained shorter in the Fgf8-rescued mutants than in controls. Cultured embryos of the four series (controls and mutants cultured with and without Fgf8) were subjected to in situ hybridization with a *Mox1* probe (Fig. 5G-J) and their somites counted again. This confirmed the rescue of the posterior truncation of the *Cdx2* mutants by Fgf8 (Fig. 5K). The restoration of posterior axial extension of *Cdx2* mutant embryos by Fgf8 was also documented by measuring the axial length beyond the forelimb buds in stage-matched mutants cultured with (n=4) and without (n=4) Fgf8. The axial portion added to the embryos posterior to the forelimb bud was significantly longer for the mutant embryos cultured with added Fgf8 (median value 472 mm) than for mutants cultured in the same conditions but without Fgf8 (median value 320 mm) (p=0.002) (data not shown). A significant rescue of axial extension is thus taking place when the mutants are grown in the presence of exogenous Fgf8. Importantly, exogenous Fgf8 allowed the *Cdx2* mutant embryos to generate seven somites more than they ever generate in vivo (Fig. 5K). Fgf8-rescued *Cdx2* mutants also by re-expressing *Cyp26a1* at their posterior end similarly to wild-type embryos (Fig. S3). The restoration of axial elongation and posterior gene expression by supplemented Fgf suggests that Fgf signaling reactivates the growth zone in Cdx mutants. We conclude that decreased Fgf signaling in the posterior growth zone in Cdx mutants is crucially involved in causing the exhaustion of tissue emergence from this growth zone. The data are summarized in Fig. 6 and Fig. S4.
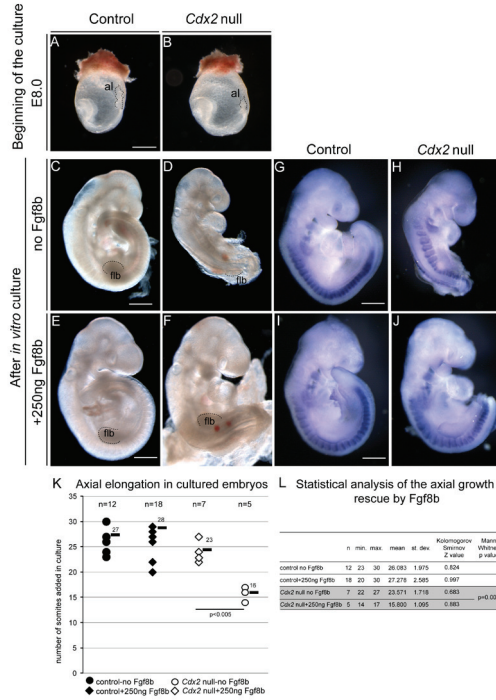
2

2

Figure 5. Addition of Fgf8 to the whole embryo culture medium of *Cdx2* null embryos rescues their axial elongation. (A,B) E 8.0 (early somite) embryos at the start of the culture (A, wild-type, B, *Cdx2* null). (C–F) Embryos after their culture for the same period without (C,D) or with (E,F) Fgf8 added to the culture medium. C,E are controls, and D,F are *Cdx2null* mutants. (G-J) *Mox1* expression in another set of *Cdx2null* mutants (H,J) and controls (G,I) that have been cultured for the same period with (I,J) and without Fgf8 (G,H). (K) Comparison of posterior elongation of *Cdx2null* and control embryos cultured without and with Fgf8. Y axis, total number of somites generated in culture; median values, bars on the graph; n, number of embryos; several experimental data are superimposed as one symbol in the graph as they had the same value; p, statistical significance (L). Statistical analysis of the axial growth rescue of Cdx mutants by Fgf8 using the Mann Whitney test. al, allantois; flb, forelimb bud. Anterior is to the right in A,B and up in C-J. Scale bars: 0.5 mm. See also Fig. S3.
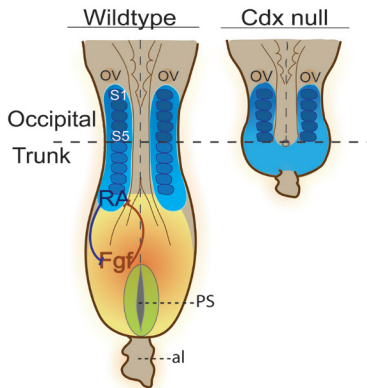

Figure 6. Schematic representation of the loss of Fgf signaling and posterior growth zone in Cdxnull mutant embryos. Schematic dorsal view of a E8.5 wild-type (lower left) and *Cdxnull* mutant (lower right) embryos. Domains of RA synthesis are in blue and Fgf signaling in orange to yellow; posterior growth zone is in green. PS, primitive streak; al, allantois. Anterior is up in the lower panels.

Discussion

Cdx genes are obligatory players in the emergence of the entire trunk and tail. They implement the dichotomy between the pre- and post-occipital tissues. It is known that head tissues are generated early during vertebrate embryogenesis whereas the rest of the axial structures are added subsequently from the posterior growth zone. The absence of active Cdx genes does not affect the generation of head and occipital tissues (the 'extended head'), but it prevents trunk and tail tissues to be formed as a result of the depletion of axial progenitor populations from the growth zone. Examination of *T* expression in the *Cdx^null^* embryos confirms that early nascent mesoderm emerges normally but stops being generated after five somites have formed. The Cdx-dependence of axial elongation is confined to the post-occipital tissues.

These data, together with recent research in lower bilaterians, support the hypothesis that the role of Cdx genes in 'post-head' body extension is ancestral and exists in arthropods with short germ band development. *Cdx/caudal* must have been involved in generating post-head axial structures since before protostomes and deuterostomes diverged from each other, as witnessed by the obligatory role of Cdx in generation of post-head tissues in the short-germ band beetle *Tribolium castaneum*, the crustacean *Artemia franciscana* (Copf et al., 2004) and the intermediate-germ band cricket *Gryllus bimaculatus* (Shinmyo et al., 2005). Caudal is therefore an ancestral master organizer of post-head morphogenesis. Its role has been conserved in all animals that sequentially add their trunk and tail structures from a posterior growth zone, and has been reduced in the derived higher dipterans, such as *Drosophila melanogaster* (Olesnicky et al., 2006).

Although *Drosophila caudal* does not directly regulate Hox genes, regulatory interactions are known to occur between mouse Cdx and Hox genes (Young et al., 2009). We show here that Cdx genes are clearly not required for the transcriptional activation of the early (3') genes of the Hox clusters. Transcriptional initiation of 3' Hox genes in the primitive streak is not affected by the absence of Cdx function, and 3' Hox expression in the hindbrain is intact, in agreement with the fact that anterior morphogenesis and signaling are normal in the mutants. In the absence of Cdx activity, no axial tissue emerges after occipital somites have been generated, and therefore

2

2

the later and more 5' Hox genes are not expressed.

Our data in the mouse suggest that Fgf signaling works downstream of Cdx in driving post-occipital tissue emergence. Strikingly, in *Tribolium*, *Tc-Fgf8* is expressed in a region of the posterior growth zone involved in axial elongation, and the Fgf signaling pathway in this insect has been suggested to play a role in posterior mesoderm formation and expansion (Beermann et al., 2011; Beermann and Schroder, 2008). It could therefore be that both Cdx and its downstream Fgf signaling have been evolutionarily conserved in permitting post-head axial extension. The rescuing activity on axial growth of adding Fgf8 during culture of *Cdx2* mutant embryos suggests that Fgfr1 signaling is a main contributing intermediate between Cdx and posterior axial extension. The spectrum of posterior abnormalities of Cdx mutants matches well with the phenotype of *Fgfr1* mutants. The posterior notochord of *Cdx^{null}* embryos is thickened, and so is the notochord in *Fgfr1* mutant embryos. Chimeric embryos generated with *Fgfr1^{null}* embryonic stem cells form ectopic neural structures (Deng et al., 1997), and this defect was observed in partial Cdx mutants as well (van de Ven et al., 2011). *Fgfr1* mutants are posteriorly truncated and exhibit neural tube closure defects. The neural tube of the severely truncated *Fgfr1^{null}* mutants described by Hoch and Soriano (Hoch and Soriano, 2006) remains open along the entire rostrocaudal axis (craniorachischisis), as a consequence of the severe posterior truncation causing a deficit of the tension that normally facilitates closure (Hoch and Soriano, 2006). *Cdx^{null}* embryos are as severely truncated as the *Fgfr1* mutants studied by Hoch and Soriano, suggesting that their lack of neural tube closure might be a consequence of their disrupted Fgfr1 signaling.

Cdx^{null} mutants arrest posterior elongation of mesoderm and neurectoderm, and downregulate both Fgf and canonical Wnt signaling in the growth zone. These data support a crucial role of Cdx-dependent Wnt and Fgf signaling in the control of post-occipital axial growth at the level of the maintenance of the bipotent neuromesodermal progenitors demonstrated in the mouse tailbud (Cambray and Wilson, 2002, 2007; Tzouanacou et al., 2009).

Funding

2

Acknowledgements

Methods

Mice. All mice were in the C57Bl6j/CBA mixed background. *Cdx2* heterozygotes and *Cdx1* and *Cdx4^{null}* mutant mice as well as the protocols to genotype them have been described previously (Chawengsaksophak and Beck, 1996; Subramanian et al., 1995; van Nes et al., 2006). Generation and genotyping of the strain carrying *Cdx2* conditional allele was described by Stringer et al. (Stringer et al., 2012). Epiblast-specific *Cdx1^{null}* mutants were obtained by crossing *Cdx2* floxed homozygotes and *Cdx2$^{+/-}$ Sox2Cre* transgenic mice (Hayashi et al., 2002). *Cdx^{null}* embryos were generated by crossing *Cdx1$^{-/-}$ Cdx2$^{flox/flox}$ Cdx4$^{-/-}$* females with *Cdx1$^{-/-}$ Cdx2$^{+/-}$* males, which carry the *Sox2Cre* transgene. Embryos of the genotype *Cdx1$^{-/-}$Cdx2$^{-/-}$ Cdx4$^{+/-}$* were obtained in the same cross. All experiments using mice were performed in accordance with the institutional and national guidelines and regulations, under control of the Dutch Committee for Animals in Experiments, and under the licenses required in The Netherlands.

Histology and immunohistochemistry. For histological analysis, tissues

were fixed with 4% paraformaldehyde (PFA) overnight at 4°C. Whole mount in situ hybridization of mutant and control embryos was performed according to Young et al. (Young et al., 2009). Embryos were imbedded in plastic (GMA Technovit type 8100) and sectioned at 7 µm. For immunofluorescence staining, 70 µm-thick vibratome sections were made from embryos embedded in 4% low melting point agarose. Antibodies used were anti-Sox2 (polyclonal rabbit anti- mouse Sox2, Millipore, AB5603), and anti-T (polyclonal goat anti-mouse T, Santa Cruz, SC-17743). Counterstaining was with DAPI.

Whole embryo culture. Embryos were cultured for 48 hours as described by Bialecka et al. (Bialecka et al., 2010). Each experiment contained control and Cdx mutant embryos with and without Fgf8. At the end of the culture period embryos were fixed in 4% PFA overnight at 4°C, and photographed. Somites were counted using a Leica MZ16FA microscope with a DFC480 camera. Recombinant Fgf8 (isoform b) was purchased from R&D Systems (423- F8).

Statistical analysis. The Mann-Whitney U test was used to analyze the significance of the difference between the number of somites added, and the difference between the length of axial tissue added beyond the forelimb bud of Cdx mutant embryos cultured for 2 days with or without Fgf8. The Mann-Whitney U test was chosen because the data sets for each genotype were not normally distributed (z values obtained from the Kolmogorov-Smirnov test for each genotype were >0.05).

References

Beermann, A., Pruhs, R., Lutz, R., and Schroder, R. (2011). A context-dependent combination of Wnt receptors controls axis elongation and leg development in a short germ insect. Development *138*, 2793-2805.

Beermann, A., and Schroder, R. (2008). Sites of Fgf signalling and perception during embryogenesis of the beetle Tribolium castaneum. Development genes and evolution *218*, 153-167.

Bialecka, M., Wilson, V., and Deschamps, J. (2010). Cdx mutant axial progenitor cells are rescued by grafting to a wild type environment. Developmental biology *347*, 228-234.

Cambray, N., and Wilson, V. (2002). Axial progenitors with extensive potency are localised to the mouse chordoneural hinge. Development *129*, 4855-4866.

Cambray, N., and Wilson, V. (2007). Two distinct sources for a population of maturing axial progenitors. Development *134*, 2829-2840.

Chawengsaksophak, K., and Beck, F. (1996). Chromosomal localization of cdx2, a murine homologue of the Drosophila gene caudal, to mouse chromosome 5. Genomics *34*, 270-271.

Chawengsaksophak, K., de Graaff, W., Rossant, J., Deschamps, J., and Beck, F. (2004). Cdx2 is essential for axial elongation in mouse development. Proceedings of the National Academy of Sciences of the United States of America *101*, 7641-7645.

Chawengsaksophak, K., James, R., Hammond, V.E., Kontgen, F., and Beck, F. (1997). Homeosis and intestinal tumours in Cdx2 mutant mice. Nature *386*, 84-87.

Copf, T., Schroder, R., and Averof, M. (2004). Ancestral role of caudal genes in axis elongation and segmentation. Proceedings of the National Academy of Sciences of the United States of America *101*, 17711-17715.

Delfini, M.C., Dubrulle, J., Malapert, P., Chal, J., and Pourquie, O. (2005). Control of the segmentation process by graded MAPK/ERK activation in the chick embryo. Proceedings of the National Academy of Sciences of the United States of America *102*, 11343-11348.

Deng, C., Bedford, M., Li, C., Xu, X., Yang, X., Dunmore, J., and Leder, P. (1997). Fibroblast growth factor receptor-1 (FGFR-1) is essential for normal neural tube and limb development. Developmental biology *185*, 42-54.

Deschamps, J., and Wijgerde, M. (1993). Two phases in the establishment of HOX expression domains. Developmental biology *156*, 473-480.

Diez del Corral, R., and Storey, K.G. (2004). Opposing FGF and retinoid pathways: a signalling switch that controls differentiation and patterning onset in the extending vertebrate body axis. BioEssays : news and reviews in molecular, cellular and developmental biology *26*, 857-869.

2

2

Forlani, S., Lawson, K.A., and Deschamps, J. (2003). Acquisition of Hox codes during gastrulation and axial elongation in the mouse embryo. Development *130*, 3807-3819.

Gaunt, S.J., Miller, J.R., Powell, D.J., and Duboule, D. (1986). Homoeobox gene expression in mouse embryos varies with position by the primitive streak stage. Nature *324*, 662-664.

Gould, A., Itasaki, N., and Krumlauf, R. (1998). Initiation of rhombomeric Hoxb4 expression requires induction by somites and a retinoid pathway. Neuron *21*, 39-51.

Haldiman, J.T., and Gier, H.T. (1981). Bovine notochord origin and development. Anatomia, histologia, embryologia *10*, 1-14.

Hayashi, S., Lewis, P., Pevny, L., and McMahon, A.P. (2002). Efficient gene modulation in mouse epiblast using a Sox2Cre transgenic mouse strain. Mechanisms of development *119 Suppl 1*, S97-S101.

Hoch, R.V., and Soriano, P. (2006). Context-specific requirements for Fgfr1 signaling through Frs2 and Frs3 during mouse development. Development *133*, 663-673.

Iimura, T., and Pourquie, O. (2006). Collinear activation of Hoxb genes during gastrulation is linked to mesoderm cell ingression. Nature *442*, 568-571.

Kaufman, M.H. (1995). The Atlas of Mouse Development. London: Academic Press.

Kinder, S.J., Tsang, T.E., Quinlan, G.A., Hadjantonakis, A.K., Nagy, A., and Tam, P.P. (1999). The orderly allocation of mesodermal cells to the extraembryonic structures and the anteroposterior axis during gastrulation of the mouse embryo. Development *126*, 4691-4701.

Larochelle, C., Tremblay, M., Bernier, D., Aubin, J., and Jeannotte, L. (1999). Multiple cis-acting regulatory regions are required for restricted spatio-temporal Hoxa5 gene expression. Developmental dynamics : an official publication of the American Association of Anatomists *214*, 127-140.

Lawson, K.A., Meneses, J.J., and Pedersen, R.A. (1991). Clonal analysis of

epiblast fate during germ layer formation in the mouse embryo. Development *113*, 891-911.

Mansouri, A., Yokota, Y., Wehr, R., Copeland, N.G., Jenkins, N.A., and Gruss, P. (1997). Paired-related murine homeobox gene expressed in the developing sclerotome, kidney, and nervous system. Developmental dynamics : an official publication of the American Association of Anatomists *210*, 53-65.

Naiche, L.A., Holder, N., and Lewandoski, M. (2011). FGF4 and FGF8 comprise the wavefront activity that controls somitogenesis. Proceedings of the National Academy of Sciences of the United States of America *108*, 4018-4023.

Olesnicky, E.C., Brent, A.E., Tonnes, L., Walker, M., Pultz, M.A., Leaf, D., and Desplan, C. (2006). A caudal mRNA gradient controls posterior development in the wasp Nasonia. Development *133*, 3973-3982.

Ribes, V., Le Roux, I., Rhinn, M., Schuhbaur, B., and Dolle, P. (2009). Early mouse caudal development relies on crosstalk between retinoic acid, Shh and Fgf signalling pathways. Development *136*, 665-676.

Savory, J.G., Bouchard, N., Pierre, V., Rijli, F.M., De Repentigny, Y., Kothary, R., and Lohnes, D. (2009). Cdx2 regulation of posterior development through non-Hox targets. Development *136*, 4099-4110.

Savory, J.G., Mansfield, M., Rijli, F.M., and Lohnes, D. (2011). Cdx mediates neural tube closure through transcriptional regulation of the planar cell polarity gene Ptk7. Development *138*, 1361-1370.

Shinmyo, Y., Mito, T., Matsushita, T., Sarashina, I., Miyawaki, K., Ohuchi, H., and Noji, S. (2005). caudal is required for gnathal and thoracic patterning and for posterior elongation in the intermediate-germband cricket Gryllus bimaculatus. Mechanisms of development *122*, 231-239.

Stringer, E.J., Duluc, I., Saandi, T., Davidson, I., Bialecka, M., Sato, T., Barker, N., Clevers, H., Pritchard, C.A., Winton, D.J.*, et al.* (2012). Cdx2 determines the fate of postnatal intestinal endoderm. Development *139*, 465-474.

Subramanian, V., Meyer, B.I., and Gruss, P. (1995). Disruption of the murine homeobox gene Cdx1 affects axial skeletal identities by altering the

mesodermal expression domains of Hox genes. Cell *83*, 641-653.

Tam, P.P., and Beddington, R.S. (1987). The formation of mesodermal tissues in the mouse embryo during gastrulation and early organogenesis. Development *99*, 109-126.

Tzouanacou, E., Wegener, A., Wymeersch, F.J., Wilson, V., and Nicolas, J.F. (2009). Redefining the progression of lineage segregations during mammalian embryogenesis by clonal analysis. Developmental cell *17*, 365-376.

van de Ven, C., Bialecka, M., Neijts, R., Young, T., Rowland, J.E., Stringer, E.J., Van Rooijen, C., Meijlink, F., Novoa, A., Freund, J.N.*, et al.* (2011). Concerted involvement of Cdx/Hox genes and Wnt signaling in morphogenesis of the caudal neural tube and cloacal derivatives from the posterior growth zone. Development *138*, 3451-3462.

van den Akker, E., Forlani, S., Chawengsaksophak, K., de Graaff, W., Beck, F., Meyer, B.I., and Deschamps, J. (2002). Cdx1 and Cdx2 have overlapping functions in anteroposterior patterning and posterior axis elongation. Development *129*, 2181-2193.

van Nes, J., de Graaff, W., Lebrin, F., Gerhard, M., Beck, F., and Deschamps, J. (2006). The Cdx4 mutation affects axial development and reveals an essential role of Cdx genes in the ontogenesis of the placental labyrinth in mice. Development *133*, 419-428.

Wilson, V., Olivera-Martinez, I., and Storey, K.G. (2009). Stem cells, signals and vertebrate body axis extension. Development *136*, 1591-1604.

Young, T., Rowland, J.E., van de Ven, C., Bialecka, M., Novoa, A., Carapuco, M., van Nes, J., de Graaff, W., Duluc, I., Freund, J.N.*, et al.* (2009). Cdx and Hox genes differentially regulate posterior axial growth in mammalian embryos. Developmental cell *17*, 516-526.

Supplementary Materials

Figure S1. Phenotype of *Cdx^null^* embryos and expression of the nascent somite marker *Mesp2*. Control (A,C,E) and *Cdx^null^* embryos (B,D and F) at E7.5 (headfold stage, A,B), E8.5 (C, 10 somites, and D, 5 somites but similar stage as the control as seen from head developmental aspect), and at E10.5 (E,F). (G,H) Expression of the nascent somite marker *Mesp2* in E8.5 wild-type (G) and *Cdx^null^* (H) embryo. The wild-type is photographed in a way that the two Mesp2 expression stripes are visible (white arrows); they correspond to one of the phases of somitogenesis when one stripe is still visible once the following comes up. The *Cdx^null^* embryo did not exhibit any expression of *Mesp2* in the PSM. Scale bars: 0.5 mm.
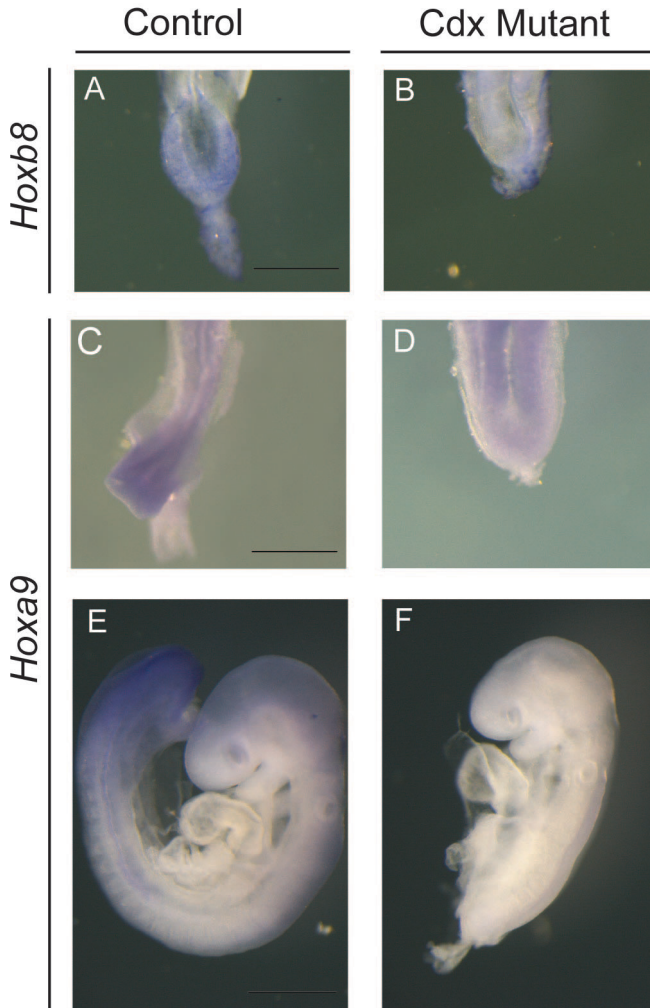
2

Figure S2. Expression of *Hoxb8* and *Hoxa9* in *Cdx^{null}* embryos and controls. (A,B) Expression of *Hoxb8* in a E8.5 wild-type (A) and *Cdx^{null}* mutant (B) embryo. (C-F) Expression of *Hoxa9* in E8.5 (C,D) and E9.5 (E,F) wild-type (C,E) and *Cdx^{null}* (D,F) embryos. Scale bars: 0.5 mm.
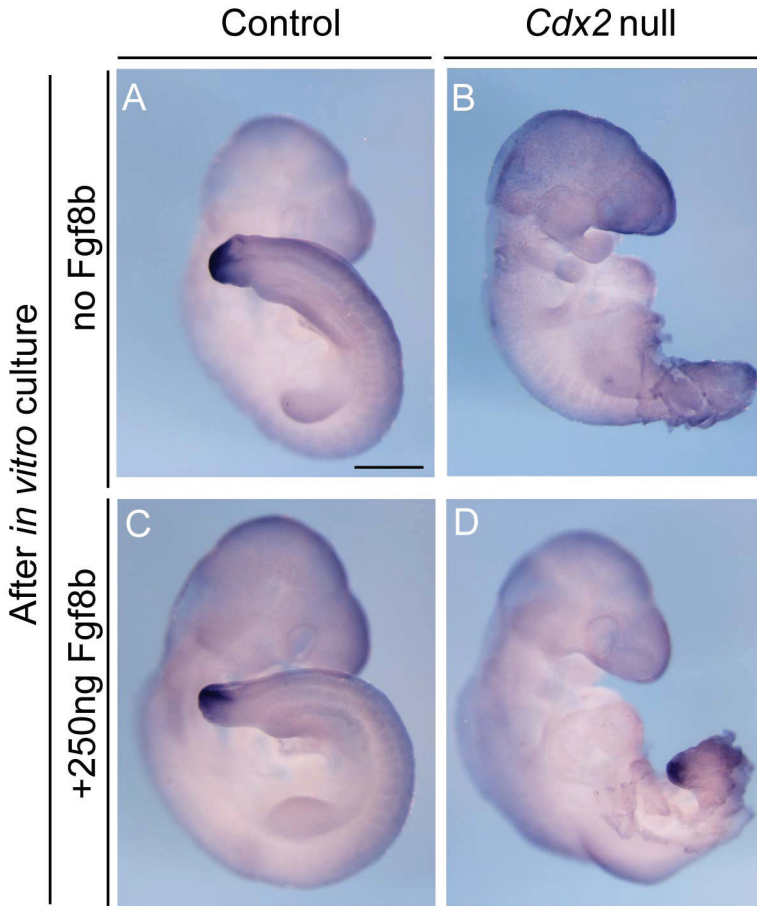
Figure S3. *Cdx2^null* embryos rescued by Fgf8 re-express posterior genes in their growth zone. Expression of *Cyp26a1* in *Cdx2^null* mutants (B,D) and controls (A,C) that have been cultured for the same 2-day period with (C,D) and without (A,B) Fgf8b. The posterior axis of the Cdx mutant embryo cultured with Fgf8 is curled and is therefore longer than it may seem.
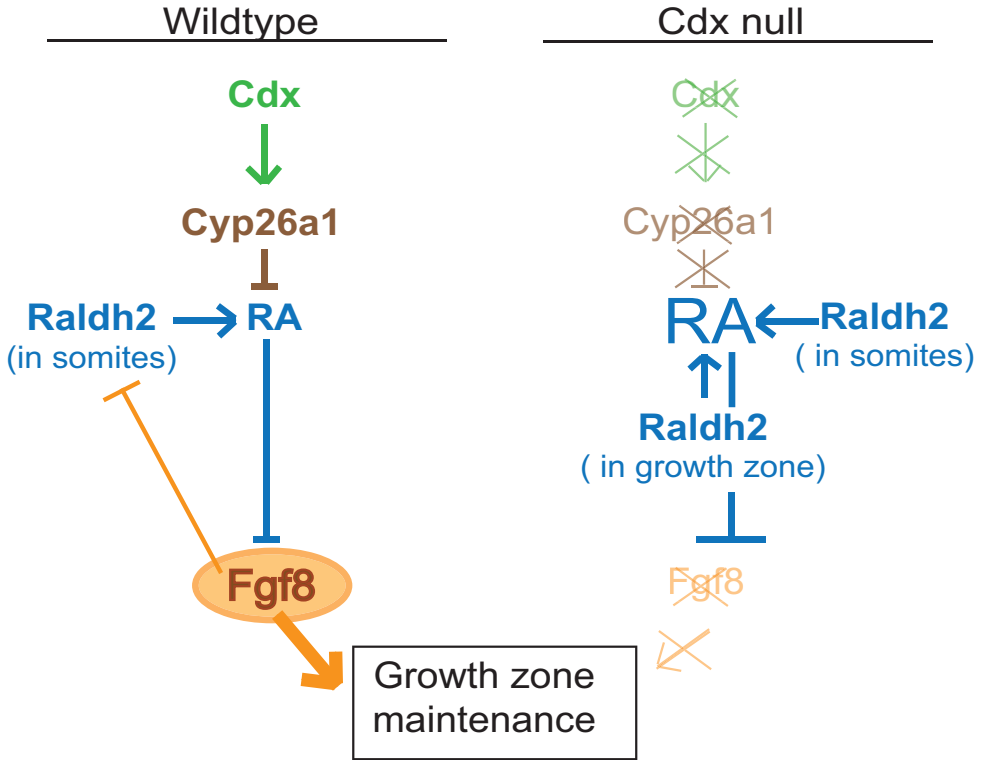
2

Posterior growth zone

Figure S4. Schematic representation of the signaling cascades underlying axial elongation in the posterior growth zone of *Cdx^null* embryos. Genetic interactions downstream of Cdx in the growth zone region of a wild-type (left) and a *Cdx^null* mutant embryo (right). These interactions focus on the role of posterior Fgf8 signaling, absent in the mutant. Not mentioned here is the role of Wnt signaling, shown earlier to play a role in axial extension as well in the mouse (Young et al., 2009).

2

Chapter 3
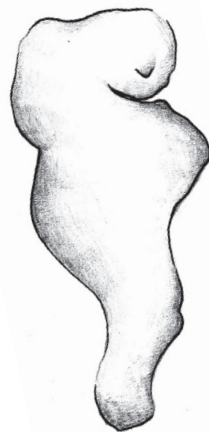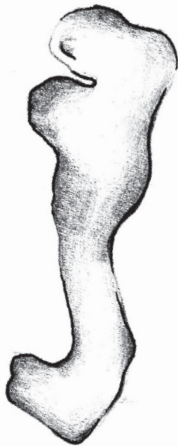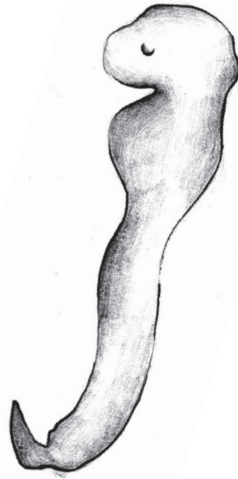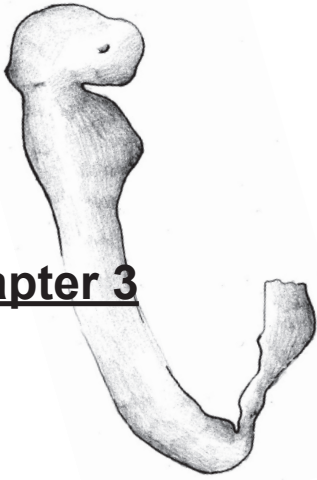
Genetic pathways driving progressive posterior axial elongation in mice: cross-talk between Cdx and T Brachyury

Salvatore Simmini, Roel Neijts, Lennart Kester, Carina van Rooijen, Alexander van Oudenaarden, Jacqueline Deschamps

Hubrecht Institute and UMC Utrecht, Uppsalalaan 8 3584 CT Utrecht, The Netherlands

Abstract

Many aspects of the genetic regulation of posterior axial elongation in vertebrates are still unknown. A number of transcription factors and signaling pathways are involved to sustain progenitors that supply cells for the laying down of the trunk and tail primordia. *Cdx2* and *T Brachyury* code for DNA binding proteins that are crucially required for axial elongation of the embryo. They both work by stimulating the Wnt and the Fgf pathways but whether they interact in another way it is still unclear. In order to better understand how *Cdx2* and *T Brachyury* regulate axial elongation we generated *Cdx2^{null}/T Brachyury^{null}* double mutant mouse embryos and we compared them with *Cdx2^{null}* and *T Brachyury^{null}* single mutants. The simultaneous loss of function of these two genes disrupts axial elongation of the embryo, much more severely than each single mutation. We found confirmation that *Cdx2* and *T Brachyury* cooperate in affecting parallel pathways during mouse development. Analysis of transcriptional profiles of the different mutants suggests that *Cdx2* and *T Brachyury* ynergistically stimulate the Fgf pathway in order to generate the mouse embryonic trunk and tail. We present a model proposing that Cdx mainly ensures the maintenance of self-renewing axial progenitors via activation of Wnt signaling. *T Brachyury* instead would enable nascent mesoderm to ingress in and leave the primitive streak via Fgf signaling. This would ensure a balanced neuroectoderm/mesoderm fate choice of the axial progenitors. Both pathways would interact via a reciprocal regulation of Wnt and Fgf.

Introduction

The genetic regulation of posterior axial elongation in vertebrates has become increasingly better understood during the last decade. Transcription factors and signaling pathways at work in the posterior-most embryonic tissues act to sustain progenitors that supply cells for the different axial tissues of the trunk and tail during the sequential laying down of the anteroposterior axial tissues. Among the progenitors present along the primitive streak, some are generating mesoderm whereas an anterior population consists in bipotent neuromesodermal precursors (Tzouanacou et al., 2009). The latter axial progenitors have received considerable attention as they possess self-renewing properties (Cambray and Wilson, 2002), and might be the core cell population on which differential influences play to modulate the successive steps of axial tissue generation. Mutants in signaling molecules and in transcription factors driving these pathways [Wnt (Takada et al., 1994), Fgf (Boulet and Capecchi, 2012; Olivera-Martinez et al., 2012), Retinoic acid (RA) metabolism (Janesick et al., 2014; Olivera-Martinez et al., 2012), T Brachyury (Dobrovolskaia-Zavadskaia, 1927; Herrmann et al., 1990), Cdx (Chawengsaksophak et al., 2004; van den Akker et al., 2002; van Rooijen et al., 2012)] independently made it clear that axial extension occurs in a succession of windows that each depends on higher and higher dosage of the corresponding effectors. Not only, is it still unclear how this progressive higher dependence of the axial progenitors on signaling pathways is molecularly regulated and imparted to the downstream program of the cell descendants, but the relationship between pathways is still enigmatic.

T Brachyury deficient mice were the very first genetic mutant identified after mutagenesis almost a century ago (Dobrovolskaia-Zavadskaia, 1927). *T Brachyury*^{null} embryos die around E10.5 due to their failure to grow an allantois and their resulting incapacity to generate the chorio-allantoic placenta. Before this stage already, embryonic tissues posterior to the forelimb buds are severely disturbed. A maximum of seven somites are generated, the somites are often misformed and the neural tube at posterior levels is kinked and abnormal. *T Brachyury* is expressed in the early mesoderm and its epiblast progenitors along the primitive streak at gastrulation stages, and in the growth zone of the tailbud subsequently until around E14 (Wilkinson et al., 1990). *T Brachyury* is also strongly expressed in the axial mesoderm-derived notochord, a structure also affected in the

3

T Brachyury[null] mutant embryos. Hypotheses have been proposed that the progressive accumulation of T Brachyury defective cells in the primitive streak disturbs gastrulation and mesoderm production (Beddington et al., 1992b). Rescue of the phenotypic deficiency of *T Brachyury*[null] mutant embryos in chimeras with *T Brachyury* overexpressing cells proved that T Brachyury activity is required at increasing levels during the generation of more and more posterior mesoderm (Beddington et al., 1992a; Wilson and Beddington, 1997). From these *in vivo* experiments, and other work in differentiation of pluripotent cells such as ES cells (Trott and Martinez Arias, 2013; Turner et al., 2014), it appeared that the function of *T Brachyury* during embryogenesis includes a role in mesoderm generation from progenitors in the primitive streak. A function of T Brachyury in the self-renewing neuromesodermal axial progenitors mentioned above was proposed, as T Brachyury is co-expressed with the stem cell marker Sox2 in the particular cell population present in the node-streak border (NSB) and chordo-neural hinge (CNH), shown to contain progenitors for the somitic mesoderm, ventral neural tube and notochord (Cambray and Wilson, 2002). *T Brachyury* would thus be required for the activity of axial stem cells and for mesoderm generation more generally at axial levels posterior to the forelimbs (around somite 7 and more posteriorly).

Cdx genes, have been known to be involved in axial elongation ever since their inactivation in mice gave rise to embryos with a shortened axis (Chawengsaksophak et al., 1997; van den Akker et al., 2002). The three Cdx genes contribute to this function, the main contributor being *Cdx2* (Chawengsaksophak et al., 2004). Recently, generation of mutants totally missing active Cdx genes revealed that they do not impair development of anterior structures but fail to generate any post-occipital tissue (posterior to somite 5) [see Chapter 2 and (van Rooijen et al., 2012)]. Cdx genes are expressed in the primitive streak, in the epiblast along this structure and in the emerging mesoderm at primitive streak stages. This includes the territory harboring the axial stem cells defined above. Cdx genes remain expressed in the three germ layers in the tailbud at subsequent stages until E12.5 for Cdx2. *Cdx2*[null] mutants are impaired in tissue generation posterior to somite 15-17. Unlike *T Brachyury* mutations which predominantly affect mesoderm generation, Cdx deficiencies affect expansion of the three germ layers. Cdx mutant embryos appear to be truncated in their mesoderm, spinal cord and gut endoderm (Chawengsaksophak et al., 2004; Savory et al., 2009).

Cdx2 and *T Brachyury* genes are each required for posterior axis elongation to proceed to completion. They are both known to stimulate the Wnt and the Fgf growth signaling pathways (Casey et al., 1998; Martin and Kimelman, 2008; van Rooijen et al., 2012; Young et al., 2009). So far, the molecular interactions underlying these transcriptional controls of *T Brachyury* and *Cdx2* on the Wnt and Fgf pathways have remained enigmatic. We set out to investigate whether the mutations in *Cdx2* and *T Brachyury* would add their effects on embryonic axial elongation, and to compare the changes in the transcriptional program downstream of these master regulators between *Cdx2^{null}/T Brachyury^{null}* double mutant, and *Cdx2^{null}* and *T Brachyury^{null}* single mutant embryos. Our objective was to gain understanding on the molecular mechanism enabling *Cdx2* and *T Brachyury* to stimulate posterior axial extension, and to reveal whether these mechanisms are independent or interactive.

Results

Cdx2 and *T Brachyury* are co-expressed in the axial progenitor region in the embryonic posterior growth zone. Expression of *T Brachyury* in the posterior part of the E6.2 egg cylinder accompanies primitive streak appearance (Rivera-Perez and Magnuson, 2005). *T Brachyury* is transcribed in the primitive streak at E7.5 and it continues in the tailbud (Fig. 1a) until the end of axial extension by production of new tissues from these structures (E13/E14) (Cambray and Wilson, 2007). Examination of *T Brachyury* expression on cross-sections of E8.0 embryos reveals that it is expressed in the epiblast abutting the streak and in the nascent mesoderm ingressing through the streak. The gene is dowregulated as the mesoderm migrates away from the streak, except in the notochord where it remains highly expressed (Fig. 1b).

Expression of *Cdx2* in the embryo proper begins in the posterior part of the primitive streak at the late streak stage (E7.2). Expression expands rostrally along the streak in epiblast and in nascent mesoderm, though not in the notochord. It remains strong in the presomitic mesoderm (PSM) (Fig. 1a).

T Brachyury shows a more midline-restricted expression than *Cdx2* in the primitive streak area at E8.0 and E8.5 (Fig. 1a). Co-staining of transverse sections of the posterior part of E8.0 embryos with antibodies against T

Brachyury and Cdx2 makes it clear that both proteins are present in the node-streak border (NSB), where the axial progenitors are known to reside (Cambray and Wilson, 2002) (Fig. 1b).

These observations indicate that *T Brachyury* and *Cdx2* are co-expressed where axial tissue expands from, at the time of axial elongation.
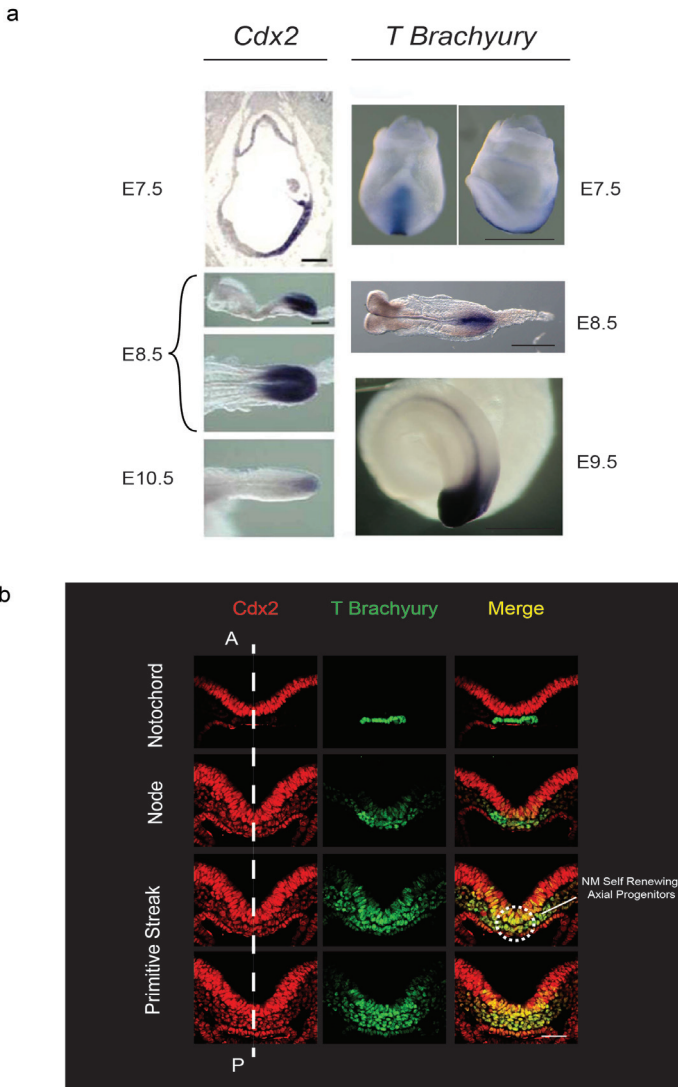

Figure 1. *Cdx2* and *T Brachyury* are co-expressed in the axial progenitor region. a. Expression of *Cdx2* and *T Brachyury* in wt embryos at E7.5, E8.5, E9.5 and E10.5. Scale bars 0.5 mm. **b.** Cdx2 and T Brachyury immunostaining on transversal sections of the posterior region of a wt mouse embryo at E8.0. The axial progenitors reside at the level between the anterior primitive streak and the node (white circle). A, Anterior and P, Posterior. Scale bar 0.05 mm.

Morphogenesis and patterning of anterior trunk tissues occur normally but fail to continue in $Cdx2^{null}$ and $T Brachyury^{null}$ mutants. Both Cdx and T Brachyury gene products are required for axial elongation in a dosage-dependent way. Loss of *Cdx1* and *Cdx4* does not impair axis extension (van den Akker et al., 2002; van Nes et al., 2006). $Cdx2^{het}$ mutants have a slightly shorter tail (Chawengsaksophak et al., 1997). An allelic series of Cdx mutants was generated (Fig. 2a). Compound mutants $Cdx2^{het}/Cdx4^{null}$ are truncated at sacral levels (van Nes et al., 2006), whereas mutant embryos missing the 2 alleles of *Cdx2* are arrested after about 15-17 somites (van de Ven et al., 2011). Compound mutants $Cdx2^{null}/Cdx4^{null}$, $Cdx1^{null}/Cdx2^{null}$ (Savory et al., 2011) and Cdx^{null} (van Rooijen et al., 2012) more and more severely fail in elongating their axis, only generating 12, 7-8 (Savory et al., 2011) and 5 (van Rooijen et al., 2012) somites, respectively.
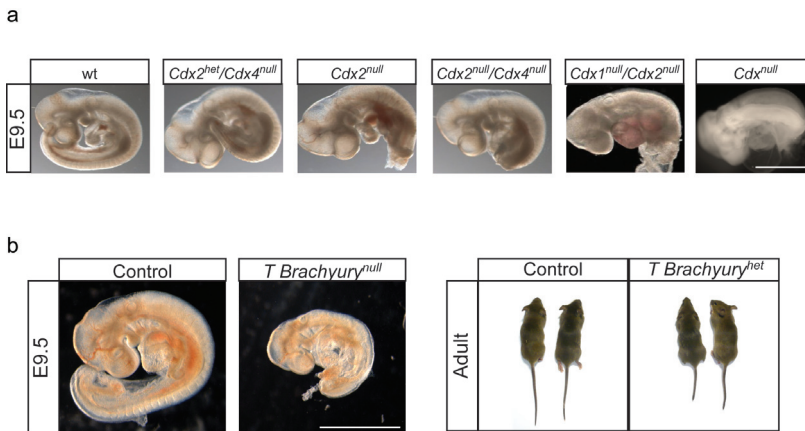
3

Figure 2. *Cdx* and *T Brachyury* regulate the axial elongation in a dosage-dependent way. a. Allelic series of Cdx compound mutant embryos at E9.5. The severity of the posterior truncation progressively increases with the loss of Cdx alleles. Scale bar 2 mm. **b.** $T Brachyury^{null}$ mutant compared with wt embryo at E9.5. The $T Brachyury^{null}$ mutant embryo shows a severe posterior truncation. Scale bar 2 mm. Adult mice heterozygous for the *T Brachyury* mutation are characterized by a shorter and kinky tail.
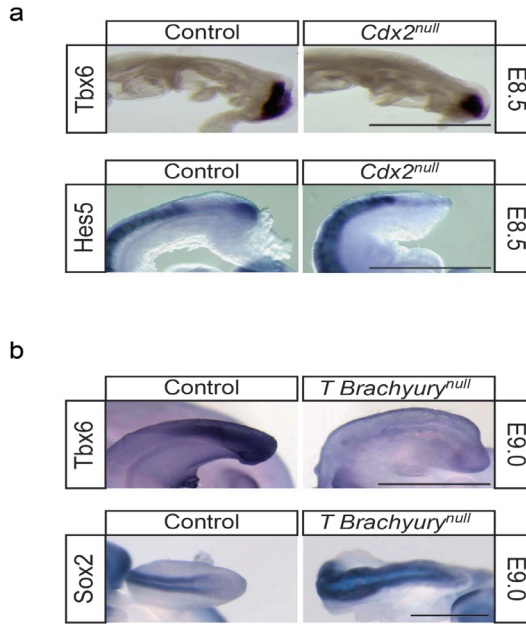
3

Figure 3: Mesodermal (*Tbx6*) and neuroectodermal (*Hes5* and *Sox2*) marker expression in *Cdx2^{null}* and *T Brachyury^{null}* mutant embryos. a. Expression of *Tbx6* and *Hes5* at E8.5 in *Cdx2^{null}* compared to control embryo. *Tbx6* is not downregulated in the *Cdx2^{null}* mutants but the PSM expressing the gene is reduced; *Hes5* posterior expression does not seem to be affected in the caudal neural tube. The posterior region of *Hes5* expression in wt corresponds to the expression in the PSM. Scale bars 0.5 mm. **b.** Expression of *Tbx6* and *Sox2* at E9.0 in *T Brachyury^{null}* compared to control embryo. A significant *Tbx6* downregulation occurs at E9.0, whereas *Sox2* shows upregulation in the *T Brachyury^{null}* mutants compared to the control. Right is posterior. Scale bars 0.5 mm.
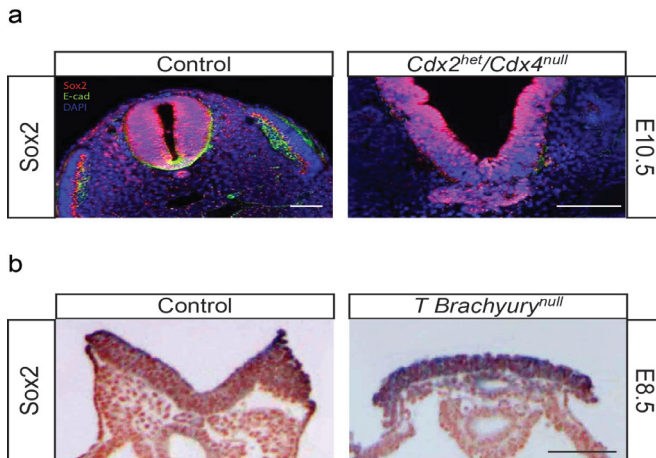
Figure 4. Ectopic neural structures at posterior levels in Cdx compound mutants and in *T Brachyury^{null}* embryos. a. *Sox2* expressing neural structures in *Cdx2^{het}/Cdx4^{null}* mutants compared to controls on transversal sections of the tailbud region of E10.5 embryos. These ectopic neural structures are formed outside the posterior neural tube. Scale bar 50 μm. **b.** *Sox2* expression in *T Brachyury^{null}* mutant compared to control. Transversal sections of the posterior region of E8.5 embryos: *T Brachyury^{null}* mutants exhibit clear Sox2-expressing posterior ectopic neural structures. Scale bar 0.1 mm.

T Brachyury^{null} mutant embryos, do not generate more than about 7-8 somites and their neural tube at posterior levels is kinked and abnormal. The *T Brachyury^{null}* mutation is semi-dominant, resulting in an abnormal tail phenotype of the heterozygote adults (Fig. 2b).

At gene expression level, the transcription of the PSM marker *Tbx6* and the neural markers *Hes5* and *Sox2* was investigated. *Tbx6* is expressed in the PSM of *Cdx2^{null}* mutant, which is reduced at E8.5 due to axial truncation (Fig. 3a). *Tbx6* is downregulated at E9.0 in *T Brachyury^{null}* mutants (Fig. 3b). Posterior *Hes5* is not increased in *Cdx2^{null}* (Fig. 3a) whereas *Sox2* expression is posteriorly expanded in *T Brachyury^{null}* mutants compared to the wild-type (wt) situation (Fig. 3b). Upregulation of posterior *Sox2* expression in *T Brachyury^{null}* mutants is presumably the origin of the ectopic neural structures observed. Such ectopic neural structures in Cdx mutants are more rare and less extensive (Fig. 4a, b).

T Brachyury expression is intact in Cdx2^{null} mutants and Cdx2 expression is normal in early T Brachyury^{null} embryos. Expression of *T Brachyury* appears not to be altered in the *Cdx2^{null}* embryos at E8.5. Expression of *Cdx2* in *T Brachyury^{null}* mutants is not affected either (Fig. 5) at the same embryonic stage. This indicates that *T Brachyury* and *Cdx2* are not linearly upstream to one another in early posterior morphogenesis.

Cdx2^{null}/T Brachyury^{null} double mutants exhibit a posteriorly truncated phenotype more severe than each single mutant. Double mutant embryos were generated from intercrosses of *Cdx2* conditional homozygotes carrying a null allele of *T Brachyury*. The *T Brachyury^{null}* mutants affect somite morphology and it is therefore more difficult to precisely count the somites in *T Brachyury^{null}* and *Cdx2^{null}/T Brachyury^{null}* than in *Cdx2^{null}* mutants. Comparison between the phenotype of *Cdx2^{null}* and *T Brachyury^{null}* embryos indicated that, in addition to the fact that axial extension stops at about 15-17 somite stage in *Cdx2^{null}* mutants and around 7-8 somite stage in *T Brachyury^{null}* mutants, the posterior aspect of the *T Brachyury^{null}* embryos seems slightly thicker than that of the *Cdx2^{null}* mutants (Fig. 6). This difference might be inherent to the persistence of nascent mesoderm in the streak in *T Brachyury^{null}* mutants (see Introduction).

Double mutant embryos clearly exhibit a more severely truncated phenotype than each single mutant (Fig. 6), and develop only 3 to 5 disorganized somites.
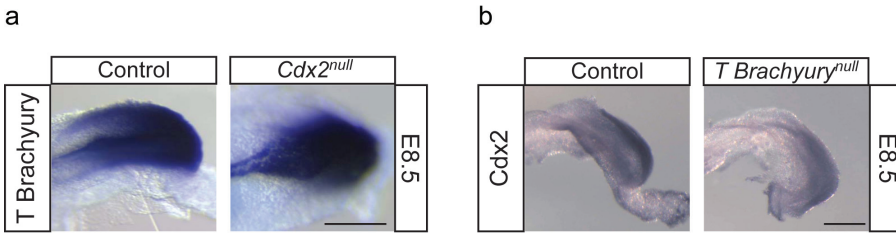
a

b

Figure 5. *Cdx2* and *T Brachyury* do not affect each other's expression. a. Expression of *T Brachyury* in the posterior part of a E8.5 *Cdx2^null* mutant embryo compared to a control. Scale bar 0.25 mm. **b.** Expression of *Cdx2* in the posterior part of a E8.5 *T Brachyury^null* mutant embryo compared to a control. Scale bar 0.25 mm.
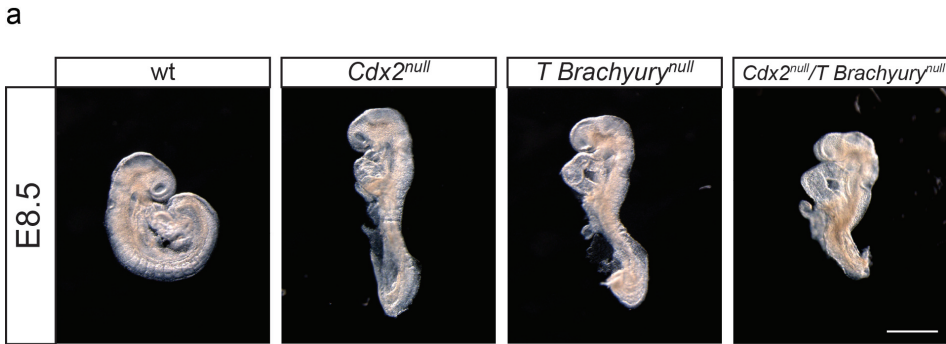
a

Figure 6. *Cdx2^null/T Brachyury^null* mutant embryos exhibit a posterior truncation more severe than each single mutant. From left to right E8.5 wt, *Cdx2^null* mutant, *T Brachyury^null* mutant, *Cdx2^null/T Brachyury^null* mutant embryos. The wt embryo has 14 somites, the *Cdx2^null* shown here has 10 somites, the *T Brachyury^null* 6 recognizable somites and the *Cdx2^null/T Brachyury^null* mutant 4 or 5 identifiable somites. As noted in the text, *T Brachyury^null* mutants affect somites morphology and it is therefore more difficult to precisely count the somites in *T Brachyury^null* and *Cdx2^null/T Brachyury^null* mutants than in *Cdx2^null* mutants. Scale bar 0.5 mm.

Impact of the *Cdx2^null* and *T Brachyury^null* mutations on the Wnt and Fgf signaling pathways. E7.5 and E8.0 wt and mutant embryos were subjected to *in situ* hybridization to detect the expression *Axin2* and *Spry4*, as readouts of the Wnt and Fgf pathways, respectively (Fig. 7). At head fold stages (E7.5) *Axin2* is expressed at comparable levels in the posterior streak of all mutant embryos and in the wt (Fig. 7a). At later stages (E8.0) *Cdx2^null* embryos show an evident downregulation of *Axin2* in the tailbud, whereas it is not the case in *T Brachyury^null* mutants. It is difficult to appreciate the posterior expression of *Axin2* in the *Cdx2^null/T Brachyury^null* mutants because of their severe truncation (Fig. 7a).

Spry4 expression seems to be decreased at the head fold stage (E7.5) in both single mutants and in the double mutants. Very low levels of *Spry4* expression is still detectable in the single *Cdx2^null* and *T Brachyury^null* mutants

at E8.0. In the *Cdx2^{null}*/*T Brachyury^{null}* embryos virtually no expression of *Spry4* is detectable at E7.5 but it is difficult to evaluate the expression of *Spry4* in the *Cdx2^{null}*/*T Brachyury^{null}* mutants at E8.0, due to the severe truncation of their posterior tissues.
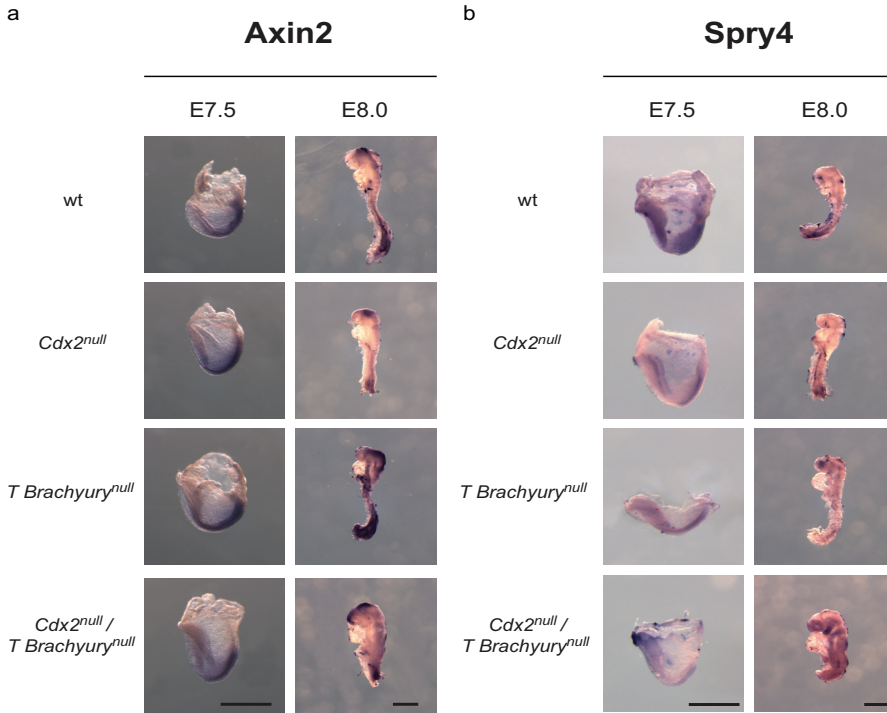

Figure 7. The Fgf pathway is more affected than the Wnt pathway in the *Cdx2^{null}*/*T Brachyury^{null}* mutant embryos. a. Expression of a Wnt target (*Axin2*) at E7.5 and E8.0 in wt, *Cdx2^{null}* mutant, *T Brachyury^{null}* mutant and *Cdx2^{null}*/*T Brachyury^{null}* mutant embryos. While *Axin2* expression at E7.5 seems not to be affected in all mutants, it is downregulated in the *Cdx2^{null}* mutants but not in the *T Brachyury^{null}* mutants compared to the wt at E8.0. It is difficult to appreciate the posterior expression of *Axin2* in the *Cdx2^{null}*/*T Brachyury^{null}* because of their truncation. The results suggest that the *T Brachyury* mutation does not affect *Axin2* expression extremely reducing the size of posterior growth zone. Scale bars 0.5 mm. **b.** Expression of a Fgf target (*Spry4*) at E7.5 and E8.0 in wt, *Cdx2^{null}* mutant, *T Brachyury^{null}* mutant and *Cdx2^{null}*/*T Brachyury^{null}* mutant embryos. *Cdx2^{null}* and *T Brachyury^{null}* mutants show downregulation of *Spry4* both at E7.5 and E8.0 compared to the wt. At E8.0, the *T Brachyury^{null}* mutation seems to affect the expression of *Spry4* more than the *Cdx2^{null}* mutation. Also *Spry4* expression is more downregulated in the *Cdx2^{null}*/*T Brachyury^{null}* mutants at E7.5 compared to the *Cdx2^{null}* and *T Brachyury^{null}* mutants, and compared to the wt. Posterior *Spry4* expression in the *Cdx2^{null}*/*T Brachyury^{null}* mutants at E8.0 is difficult to appreciate because their severe truncation leaves a very reduced posterior part. Scale bars 0.5 mm.

Transcriptional changes of the *Cdx2^{null}*/*T Brachyury^{null}* mutant embryos versus *Cdx2^{null}* and *T Brachyury^{null}* mutants. Knowing that *Cdx2* and *T Brachyury* add their effects in jeopardizing axial elongation of the trunk, we wanted to compare the transcriptome of single and double mutants at a developmental time point just before morphogenesis is severely affected
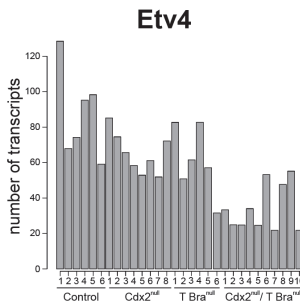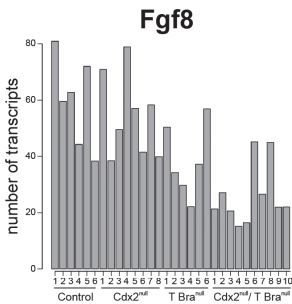
3

at E8.0 (2-5 somites stage). We performed RNA-Seq using the embryonic part posterior to the first formed somite of E8.0 embryos, given the fact that the axial elongation process that we study does not involve anterior tissues. We set out to sequence the transcriptome of *Cdx2^{null}* (n=8), *T Brachyury^{null}* (n=6) and *Cdx2^{null}/T Brachyury^{null}* (n=10) individual mutant embryos and to compare them with the transcriptome of Control embryos (n=6) (Fig. 8a). We normalized the transcripts output of each mutant embryo with the mean of the transcriptomes of control embryos and we looked for genes significantly affected in their expression in the *Cdx2^{null}/T Brachyury^{null}* compared to the single mutants. Even though the stages of the embryos analysed were similar (Fig. 8a), we observed important variability in gene expression between samples of the same groups. In agreement with the *in situ* hybridization experiments, we found that components of the Fgf pathway, namely *Fgf8* and *Etv4* transcripts, were more heavily downregulated in the *Cdx2^{null}/T Brachyury^{null}* than in the single mutants compared to the controls (Fig. 8b). The expression of these two genes was significantly (2-fold difference in log2 fold-scale) downregulated in the *Cdx2^{null}/T Brachyury^{null}* mutants compared to the controls (Fig. 8c). In addition*,* we also found that the expression of the mesodermal marker *Tbx6*, was significantly downregulated in the *T Brachyury^{null}* and *Cdx2^{null}/T Brachyury^{null}* mutants compared to the controls (Fig. 8d). This validate the RNA-Seq experiment since *Tbx6* has been reported to be a direct target of T Brachyury (Lolas et al., 2014). We found components of the Wnt pathway, such as *Wnt3a*, to be expressed at lower levels in the *Cdx2^{null}/T Brachyury^{null}* mutant embryos, compared to the single mutants. However, the difference in gene expression is not significant in the current available data (not shown).

a

Control	Stage (n.somites)	*Cdx2^null*	Stage (n.somites)	*T Brachyury^null*	Stage (n.somites)	*Cdx2^null/ T Brachyury^null*	Stage (n.somites)
1	2	1	4	1	2/3	1	4
2	3	2	3	2	2/3	2	2
3	2	3	2	3	3/4	3	3
4	2/3	4	4/5	4	2	4	4
5	2/3	5	4/5	5	3	5	3
6	3	6	3	6	2	6	4
		7	3			7	3
		8	2/3			8	4
						9	4
						10	3

Figure 8. Simultaneous loss of *Cdx2* and *T Brachyury* mainly affects the expression of components of the Fgf pathway. a. List of embryos with their relative genotype and stage (indicated in number of somites) submitted for the RNA-Seq analysis. **b.** Comparison of expression levels of *Fgf8* and *Etv4* (expressed in absolute number of transcripts) among all samples. **c.** Comparative analysis of *Fgf8* and *Etv4* expression in *Cdx2^null/T Brachyury^null* compared with control. **d.** Analysis of *Tbx6* expression in *T Brachyury^null* and *Cdx2^null/T Brachyury^null* compared with control. **e.** Representation of our model regarding Cdx and T Brachyury functions during axial elongation.

Discussion

The transcription factors-encoding genes *Cdx2* and *T Brachyury* are both required for embryonic posterior body elongation, and their inactivation compromises tissue generation in the three germ layers in the upper trunk. *T Brachyury* is expressed in the axial progenitor region of the posterior growth zone from which tissues are generated as the embryo grows (Cambray and Wilson, 2007), and we showed in the present work that *Cdx2* is expressed in this progenitor region as well. Double mutants in *Cdx2* and *T Brachyury* were generated and found to be dramatically more severely affected than each single mutant. They are arrested in axial extension at a level corresponding to somite 5 or 6, and thus fail to generate trunk and tail structures. Because the two genes do not regulate each other's transcription, at least until these early somite stages, we wanted to elucidate the mechanism underlying their cooperativity, in order to better localize these players in the network that controls embryonic axial elongation. *Cdx2* and *T Brachyury* were known from mutant rescue experiments in previous work to have the Wnt and Fgf pathways as downstream target programs [(Bialecka et al., 2010) for *Cdx2* in the mouse, (Martin and Kimelman, 2008) for *T Brachyury* and Fgf in zebrafish]. Here we documented the expression of components of the Wnt and Fgf pathways by *in situ* hybridization in early somite embryos single and double mutants for *Cdx2* and *T Brachyury*. We conclude that the Wnt pathway is more affected in the *Cdx2^{null}* mutants than in the *T Brachyury^{null}* mutants, and that Fgf pathway is more affected in the *T Brachyury^{null}* mutants than in the *Cdx2^{null}* mutants. The Fgf pathway is even more downregulated in the *Cdx2^{null}/T Brachyury^{null}* mutants than in the single mutants. We confirmed the downregulation of the Fgf pathway in the double mutants by RNA-Seq experiments using single early somite embryos. This transcriptome analysis surprisingly seemed to reveal less changes than the *in situ* hybridization. This probably originates from the fact that the RNA was extracted from a relatively large part of the embryos, of which the progenitor cell population that supports axial elongation (for which there is no specific marker) represents only a small subset. In spite of this limitation, the significant detection of a decrease of *Fgf8* expression in *T Brachyury^{null}* mutants and to a larger extent in the *Cdx2^{null}/T Brachyury^{null}* mutants, is in agreement with the independent gene expression analyses performed by *in situ* hybridization. In addition, the fact that transcripts of Wnt pathway components that were detected are not found to be significantly different in double mutants suggests that

these changes are less extensive than the changes in the Fgf pathway, also in line with the *in situ* hybridization experiments. A conclusion from the gene expression experiments, therefore, is that the *Cdx2^{null}/T Brachyury^{null}* double mutations decrease the activity of the Fgfr1-dependent Fgf signaling pathway, that the *Cdx2* impairment does that in a much lesser extent than the *T Brachyury* mutation. A common action of T Brachyury and Fgfr1-dependent Fgf signaling in the posterior part of the early embryo is to enable the nascent mesoderm emerging from the primitive streak to migrate away from the streak (Deng et al., 1994; Wilson et al., 1995; Yamaguchi et al., 1994) and their invalidation results in a wider tailbud. These mutants also manifest a bias in their differentiation of mesoderm versus neurectoderm, possibly as a result of the abnormal routing of the mesoderm descendants of the progenitors. This bias is likely correlated with the appearance of ectopic neural tissues in these mutants. Such features of *T Brachyury^{null}* and *Fgfr1^{null}* mutants are less characteristic of *Cdx2^{null}* mutants, where no abnormality was noticed in mesoderm migration, and much less extensive ectopic neural structures were scored.

These results and considerations lead us to propose the following model of involvement of *Cdx2* and *T Brachyury* in posterior axial elongation (Fig. 8e): *Cdx2*, and the other Cdx transcription factors, would mainly activate the Wnt pathway and in this way maintain the self-renewal of the neuromesodermal axial progenitors in the posterior stem zone. *T Brachyury* would mainly activate the Fgf pathway and ensure the correct outmigration of the nascent mesoderm from the streak, thereby allowing the balanced fate choice decisions of the neurectodermal and mesodermal descendants of the bipotent progenitors. A secondary reciprocal stimulation of Wnt and Fgf on each other would lead to some involvement of *T Brachyury* in progenitor maintenance, and of Cdx in progenitor differentiation choice, and explain why Fgf and Wnt both can partially rescue the *Cdx2^{null}* and *T Brachyury^{null}* mutants (Martin and Kimelman, 2008; van Rooijen et al., 2012; Young et al., 2009).

Validation of this model will require additional work. A new series of RNA-Seq experiments using RNA from dissected embryonic growth zones (possibly amounting about 1000 cells) should confirm the data obtained so far and possibly point to additional genes differentially regulated by Cdx2 and T Brachyury. In addition, defining and comparing Cdx2 and T Brachyury

binding profiles in the genome by ChIP-Seq on dissected embryonic tail buds, and a subsequent validation of selected targets should allow us to reach a deeper degree of understanding of the activity and interaction of these transcription factors during axial elongation.

Methods

Mice. All mice were in the C57Bl6j/CBA mixed background. Generation of the strain carrying *Cdx2* conditional allele was described by Stringer *et al.,* (Stringer et al., 2012). The RosaCreER[T2] mice come from Lars Grotewold and Austin Smith, Wellcome Trust Centre for Stem Cell Research, University of Cambridge, UK. *Cdx2^{fl/fl}/RosaCreERT2* mice were generated by interbreeding *Cdx2^{fl/fl}* and *RosaCreERT2* mice. The generation of the strain carrying *T Brachyury[2J]* deletion (deletion of 80-110kb on chromosome 17) was described by Herrmann B.G. *et al*., 1990 (Herrmann et al., 1990). Cdx2[null]/T Brachyury[null] embryos were generated by interbreeding *Cdx2^{fl/fl}/ RosaCreERT2/T Brachyury[het].* Mouse females resulted positive at the plug check underwent intraperitoneal tamoxifen injection [100 ul from 500 ul working diluition (200 ul of 25 mg/ml tamoxifen dissolved in 100% ethanol stock diluted in 300 ul of corn oil)] at E5.0 in order to activate Cre recombinase and to induce *Cdx2[null]*.

All experiments using mice were performed in accordance with the institutional and national guidelines and regulations, under control of the Dutch Committee for Animals in Experiments, and under the licenses required in The Netherlands.

Genotyping. Genotyping of the strain carrying *Cdx2* conditional allele was described by Stringer *et al.,* (Stringer et al., 2012). Short or no tail phenotype was used to select mice heterozygous mutants for *T Brachyury[2J]* deletion. Genotyping of *T Brachyury[null]* embryos was performed by using real time quantitative PCR analysis. DNA was measured by Nanodrop and 5 ul of 2 ng/ul DNA dilution was loaded for PCR reaction. DNA was amplified with iQSyberGreenSupermix (Biorad) on a Biorad CFX Connect Real-Time PCR System. Data was analysed using Biorad CFX Manager Software Version 2.1. Embryos genotyping was calculated as difference between *T Brachyury* and *Gapdh* and β-Actin1 measurements. The following primers were used:

Primer	Sequence
T Bra-For	AGTCTGCAAAGCCCTGTGAT
T Bra-Rev	ATCGGAGAACCAGAAGACGA
Gapdh-For	AGCTGATGGCTGCAGGTTCTC
Gapdh-Rev	GCCACTGCAAATGGCAGCCCT
β-Act1-For	AGGCCCCAGCAACACGTCATT
β-Act1-Rev	GGCCCTTCATTGTGGCTGCCT

Histology and immunostaining. For histological analysis, tissues were fixed with 4% paraformaldehyde (PFA) overnight at 4°C. Whole mount *in situ* hybridization of mutant and control embryos was performed according to Young et al. (Young et al., 2009). Images of the embryos were acquired using a Leica MZ16FA microscope with a DFC480 camera. Images were analysed using the Leica LAS AF Lite software.

Embryos were imbedded in plastic (GMA Technovit type 8100) and sectioned at 7 µm. Images of the organoids were acquired using Leica DFC500 camera and Nikon Eclipse E600 microscope.

For immunofluorescence staining, 70 µm-thick vibratome sections were made from embryos embedded in 4% low melting point agarose. Antibodies used were rabbit anti-Sox2 (Millipore), goat anti-T Brachyury (Santa Cruz, SC-17745) and mouse anti-Cdx2 (Biogenex). For nuclear staining was used DAPI. Images of the fluorescent staining on sections were acquired using Leica TCS SPE Live microscope. Images were analysed using the Leica LAS AF Lite software.

Embryo material harvested for RNA-Seq. Mouse embryos were isolated at 2-4 somites stage. Glass needle was used to separate the head from the trunk and tail tissues (embryos were cut at the level of the first somite formed). Trunk and tail were dissolved in 200ul of Trizol (Ambion by Life Technology) and stored and -80˚C until RNA isolation. Yolk sacks were used for DNA isolation and genotyping.

Transcriptome analysis by RNA-Seq. For mRNA sequencing 10 ng of total RNA was used as starting material. The RNA was processed using the CEL-Seq protocol (Hashimshony et al., 2012) and sequenced on an Illumina Nextseq using 75 bp paired end sequencing. After sequencing read 1 was

aligned to the mm10 RefSeq mouse transcriptome downloaded from the UCSC genome browser (Meyer et al., 2013) using bwa (Li and Durbin, 2010) with default parameters. Read 2 contains a barcode identifying the sample from which the read originated. CEL-Seq only sequences the most 3' end of a transcript and generates one read per transcript. Samples were rpm (reads per million) normalized. Only genes with more than 10 rpm in at least 4 samples were used for subsequent analysis. Sequencing data are being deposited in Gene Expression Omnibus.

References

Beddington, R.S., Puschel, A.W., and Rashbass, P. (1992a). Use of chimeras to study gene function in mesodermal tissues during gastrulation and early organogenesis. Ciba Foundation symposium *165*, 61-74; discussion 74-67.

Beddington, R.S., Rashbass, P., and Wilson, V. (1992b). Brachyury--a gene affecting mouse gastrulation and early organogenesis. Dev Suppl, 157-165.

Bialecka, M., Wilson, V., and Deschamps, J. (2010). Cdx mutant axial progenitor cells are rescued by grafting to a wild type environment. Developmental biology *347*, 228-234.

Boulet, A.M., and Capecchi, M.R. (2012). Signaling by FGF4 and FGF8 is required for axial elongation of the mouse embryo. Developmental biology *371*, 235-245.

Cambray, N., and Wilson, V. (2002). Axial progenitors with extensive potency are localised to the mouse chordoneural hinge. Development *129*, 4855-4866.

Cambray, N., and Wilson, V. (2007). Two distinct sources for a population of maturing axial progenitors. Development *134*, 2829-2840.

Casey, E.S., O'Reilly, M.A., Conlon, F.L., and Smith, J.C. (1998). The T-box transcription factor Brachyury regulates expression of eFGF through binding to a non-palindromic response element. Development *125*, 3887-3894.

Chawengsaksophak, K., de Graaff, W., Rossant, J., Deschamps, J., and Beck, F. (2004). Cdx2 is essential for axial elongation in mouse development.

Proceedings of the National Academy of Sciences of the United States of America *101*, 7641-7645.

Chawengsaksophak, K., James, R., Hammond, V.E., Kontgen, F., and Beck, F. (1997). Homeosis and intestinal tumours in Cdx2 mutant mice. Nature *386*, 84-87.

Deng, C.X., Wynshaw-Boris, A., Shen, M.M., Daugherty, C., Ornitz, D.M., and Leder, P. (1994). Murine FGFR-1 is required for early postimplantation growth and axial organization. Genes & development *8*, 3045-3057.

Dobrovolskaia-Zavadskaia, N. (1927). Sur la mortification spontanee de la queue chez la souris nouveau-nee et sur l'existence d'un caractere hereditaire "non viable". C R Hebd Soc Biol, 114-116.

Hashimshony, T., Wagner, F., Sher, N., and Yanai, I. (2012). CEL-Seq: single-cell RNA-Seq by multiplexed linear amplification. Cell reports *2*, 666-673.

Herrmann, B.G., Labeit, S., Poustka, A., King, T.R., and Lehrach, H. (1990). Cloning of the T gene required in mesoderm formation in the mouse. Nature *343*, 617-622.

Janesick, A., Nguyen, T.T., Aisaki, K., Igarashi, K., Kitajima, S., Chandraratna, R.A., Kanno, J., and Blumberg, B. (2014). Active repression by RARgamma signaling is required for vertebrate axial elongation. Development *141*, 2260-2270.

Li, H., and Durbin, R. (2010). Fast and accurate long-read alignment with Burrows-Wheeler transform. Bioinformatics *26*, 589-595.

Lolas, M., Valenzuela, P.D., Tjian, R., and Liu, Z. (2014). Charting Brachyury-mediated developmental pathways during early mouse embryogenesis. Proceedings of the National Academy of Sciences of the United States of America *111*, 4478-4483.

Martin, B.L., and Kimelman, D. (2008). Regulation of canonical Wnt signaling by Brachyury is essential for posterior mesoderm formation. Developmental cell *15*, 121-133.

Meyer, L.R., Zweig, A.S., Hinrichs, A.S., Karolchik, D., Kuhn, R.M., Wong,

3

M., Sloan, C.A., Rosenbloom, K.R., Roe, G., Rhead, B*., et al.* (2013). The UCSC Genome Browser database: extensions and updates 2013. Nucleic acids research *41*, D64-69.

Olivera-Martinez, I., Harada, H., Halley, P.A., and Storey, K.G. (2012). Loss of FGF-dependent mesoderm identity and rise of endogenous retinoid signalling determine cessation of body axis elongation. PLoS biology *10*, e1001415.

Rivera-Perez, J.A., and Magnuson, T. (2005). Primitive streak formation in mice is preceded by localized activation of Brachyury and Wnt3. Developmental biology *288*, 363-371.

Savory, J.G., Bouchard, N., Pierre, V., Rijli, F.M., De Repentigny, Y., Kothary, R., and Lohnes, D. (2009). Cdx2 regulation of posterior development through non-Hox targets. Development *136*, 4099-4110.

Savory, J.G., Mansfield, M., Rijli, F.M., and Lohnes, D. (2011). Cdx mediates neural tube closure through transcriptional regulation of the planar cell polarity gene Ptk7. Development *138*, 1361-1370.

Stringer, E.J., Duluc, I., Saandi, T., Davidson, I., Bialecka, M., Sato, T., Barker, N., Clevers, H., Pritchard, C.A., Winton, D.J*., et al.* (2012). Cdx2 determines the fate of postnatal intestinal endoderm. Development *139*, 465-474.

Takada, S., Stark, K.L., Shea, M.J., Vassileva, G., McMahon, J.A., and McMahon, A.P. (1994). Wnt-3a regulates somite and tailbud formation in the mouse embryo. Genes & development *8*, 174-189.

Trott, J., and Martinez Arias, A. (2013). Single cell lineage analysis of mouse embryonic stem cells at the exit from pluripotency. Biology open *2*, 1049-1056.

Turner, D.A., Rue, P., Mackenzie, J.P., Davies, E., and Martinez Arias, A. (2014). Brachyury cooperates with Wnt/beta-catenin signalling to elicit primitive-streak-like behaviour in differentiating mouse embryonic stem cells. BMC biology *12*, 63.

Tzouanacou, E., Wegener, A., Wymeersch, F.J., Wilson, V., and Nicolas, J.F. (2009). Redefining the progression of lineage segregations during mammalian embryogenesis by clonal analysis. Developmental cell *17*, 365-

376.

van de Ven, C., Bialecka, M., Neijts, R., Young, T., Rowland, J.E., Stringer, E.J., Van Rooijen, C., Meijlink, F., Novoa, A., Freund, J.N.*, et al.* (2011). Concerted involvement of Cdx/Hox genes and Wnt signaling in morphogenesis of the caudal neural tube and cloacal derivatives from the posterior growth zone. Development *138*, 3451-3462.

van den Akker, E., Forlani, S., Chawengsaksophak, K., de Graaff, W., Beck, F., Meyer, B.I., and Deschamps, J. (2002). Cdx1 and Cdx2 have overlapping functions in anteroposterior patterning and posterior axis elongation. Development *129*, 2181-2193.

van Nes, J., de Graaff, W., Lebrin, F., Gerhard, M., Beck, F., and Deschamps, J. (2006). The Cdx4 mutation affects axial development and reveals an essential role of Cdx genes in the ontogenesis of the placental labyrinth in mice. Development *133*, 419-428.

van Rooijen, C., Simmini, S., Bialecka, M., Neijts, R., van de Ven, C., Beck, F., and Deschamps, J. (2012). Evolutionarily conserved requirement of Cdx for post-occipital tissue emergence. Development *139*, 2576-2583.

Wilkinson, D.G., Bhatt, S., and Herrmann, B.G. (1990). Expression pattern of the mouse T gene and its role in mesoderm formation. Nature *343*, 657-659.

Wilson, V., and Beddington, R. (1997). Expression of T protein in the primitive streak is necessary and sufficient for posterior mesoderm movement and somite differentiation. Developmental biology *192*, 45-58.

Wilson, V., Manson, L., Skarnes, W.C., and Beddington, R.S. (1995). The T gene is necessary for normal mesodermal morphogenetic cell movements during gastrulation. Development *121*, 877-886.

Yamaguchi, T.P., Harpal, K., Henkemeyer, M., and Rossant, J. (1994). fgfr-1 is required for embryonic growth and mesodermal patterning during mouse gastrulation. Genes & development *8*, 3032-3044.

Young, T., Rowland, J.E., van de Ven, C., Bialecka, M., Novoa, A., Carapuco, M., van Nes, J., de Graaff, W., Duluc, I., Freund, J.N.*, et al.* (2009). Cdx and Hox genes differentially regulate posterior axial growth in mammalian embryos. Developmental cell *17*, 516-526.

3

Chapter 4
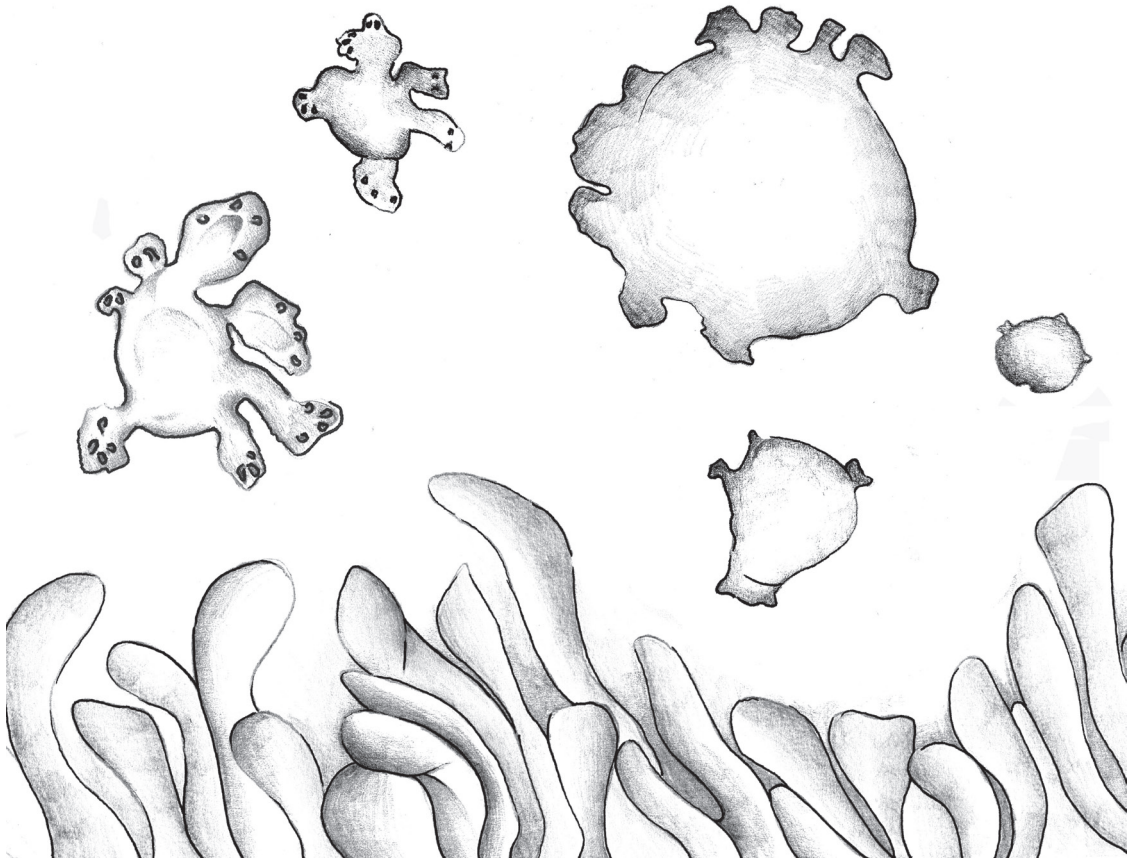
Transformation of intestinal stem cells into gastric stem cells on loss of transcription factor Cdx2

Salvatore Simmini[+], Monika Bialecka[+,1], Meritxell Huch[2], Lennart Kester, Marc van de Wetering, Toshiro Sato[3], Felix Beck[4], Alexander van Oudenaarden, Hans Clevers and Jacqueline Deschamps[*]

Hubrecht Institute and UMC Utrecht, Uppsalalaan 8 3584 CT Utrecht, the Netherlands
[1] Present address, University of Cambridge, Department of Physiology, Development & Neuroscience and Gurdon Institute Downing Street, Cambridge, CB2 3DY, UK
[2] Present address, Wellcome Trust/Cancer Research UK Gurdon Institute, University of Cambridge, Tennis Court Road, Cambridge CB2 1QN, UK
[3] Present address, Department of Gastroenterology, School of Medicine, Keio University Tokyo, Japan
[4] University of Leicester, Department of Biochemistry, Leicester LE1 7RH, UK
[+] Equal contribution
[*] Corresponding author: j.deschamps@hubrecht.eu

Abstract

The endodermal lining of the adult gastro-intestinal tract harbors stem cells that are responsible for the day-to-day regeneration of the epithelium. Stem cells residing in the pyloric glands of the stomach and in the small intestinal crypts differ in their differentiation program and in the gene repertoire that they express. Both types of stem cells have been shown to grow from single cells into 3D structures (organoids) *in vitro*. We show that single adult Lgr5-positive stem cells, isolated from small intestinal organoids, require Cdx2 to maintain their intestinal identity and are converted cell-autonomously into pyloric stem cells in the absence of this transcription factor. Clonal descendants of *Cdx2^{null}* small intestinal stem cells enter the gastric differentiation program instead of producing intestinal derivatives. We show that the intestinal genetic program is critically dependent on the single transcription factor encoding gene *Cdx2*.

Introduction

Adult stem cells from the digestive tract have been characterized *in vivo* and in organoid structures growing *in vitro* (Barker et al., 2010; Barker et al., 2007; Sato et al., 2009). Although small intestinal stem cells and gastric stem cells both express the stem cell marker Lgr5, they each express their own set of stem cell markers (Barker et al., 2010; Munoz et al., 2012; van der Flier et al., 2009). In addition, stem cells of the gastric and small intestinal segments of the digestive tract already express some markers of their respective differentiation programme. Small intestinal stem cells (SI SCs) express low levels of Villin, Mucin2 and Lysozyme (Munoz et al., 2012), whereas gastric stem cells (Sto SCs) fail to express these markers and express low levels of gastric intrinsic factor (Gif) (Barker et al., 2010). Therefore, they are already engaged in their tissue-specific differentiation programme. A comparison between the transcriptome of stem cells isolated from organs *in vivo* and from cultured organoids *in vitro* revealed the robustness and stability of these cells: each of these stem cells maintains its *in vivo* properties when cultured into organoids *in vitro* (Barker et al., 2010; Sato et al., 2009).

We find that the properties and transcriptional signature of adult SI SCs cultured *in vitro* as organoids are critically dependent on the expression of the transcription factor Cdx2. We show that single SI SCs wherein Cdx2 was inactivated rapidly lose their intestinal identity and acquire a gastric pyloric identity. They cannot give rise to intestinal organoids *in vitro* as their wild-type counterparts do, and instead manifest growth properties and transcriptional profile of gastric pyloric SCs. *Cdx2^{null}* SI SCs exclusively express the transcriptional programme of gastric pyloric stem cells and generate differentiated derivatives of all pyloric lineages. These data indicate that Cdx2 is a major determinant of the identity and fate of adult small intestinal stem cells.

Results

Single *Cdx2^null* intestinal SCs form stomach organoids. It had been found that inactivation of the intestinal-specific transcription factor Cdx2 in the adult mouse intestinal epithelium leads to the transformation of some of the crypts into submucosal empty cysts expressing stomach markers (Hryniuk et al., 2012; Stringer et al., 2012). This raised the fundamental question of whether the sole transcription factor Cdx2 was able to change the identity of adult intestinal stem cells into stem cells with a different commitment.
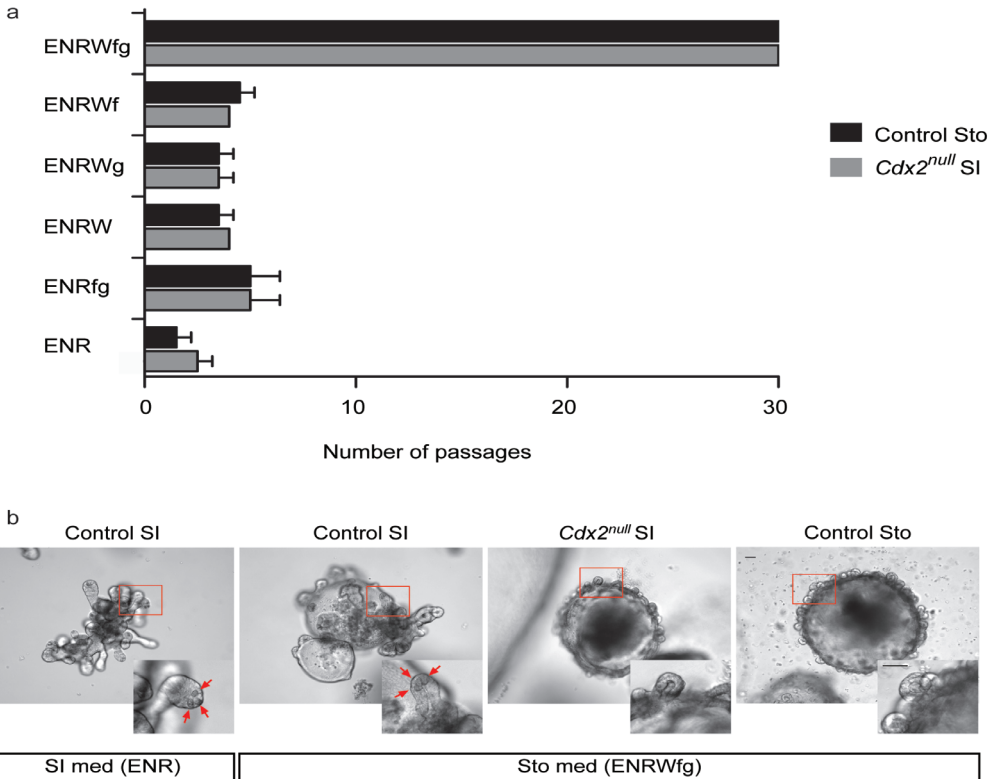
Fig. 1. Isolated *Cdx2^null* SI SCs form gastric organoids. a. Graph summarizing the growth performance (two independent experiments) of *Cdx2^null* SI SC-derived organoids and control Sto SC-derived organoids (issued from single Sto SCs) in medium dedicated to SI organoids (ENR, last rows of the graph, containing Egf, Noggin and R-Spondin1), in medium dedicated to Sto organoids [ENRWfg, top rows of the graphs, containing in addition to ENR, Wnt3a conditioned medium (W), Fgf10 (f) and Gastrin (g)], in SI medium supplemented with Fgf and Gastrin (ENRfg), SI medium supplemented with Wnt (ENRW), SI medium supplemented with Wnt and Gastrin (ENRWg), and SI medium supplemented with Wnt and Fgf (ENRWf). Black bars, stomach control organoids; dark grey bars, *Cdx2^null* SI organoids. x axis, number of passages (1 passage in average every 7 or 8 days). Error bars, standard deviations. **b.** Control SI organoids in intestinal and stomach conditions (left two panels); inserts, higher magnification of buds; red arrows, Paneth cells; *Cdx2^null* SI organoids (third panel from left) and control Sto organoids (right panel) in stomach conditions. Bars, 150 μm. med, medium. Images are representative of the results of more than 30 experiments.

We set out to investigate whether the ablation of *Cdx2* in Lgr5-positive stem cells isolated from adult small intestinal organoids would convert them into gastric stem cells. We used a stem cell (SC) specific *Lgr5-EGFP-Ires-CreERT2* knock-in allele (Barker et al., 2007) to inactivate *Cdx2* specifically in the stem cells of intestinal crypts. We induced inactivation of the floxed *Cdx2* allele (Stringer et al., 2012) in primary cultures of proximal small intestinal organoids derived from *Cdx2$^{-/fl}$/Lgr5-EGFP-Ires-CreERT2* mice by overnight exposure to 4-hydroxytamoxifen (Koo et al., 2012; Sato et al., 2009). After dissociation of the organoids, the Lgr5-EGFP^{hi} SI SCs were FACS-sorted, genotyped (Supplementary Fig. 1) and grown as single stem cell-derived clonal organoids. Unlike SI SCs from 4-hydroxytamoxifen-untreated *Cdx2$^{-/fl}$/Lgr5-EGFP-Ires-CreERT2* organoids (from here on called control SI SCs), *Cdx2^{null}/Lgr5-EGFP-Ires-CreERT2* SI SCs (from here on called *Cdx2^{null}* SI SCs) did not grow and form organoids in conditions established for culturing intestinal stem cells and intestinal organoids (ENR medium) (Sato et al., 2009) (Fig. 1a and Supplementary Fig. 2a, c). We wondered whether they would grow in conditions designed for gastric stem cells (Barker et al., 2010). Shifting to medium conditions for stomach (Sto) organoids by using Wnt3a-conditioned medium (W), Fgf10 (f) and Gastrin (g) in addition to the ENR culture medium (Barker et al., 2010), rescued the growth of *Cdx2^{null}* SI SCs and allowed them to form gastric-like organoids (Fig. 1a, b and Supplementary Fig. 2b, c), while control SI SCs formed intestinal organoids in the same medium. SC-derived *Cdx2^{null}* SI organoids cultured in stomach medium never generated Paneth cells, unlike their control SI organoids counterparts do (Fig. 1b).

***Cdx2^{null}* SI organoids depend on gastric culture conditions.** To rule out any impact of the culture conditions on the type of organoids generated by Sto and SI SCs, and on their differentiation marker expression, we analysed the transcriptome of organoids grown from wild-type stomach glands and small intestinal crypts by microarray. We show that they express a gastric and intestinal signature, respectively, regardless of whether they are cultured in stomach or intestinal conditions (Supplementary Fig. 3a). Hierarchical clustering on RNA-Seq analysis and data recovery for intestinal and stomach markers show that SC-derived SI organoids maintain their intestinal identity when grown in gastric medium (Supplementary Fig. 3b). The gene expression signature of both types of organoids is specific to the tissue of origin (Supplementary Fig. 3a, b). The stomach growth specificity

of *Cdx2^null* SI organoids is therefore not the result of their culture in stomach conditions.

The inability of *Cdx2^null* SI SCs to grow and form organoids in intestinal conditions is not alleviated by a pulse of Wnt alone (Fig. 1a and Supplementary Fig. 2c), unlike it is the case for isolated wild-type SI SCs without Paneth cells (Sato et al., 2011). The growth impairment of the *Cdx2^null* SI SCs in intestinal conditions *in vitro* is therefore not a mere consequence of their inability to generate Paneth cells, shown previously to reconstitute the niche of isolated SI SCs (Sato et al., 2011). The growth of *Cdx2^null* SI SCs has become strictly dependent on Wnt, Fgf and Gastrin altogether, like the growth of control Sto SCs (Barker et al., 2010) (Fig. 1a and Supplementary Fig. 2c). This suggests a conversion of the *Cdx2^null* SI SCs into Sto SCs, and a change in identity and fate of the SI SCs by the loss of Cdx2. Failure to produce Paneth cells results from this identity change.

4

Cdx2^null SI SCs lose intestinal and gain gastric markers. The panel of markers expressed by the organoids derived from *Cdx2^null* SI SCs grown in stomach conditions clearly reveals a gastric signature, unlike the panel of markers expressed by the intestinal controls in the same medium (Fig. 2a-f). As shown in Fig. 2a-c, ablation of Cdx2 led to strong downregulation of the intestinal stem cell markers *Olfactomedin4* (*Olfm4*) (Munoz et al., 2012) and *Cadherin17* (*Cdh17*) (Hinoi et al., 2002)*,* of the intestinal epithelial markers Villin (Maunoury et al., 1992), *Cdx1* (Coskun et al., 2011; Silberg et al., 2000), *Mucin13 (Muc13)* (Sheng et al., 2013), *Reg4* (Naito et al., 2012), and of markers of the different intestinal lineages, such as goblet cells [*Mucin2* (*Muc2*) (Ikeda et al., 2007; Lee et al., 2001; Mesquita et al., 2003; Mutoh et al., 2002; Yamamoto et al., 2003) and *Trefoil factor 3* (*Tff3*) (Leung et al., 2002)], Paneth cells [*Lysozyme1* (*Lyz1*)] (Sato et al., 2011), and enterocytes [apical Alkaline Phosphatase (ALP)] (Silberg et al., 2002) (Fig. 2a-c). For all these markers, it is clear that they are expressed in control SI organoids, regardless of whether the culture conditions are the preferred conditions for intestinal or gastric organoids. In all cases these intestinal markers are not expressed in *Cdx2^null* SI organoids. Genes upregulated in *Cdx2^null* SI SC-derived organoids include markers of different gastric lineages, like *Gastric intrinsic factor* (*Gif*) (Barker et al., 2010; Stringer et al., 2012) and *PepsinogenC* (*Pgc*) (Barker et al., 2010; Mutoh et al., 2002; Stringer et al., 2012) in chief cells, *Mucin1* (*Muc1*) (Sheng et al., 2013) and *Mucin5AC* (*Muc5AC*) (Barker et al., 2010;
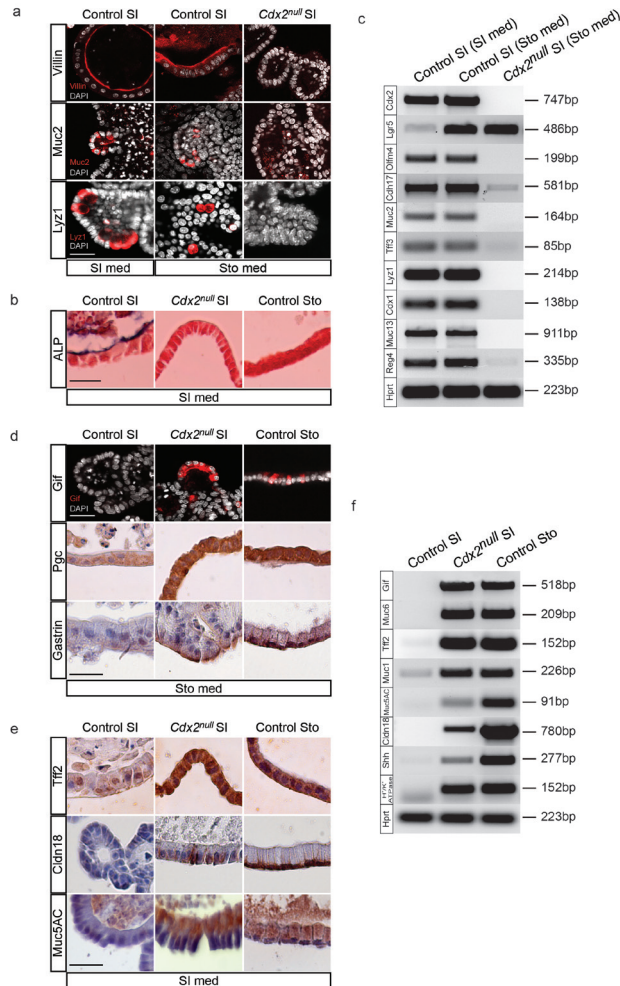
Fig. 2. ***Cdx2^null* SI organoids lost intestinal and express stomach markers. a.** *Cdx2^null* SI organoids grown from single SCs fail to express the intestinal markers Villin, Muc2 and Lyz1, whereas control SI organoids grown in the same stomach conditions (ENRWfg) do, like they do in intestinal (ENR) growth conditions. **b.** *Cdx2^null* SI organoids and control Sto organoids grown for 10 days in intestinal culture medium do not express the intestinal differentiation marker ALP whereas this marker is expressed in control SI organoids in the same growth conditions. Bar, 25 μm. **c.** RT-PCR experiments using RNA from independent clones of control SI SC-derived organoids grown in intestinal and gastric conditions, and from *Cdx2^null* SI SC-derived organoids grown in gastric conditions; intestinal markers, *Olfm4, Cdh17, Muc2, Tff3, Lyz1, Cdx1, Muc13* and *Reg4*. **d.** Organoids growing from single *Cdx2^null* SI SCs express the gastric markers Gif, Pgc and Gastrin, like control Sto organoids do, but unlike control SI organoids, all samples were grown in the same gastric conditions. **e.** *Cdx2^null* SI organoids and control Sto organoids grown for 10 days in culture medium to allow gastric differentiation of control Sto organoids, do express the gastric differentiation markers Tff2, Cldn18 and Muc5AC, Control SI organoids do not. Bar, 25 μm. **f.** Expression detected by RT-PCR of the gastric markers *Gif, Muc6, Tff2, Muc1, Muc5AC, Claudin18, Shh,* and *H^+/K^+ ATPase* in *Cdx2^null* SI organoids, compared with control SI and control Sto organoids. For *Gif, Muc6* and *Muc1* detection, the culture medium for all three samples was Sto medium; for *Tff2, Muc5AC, Claudin18, Shh,* and *H^+/K^+ ATPase* detection, the medium used for all three samples was stomach differentiation medium allowing gastric differentiation of control Sto organoids; this medium corresponds to SI medium. med, medium. Images are representative of the results obtained in three independent experiments performed on each of two independent clones.

Lee et al., 2001; Mutoh et al., 2002) in pit cells, *Mucin6* (*Muc6*) (Barker et al., 2010; Lee et al., 2001; Mutoh et al., 2002) and *Trefoil factor 2* (*Tff2*) (Barker et al., 2010; Leung et al., 2002; Stringer et al., 2012) in neck cells, Gastrin (stomach-specific hormone) (Barker et al., 2010) and *Claudin18* (*Cldn18*) (Stringer et al., 2012) in tight junctions of gastric epithelium, and *Sonic hedgehog* (*Shh*) and *H^+/K^+ ATPase* (Stringer et al., 2012) in parietal cells (Fig. 2d-f).

The conversion into gastric stem cells on loss of Cdx2 activity was not limited to the proximal SI SCs, known to reside in the digestive tract compartment abutting the stomach. *Cdx2^null* stem cells from proximal and distal small intestine both formed organoids that exhibited a gastric phenotype in terms of growth requirement and marker expression (Supplementary Fig. 4, showing downregulation of intestinal markers *Olfm4, Muc2*, *Lyz1* and *Cdx1*, and upregulation of gastric markers *Gif, Tff2, Muc6* and *Muc1* in *Cdx2^null* distal small intestine). For further analysis hereafter, we focus on the effect of inactivating Cdx2 in proximal SI SCs.

Transcriptome analysis of *Cdx2^null* SI SCs. In addition to testing a large number of markers specific to the small intestinal and gastric commitment of SC-derived organoids, we cultured organoids derived from single stem cells, FACS-sorted the Lgr5-EGFP^hi stem cells again and collected RNA for microarray analysis (experimental scheme in Supplementary Fig. 5). This allowed us to determine the impact of the absence of Cdx2 in the SI stem cells themselves. Comparative transcriptome analysis confirmed that *Cdx2^null* SI SCs originating from SC-derived *Cdx2^null* SI organoids, exhibit a gastric signature and cluster with the control stomach stem cells rather than with the control intestinal stem cells (Fig. 3a, two independent samples of each type of SCs). They express all stomach differentiation markers tested (*Cldn18*, *Muc1, Muc6, Tff2*, *Gif*, indicated on the right of the heatmap, Fig. 3a) at a higher level than SI SCs, while they have downregulated all small intestinal markers tested (*Olfm4*, *Muc2, Cdx1, Cdh17, Tff3*, *Muc13, Reg4,* Fig. 3a). We further strengthened this analysis by performing RNA-Seq on four additional independent samples of SC-derived *Cdx2^null* SI organoids, and four samples of control SI and Sto organoids. This independent transcriptome analysis confirmed that SC-derived *Cdx2^null* SI organoids are extremely similar to their stomach control (Supplementary Fig. 6a). The gene expression profile of the *Cdx2^null* SI SC samples established by microarray analysis (Fig. 3a) was
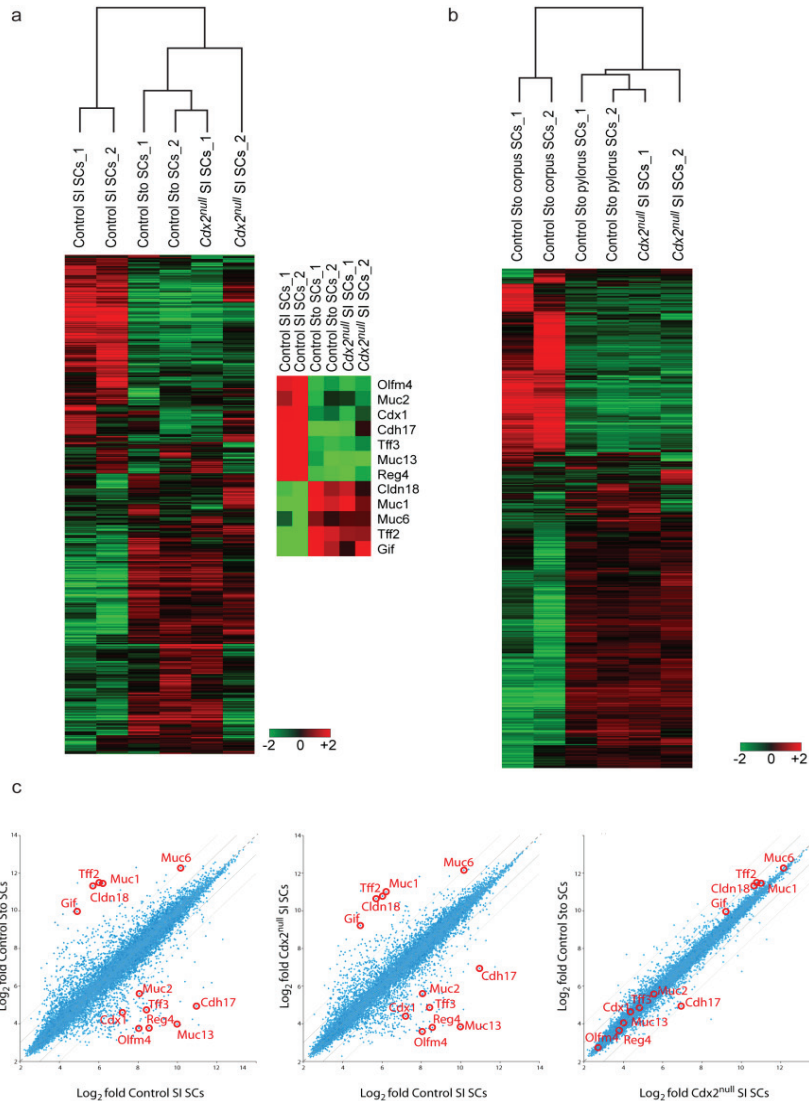
Fig. 3. Transcriptome analysis of *Cdx2^null* SI SCs. a. Heatmap comparison of the transcriptome of *Cdx2^null* SI SCs, with control SI SCs and Sto SCs (two independent samples of each) cultured in the same gastric conditions. Downregulated and upregulated genes considered to build the heatmap are the genes with at least a two-fold change in transcription. Genes characterizing the signature of SI and Sto SCs are listed on the right of the heatmap: among the downregulated genes are the intestinal markers *Olfm4*, *Muc2, Cdx1*, *Cdh17, Tff3*, *Muc13, and Reg4*; among the upregulated genes are the gastric markers *Claudin18*, *Muc1, Muc6*, *Tff2* and *Gif*. Hierarchical clustering is shown on the top. **b.** Transcriptome analysis of *Cdx2^null* SI SCs compared with control gastric pyloric and corpus SCs (two independent samples of each category of SCs). Hierarchical clustering is on the top. **c.** Pair-wise scatter plot analysis of changes in gene expression (two independent samples each time) showing that *Cdx2^null* SI SCs exhibit much more gene expression similarity with control Sto SCs (graph on the right) than with control SI SCs (graph in the middle). Each dot (blue or red) in the graph represents a gene present on the array used in the Affymetrix analysis. Dots along the bisector line are similarly expressed in the two samples compared. Dots shown in red correspond to genes with higher expression (Log$_2$ fold) in the sample indicated on the closest axis; the farther from the bisector, the bigger the difference. The genes the most altered in expression (red dots) correspond to the genes highlighted on the right of the heatmap in Fig. 3a.

compared with that of gastric corpus (Stange et al., 2013) and pylorus SCs (Fig. 3b). This comparison made it obvious that *Cdx2^null* SI SCs resemble pylorus SCs considerably, and differ from corpus SCs. Taken together, these analyses clearly established that *Cdx2* inactivation has caused the intestinal stem cells to change their identity from intestinal to gastric pylorus.

This change can be made visible at the genome-wide level, by establishing the pairwise comparison of transcriptional changes between *Cdx2^null* SI SCs and control Sto SCs (two independent samples of each), which shows much more similar transcriptional profiles than *Cdx2^null* SI SCs versus control SI SCs (Fig. 3c). The genes most altered in their expression between *Cdx2^null* SI SCs and control SI SCs (see highlighted genes on the right of the heatmap in Fig. 3a and middle graph in Fig. 3c) correspond to the set of markers that define the differences between control Sto and control SI SCs (Fig. 3c, graph on the left). These differences are absent when comparing *Cdx2^null* SI SCs and control Sto SCs (Fig. 3c, graph on the right). The changes in marker gene expression in *Cdx2^null* SI SCs have all been found to be significant in a quantitative analysis of the data from the microarray analyses (see text and Supplementary Fig. 6b where the projections on the y axis reflect statistical significance). Examples of genes with highly significant changes for upregulated stomach markers are *Cldn18*, *Muc1, Tff2*, and *Gif*, and for downregulated intestinal markers, *Olfm4, Muc2, Cdx1, Cdh17, Tff3, Muc13 and Reg4* (Fig. 3c and Supplementary Fig. 6b). These significant differences are not present between *Cdx2^null* SI SCs and control Sto SCs (graph on the right in Supplementary Fig. 6b). These pair-wise comparisons of the transcriptional changes between *Cdx2^null* SI SCs, and control Sto and SI SCs thus settle the much closer relationship between *Cdx2^null* SI SCs and Sto SCs.

Besides retrieving the expression levels of individual genes from the array data, we directly measured the transcriptional changes between *Cdx2^null^* SI organoids and their stomach and intestinal controls in independent RNA samples isolated from organoid cultures developed from single SCs (three independent samples of each). We confirmed the loss (*Olfm4*, Fig. 4a), or strong decrease in expression of the intestinal stem cell markers *Dach1, Clca4, Smoc2, Cdca7*, and *Msi1* (Munoz et al., 2012; van der Flier et al., 2009), and the increase in expression of the stomach stem cell markers *Gif*, *Col11a2* and *Pgc* (Barker et al., 2010) in *Cdx2^null^* SI SCs compared to control SI SCs (Fig. 4a, b). This quantitative marker expression analysis (Fig. 4), together with the genome-wide transcriptome comparisons (Fig. 3 and Supplementary Fig. 6), indicate that these *Cdx2^null^* SI SCs have genuinely converted to stomach pyloric stem cells.

Cdx2 ablation rapidly converts SI SCs into pyloric SCs. Candidates to cause intestinal to gastric conversion following *Cdx2* ablation are Cdx2 direct targets previously established in other studies (Coskun et al., 2011; Hinoi et al., 2002; Ikeda et al., 2007; Mesquita et al., 2003; Mutoh et al., 2002; Naito et al., 2012; Silberg et al., 2000; Yamamoto et al., 2003)*,* and clearly downregulated in the *Cdx2^null^* SI SCs compared with control SI SCs, such as *Muc2* (Ikeda et al., 2007; Mesquita et al., 2003; Mutoh et al., 2002; Yamamoto et al., 2003)*, Cdh17* (Hinoi et al., 2002), *Reg4* (Naito et al., 2012) and *Cdx1* (Coskun et al., 2011; Silberg et al., 2000) (Supplementary Fig. 7). The rapidity of the transcriptional response of genes to *Cdx2* inactivation could also indicate primary involvement of Cdx2 in this process. The kinetics of the *Cdx2^null^* SI identity conversion into stomach was followed by measuring intestinal and gastric gene expression in organoids at different time points after *Cdx2* inactivation in SI SCs. *Cdx2* transcripts seem to have disappeared by day 8 (Fig. 4c). Expression of the SI SC marker *Olfm4* begins to decrease at that time and a strong upregulation of the stomach marker *Gif* is then already noticeable (Fig. 4c). These changes in the gene repertoire manifested upon *Cdx2* inactivation therefore are quite rapid, occurring after a week of culture and preceding further passaging, in keeping with the hypothesis of a key role of Cdx2 in sustaining the intestinal programme.
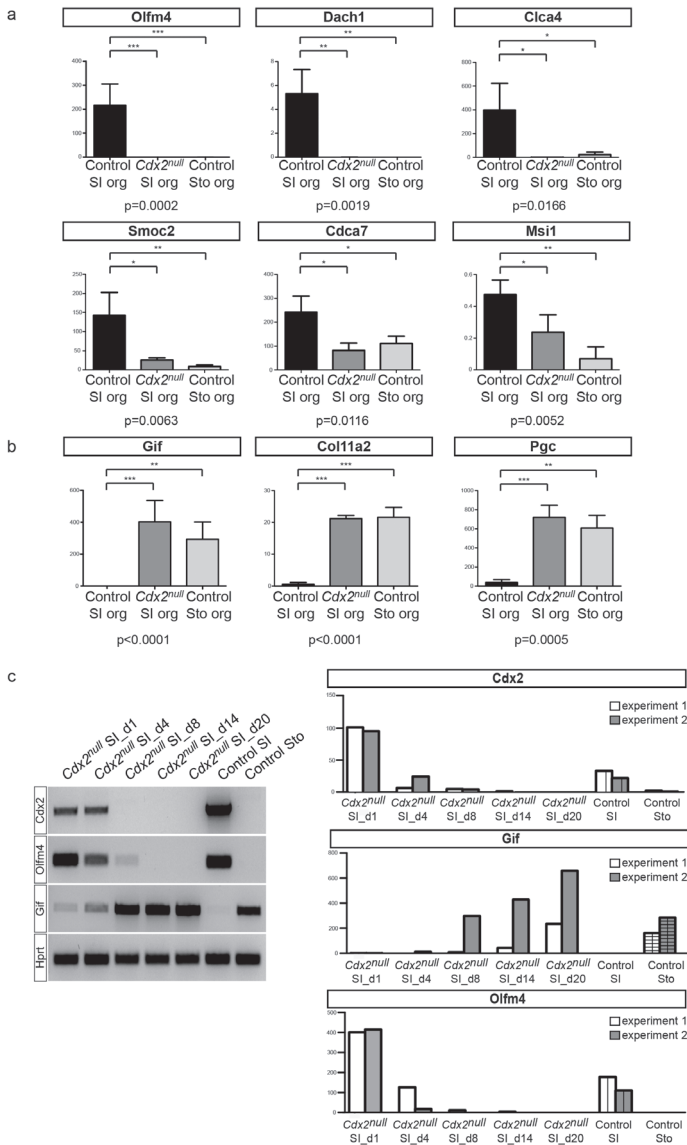
4

Fig. 4. SI and Sto SC marker gene expression in *Cdx2^null* SI organoids. a. Expression of the SI SC markers *Olfm4*, *Dach1, Clca4, Smoc2, Cdca7* and *Msi1*. org, organoids. **b.** Expression of the stomach-specific SC markers *Gif, Col11a2, and PepsinogenC (Pgc)* in control SI organoids (black bar), *Cdx2^null* SI organoids (dark grey) and control Sto organoids (lighter grey). Along the y axis, relative RNA amounts measured in three independent samples per condition, normalized for *Gapdh* expression. Error bars are s.d. values. For each marker, one way analysis of variance according to the ANOVA test is indicated by the p value underneath the graph. p<0.05 indicates that the differences are significant. Tuckey's test for multiple comparison was run for pair-wise comparison of the means of the samples, with *** meaning highly significant difference, ** very significant difference and * significant difference (see Methods for more details). org, organoids. **c.** Time course of the downregulation of intestinal markers and the upregulation of gastric markers in SI SCs on inactivation of *Cdx2*. **Left panel**, RT-PCR for *Cdx2, Olfm4, Gif,* and the house keeping gene *Hprt*. **Right panel**, graph representing the quantitative RT-PCR results of two independent time course experiments; light grey, five time points in experiment 1; dark grey, five time points in experiment 2; grey with internal patterns, control SI and control Sto.

***Cdx2* expressing gastric organoids remain stomach-like.** We wondered whether Cdx2 could transform wild-type gastric epithelium in organoid cultures into tissues with intestinal identity. We generated a lentiviral stock expressing *Cdx2* from the PGK promoter (Supplementary Fig. 8), and infected dissociated wild-type pyloric stomach organoids in culture. After selection of infected cells, several clones were recovered, derived from stable infection of stem cells, which grew into organoids expressing Cdx2 (Fig. 5a) that could be passaged indefinitely. These organoids did not grow in intestinal medium. *Cdx2*-positive (*Cdx2*$^+$) Sto organoids analysed after 5 passages in stomach culture conditions appeared to express the intestinal markers *Muc2* and *Tff3* at low level (Fig. 5b, left panel). In addition, immunohistochemistry revealed the expression of the Muc2 protein in a similar percentage of *Cdx2*$^+$ Sto and control SI organoids, with the same type of epithelial distribution (Fig. 5b, right panel). Expression of these intestinal markers revealed a certain degree of intestinalization of the epithelium (Mari et al., 2014; Silberg et al., 2002; Xu et al., 2010; Yamamoto et al., 2003). The *Cdx2*$^+$ Sto organoids also downregulated stomach markers (*Gif, Muc6, Tff2* and *Cldn18*, Fig. 5c). Independent transcriptome analysis of *Cdx2*$^+$ Sto organoids confirmed very mild changes in intestinal marker expression in *Cdx2*$^+$ Sto (*Muc2* and *Muc13*) (Fig. 5d, graph on the right), but revealed that *Cdx2*$^+$ Sto are globally more similar to control Sto than to control SI organoids (Fig. 5d). Expressing *Cdx2* is thus not sufficient to fully convert adult stomach stem cells into intestinal stem cells, unlike it is for maintaining the intestinal identity and fate of the small intestinal stem cells.
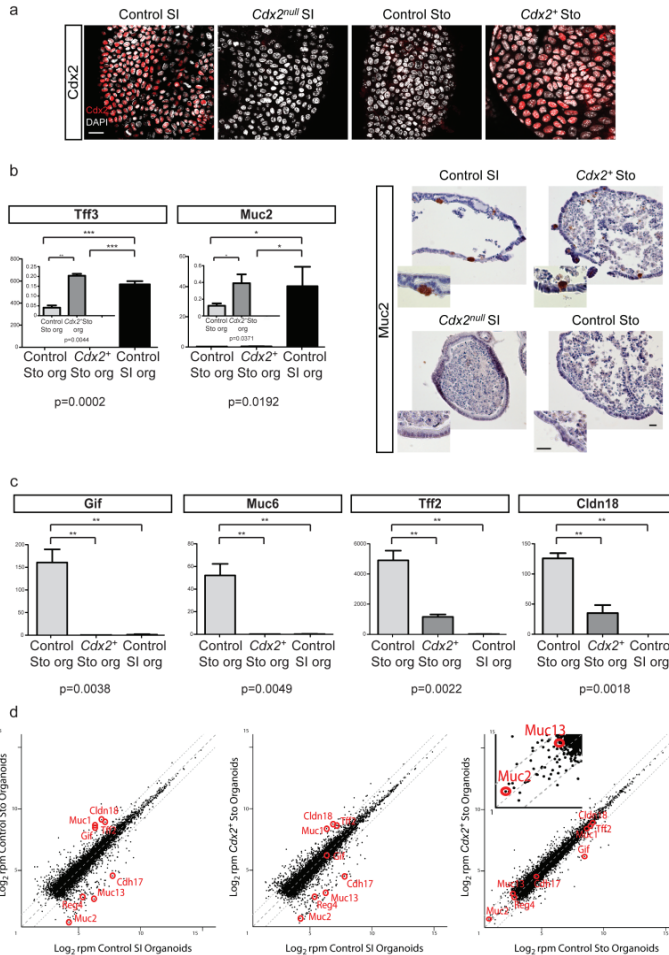
4

Fig. 5. Expression of Cdx2 in wild-type Sto organoids fails to fully convert them into SI organoids. **a.** Expression of Cdx2 in whole mounts of control SI organoids, *Cdx2null* SI and control Sto organoids and *Cdx2* expressing Sto organoids (*Cdx2+* Sto), all grown in Sto medium. Bar, 25 µm. **b. Left panel**, quantitative measurement of transcripts of the intestinal markers *Tff3* and *Muc2* in *Cdx2+* Sto compared with control Sto and SI organoids. The graph showing expression of intestinal markers in *Cdx2+* Sto versus control Sto organoids is blown up in the inserts to document the statistically significant small increase in expression (t-test, see Methods). For each marker, two independent experiments were performed, and the ANOVA and Tuckey's tests were used (See Methods for more details). Asterisks in the insert were calculated using one tail t-test. org, organoids. **Right panel**, immunostaining for Muc2 in *Cdx2+* Sto organoids, *Cdx2null* SI organoids and control SI and Sto organoids; a similar proportion of *Cdx2+* Sto and control SI organoids (about 50%) contained positive cells for the immune reaction. Bar, 25 µm. **c.** Quantitative measurement of transcripts (two independent experiments for each gene) of the gastric markers *Gif, Muc6, Tff2* and *Claudin18* in *Cdx2+* Sto organoids compared with control Sto organoids and control SI organoids. Error bars, standard deviations. org, organoids. **d.** Transcriptome analysis on performing RNA-Seq on *Cdx2+* Sto organoids and control SI and Sto organoids. Scatter plot of the Log_2 mean rpm values per gene for *Cdx2+* Sto against the Log_2 mean rpm values per gene for control organoids (four independent samples each time). The highlighted genes in the insert (graph on the right) are intestinal markers that are slightly upregulated (Log_2 fold) in the *Cdx2+* Sto compared with control Sto organoids. Dots along the bisector line are similarly expressed in the two samples compared. Outer dashed lines indicate the two-fold difference boundary. Images in **a, b** (immunostainings) are representative of the results of 3 independent experiments each time.

Discussion

The role of Cdx2 in the adult intestinal epithelium had been suggested previously but could not thoroughly be investigated. Loss of function of *Cdx2* in the endoderm of the adult gastro-intestinal tract in mice *in vivo* was either examined at one time point (Verzi et al., 2010; Verzi et al., 2011), or led to the generation of mosaic epithelium wherein wild-type crypts took over (Stringer et al., 2012). Generation of chimeras between wild-type and *Cdx2null* intestines did not allow the examination of pure clonal populations of stem cells for prolonged periods of time (Beck et al., 2003; Hryniuk et al., 2012). We now demonstrate that the inactivation of a single transcription factor Cdx2 in the adult intestinal stem cells directly, is sufficient to re-specify the identity and fate of these stem cells towards stem cells that exhibit a distinct committed programme: gastric stem cells. This re-specification is rapid and extensive, as the complete series of intestinal markers tested was downregulated while the complete series of gastric markers tested was turned on in the *Cdx2null* SI SCs. This drastic re-specification occurs in the stem cells producing the endoderm epithelium *in vitro* in the absence of mesenchyme and is irreversible regardless of the culture conditions. We therefore conclude that Cdx2 is an absolute master controller of the intestinal character of the adult stem cells of the digestive tract epithelium in a cell-autonomous way.

4

Author contribution

J.D., S.S, and M.B designed the experimental approach; S.S., M.B., M.H., L.K., and M.vd W. designed and performed the experiments; T.S. contributed to the initial discovery of the *Cdx2null* intestinal stem cell properties; F.B. participated in the generation of the *Cdx2* conditional mouse mutant line; A. v O. supervised the RNA sequencing work; H.C. provided the expertise and facilities to perform the work with organoid cultures; J.D and S.S. wrote the manuscript. The authors declare no conflict of interest.

Acknowledgements

Methods

Mice. All mice were in the C57Bl6j/CBA mixed background. The generation of the *Lgr5-EGFP-Ires-CreERT2* and *Cdx2$^{+/-}$* mice, as well as the protocols to genotype them, was described earlier respectively by Barker *et al,* (Barker et al., 2007) and Chawengsaksophak *et al*, (Chawengsaksophak et al., 1997). Generation and genotyping of the strain carrying the *Cdx2* conditional allele (*Cdx2^{fl}*) were described by Stringer *et al*, (Stringer et al., 2012). *Cdx2^{-fl}/Lgr5-EGFP-Ires-CreERT2* mice were generated by interbreeding *Lgr5-EGFP-Ires-CreERT2, Cdx2$^{fl/fl}$* and *Cdx2$^{+/-}$* mice. They have a normal phenotype. The animals used to isolate the intestine or stomach were males and females, without distinction. They were between 3 and 10 months old. All experiments using mice were performed in accordance with the institutional and national guidelines and regulations, under control of the Dutch Committee for Animals in Experiments, and under the licenses required in the Netherlands.

Generating organoids from intestinal crypts and stomach glands. Isolation of small intestinal crypts and stomach pyloric glands, cell dissociation, cell culture and organoids formation and culture were adapted from those previously described by Sato *et al*, and Barker *et al*, (Barker et al., 2010; Sato et al., 2009). In brief, an isolated small intestine was opened longitudinally. It was washed with cold PBS and chopped into pieces of about 5 mm. Gastric glands were isolated from a dissected stomach. The stomach was opened along the greater curvature and washed with saline solution. The muscular layer of the stomach was removed and the remaining epithelium was divided into 5 mm pieces. The tissue fragments were then washed with cold PBS.

Intestinal tissue fragments were incubated in 2 mM EDTA in PBS at 4ºC for 30 min. Stomach tissue fragments were incubated in 10 mM EDTA in PBS at 4ºC for 2-3 h. After removal of the EDTA solution, the tissue fragments were suspended in cold PBS with 10% Fetal Bovine Serum, using a 10-ml pipette. For the intestine, this suspension was the crypt fraction. It was passed through a 70 μm cell strainer (BD Bioscience). For the stomach, the suspension was the gland fraction and it was not filtered. Centrifugation of the suspensions at 200g for 5 min allowed separating crypts or glands from single cells. The pellet enriched in crypts and glands were resuspended in Matrigel (BD Bioscience) and plated in 24-well plates (about 100 crypts or glands per 50 μl per well). After polymerization of the Matrigel, 500 μl of intestinal or gastric culture medium was added per well [Advanced DMEM/F12, (Invitrogen) containing growth factors: for intestinal medium, 10–50 ng ml^{-1} EGF (Invitrogen), R-spondin 1 (conditioned medium) and Noggin (conditioned medium); for gastric medium, additional supplementation with 100 ng ml^{-1} FGF10 (Preprotech), Wnt3A (conditioned medium) and 10 nM Gastrin (Sigma-Aldrich)].

Single stem cell sorting and organoid culture. To obtain *Cdx2^{null}* intestinal stem cells carrying the Lgr5-EGFP marker, 5- to 6-day- old small intestinal organoids generated from *Cdx2^{-fl}/Lgr5-EGFP-Ires-CreERT2* mice were incubated with 1 μM of 4-hydroxytamoxifen in intestinal culture medium (Koo et al., 2012; Sato et al., 2009) for 16h to activate the Cre recombinase. Controls were 4-hydroxytamoxifen-untreated small intestinal (Control SI) and stomach (Control Sto) organoids issued from mice with the same genotype. The organoids were dissociated and sorted for EGFP^{hi} by using MoFlo cell sorter (DAKO) as described by Barker *et al*, (Barker et al., 2010) with some modifications. In brief, intestinal or stomach organoids were dissociated in culture medium by trituration with a glass pipette, followed by trypsinization in TrypLE Express (GIBCO). After incubation at 37 ºC for 5-10 min, cells were resupended in Advanced DMEM/F12 and spun down. Pellets were resuspended in stomach medium (ENRWfg) supplemented with 10μM Rock inhibitor Y-27632 (Sigma-Aldrich) and 0.8 Units μl^{-1} DNAse for culture purposes. The suspension was passed through a 40 μM mesh filter. EGFP^{hi} cells were sorted by flow cytometry (MoFlo; DAKO). Single viable (negative staining for propidium iodide) epithelial cells were gated by forward scatter, side scatter and pulse-width parameter. Sorted cells were collected in culture medium and embedded in Matrigel (BD Bioscience) at 1 cell per

4

well (in 96-well plates, 5 µl Matrigel per well). Intestinal or stomach culture medium (250 µl for 48-well plates, 100 µl for 96-well plates) containing the ROCK inhibitor Y-27632 (10 µM) was overlaid.

Control SI SCs grew and could be passaged indefinitely in small intestinal medium [SI med, ENR (Sato et al., 2009)] or in stomach medium [Sto med, ENRWfg (Barker et al., 2010)]. *Cdx2null* SI and control Sto SCs were cultured in stomach medium (Barker et al., 2010). Medium was refreshed every 2 days. Passage of the generated organoids was performed in split ratios of 1:4 and subsequently about once per week. Growth of the organoids and expression of Lgr5-EGFP were documented by using an EVOS fl (AMG) microscope.

59 independent clones of *Cdx2null* SI SCs were generated during these experiments, and the analysis of 15 of these is documented in detail in this work. An equivalent number of clones of both types of controls (small intestinal and stomach) was analysed.

Genotyping. *Cdx2null* and control stem cells sorted for EGFPhi by flow cytometry were genotyped upon using 1000 cells. Organoids were genotyped after collecting them from the clonal cultures. This procedure was repeated several times during the culture to rule out that organoids grew from cells that had escaped 4-hydroxytamoxifen-induced *Cdx2* inactivation (see Supplementary Fig. 1). Primers used are listed in Supplementary Materials.

Gene expression analysis by RT-PCR. For RT-PCR analysis, RNA was extracted from *Cdx2null* SI, control SI, and control Sto organoids using the RNeasy Mini RNA Extraction Kit (Qiagen) and reverse-transcribed using Moloney Murine Leukemia Virus reverse transcriptase (Promega). cDNA was amplified in a thermal cycler (Veriti 96 well Thermal Cycler, Applied Biosystems, London, UK). Primers used are listed in Supplementary Materials. For full gel panels see Supplementary Fig. 9 and Supplementary Fig. 10.

For real time quantitative PCR analysis, cDNA was amplified with iQSyberGreenSupermix (Biorad) on a Biorad CFX Connect Real-Time PCR System. Data was analysed using Biorad CFX Manager Software Version 2.1. Gene expression was normalized according to the expression of the housekeeping gene *Gapdh*. The primers usedare listed in Supplementary Materials.

Statistical Analysis. Statistical analysis was performed on Graphpad Prism Software Version 5.0. Results are expressed as mean $\pm$ s.d. One-way

analysis of variance (ANOVA) was used to evaluate the differences between group means. Student's t-test was used to analyse the difference between the means of two samples. p=0.05 was taken as the maximum value for significance. Tuckey's Multiple comparison test was used to find whether pairwise comparison of means are significantly different from each other. The level of significance is represented by asterisks (***, highly significant p<0.0001; **, very significant p<0.001; *, significant p<0.05).

Immunostaining for intestinal and stomach markers. For immunofluorescent staining on whole mounts, samples were fixed with 4% PFA for 20 min at room temperature, permeabilized with PBS 0.5% Triton-X100- 1% BSA and incubated overnight with the primary antibodies. Following several washes in PBS with 0,3% Triton-X100- 0.05% BSA, samples were incubated with the secondary antibody. Primary antibodies were mouse anti-Villin (1:100, Santa Cruz), rabbit anti-Muc2 (1:1000, Santa Cruz), rabbit anti-Lysozyme (1:1500, DAKO), rabbit anti-Gastric Intrinsic Factor (1:24000, generous gift from David Alpers) and mouse anti-Cdx2 (1:1000 Biogenex). Secondary antibodies used were Alexa Fluor 568 donkey anti-mouse IgG (H+L) (Invitrogen), Alexa Fluor 488 donkey anti-mouse IgG (H+L) (Invitrogen) and Alexa Fluor 568 donkey anti-rabbit (Life Technologies). Nuclei were stained with DAPI (Invitrogen). Images of the organoids were acquired using Leica TCS SPE and TCS SPE Live confocal microscopes. Images were analysed using the Leica LAS AF Lite software.

For immunostainings on sections, small intestinal and stomach organoids were fixed and embedded in paraffin, and staining was performed on 4 μm sections according to standard protocols. Primary antibodies were mouse anti-Muc5AC (1:200, Novocastra), rabbit anti-Gastrin (1:500, Novocastra), rabbit anti-Claudin18 (1:800, Invitrogen), rabbit anti-Muc2 (1:1000, Santa Cruz), goat anti-Tff2 (1:300, Santa Cruz), sheep anti-PepsinogenC (1:50000, Abcam). The peroxidase conjugated secondary antibodies used were Mouse EnVision+ (DAKO), BrightVision poly HRP-anti-rabbit IgG (Immunologic), Southern Biotech Rabbit anti-goat IgG (HIL)-UNLB and polyclonal rabbit anti-sheep immunoglobulins/HRP (DAKO). Images of the organoids were acquired using Leica DFC500 camera and Nikon Eclipse E600 microscope.

Cell sorting and RNA isolation for microarray analysis. Organoids were dissociated and sorted by flow cytometry (MoFlo, DAKO) as described above (Barker et al., 2010). Several independent samples were analysed for each condition. EGFP^{hi} stem cells were collected in Trizol LS (Invitrogen)

4

and RNA isolated by using RNeasy Micro RNA Extraction Kit (Qiagen). RNA concentration and quality was determined using a NanoDrop (NanoDrop Technologies, Wilmington, DE, USA) and Agilent 2100 Bioanalyzer (Agilent Technologies, Palo Alto, CA, USA), respectively. Fragmentation of cRNA, hybridization to genome-wide mRNA expression platform harboring 20819 unique genes (Affymetrix mouse gene ST1.1 Array Plate) and scanning was carried out according to the manufacturer's protocol (Affymetrix Inc., Santa Barbara, CA, USA) at the MicroArray Department of the AMC (Amsterdam, the Netherlands). Note that the array used 4 probe sets for *Cdx2*, covering the three exons of the gene, thus including the part of the gene that is still present in the *Cdx2^(null)* SI SCs. The expression data extracted from the raw files were normalized with the RMA-sketch algorithm from Affymetrix Power Tools. Pair-wise scatter plot and volcano plot were generated by using the R2 web application, which is freely available at http://r2.amc.nl "Microarray analysis and visualization platform". False discovery rate (FDR) statistical method was used to correct for multiple comparisons test. An expression difference of two-fold (Log_2 fold) and a level of significance of $p<0.05$ (t-test) was defined as a threshold for significantly changed genes. Cluster analysis was performed by using Cluster 3.0 and Tree View 1.60 softwares. An expression difference of two-fold (Log_2 fold) was defined as a threshold for significantly changed genes. Microarray data have been deposited in Gene Expression Omnibus (accession number GSE51751).

RNA extraction from organoids and RNA-Seq. Organoids were freed from Matrigel and resuspended in RLT buffer (Qiagen). RNA was extracted from *Cdx2^(null)* SI, control SI, and control Sto organoids using the RNeasy Mini RNA Extraction Kit (Qiagen). For mRNA sequencing 10 ng of total RNA was used as starting material. The RNA was processed using the CEL-Seq protocol (Hashimshony et al., 2012)and sequenced on an Illumina Nextseq using 75 bp paired end sequencing. After sequencing read 1 was aligned to the mm10 RefSeq mouse transcriptome downloaded from the UCSC genome browser (Meyer et al., 2013) using bwa (Li and Durbin, 2010)with default parameters. Read 2 contains a barcode identifying the sample from which the read originated. CEL-Seq only sequences the most 3' end of a transcript and generates one read per transcript. Samples were rpm (reads per million) normalized. Only genes with more than 10 rpm in at least 4 samples were used for subsequent analysis. Sequencing data have been deposited in Gene Expression Omnibus under accession number GSE62784.

***Cdx2* ectopic expression in wild-type stomach organoids**. Full-length *Cdx2* cDNA was cloned behind the PGK promoter into Sal1 and Xho1 restriction sites of the pLV_pGK_2A_dsRED_IRES-Puro plasmid (generous gift from Henner Farin from the Clevers lab) using the following primers:

forward, GAACTAAACCGTCGACGCCACCATGTACGTGAGCTACCTT;

reverse, CGCTTCCGGACTCGAGCTGGGTGACAGTGGAGTTTAAAAC.

To generate a lentiviral stock expressing *Cdx2*, the Human Embryonic Kidney 293T (HEK 293T) cells were cultured in 10% FCS DMEM in a 150 cm dish, to a confluency of about 80%. Cells were transiently transfected with the *Cdx2* expressing vector (30µg) in the presence of polyethylenimine (PEI) (Polysciences) in serum-free DMEM, according to the manufacturer's instructions. The medium was changed once on the next day to remove PEI. After two more days, the medium was collected, passed through a 0.45-µm filter and centrifuged it at 8000*g* overnight at 4°C. The supernatant was discarded and the pellet resuspended in 500 µl of infection medium (stomach medium plus 10 mM nicotinamide (Sigma-Aldrich) plus 10 µM Y27632 (p160 ROCK inhibitor, Sigma-Aldrich) plus 8 µg ml^{-1} Polybrene (Sigma-Aldrich).

Stomach organoids were infected by a lentiviral suspension and cultured under puromycin selection according to the protocol previously described by Koo *et al*, (Koo et al., 2012) modified as follows. In brief, about 500 organoids were transferred to a 15-ml Falcon tube, and dissociated with a fire-polished glass pipette. Organoid fragments were incubated with TripLE Express (GIBCO) for 5 min at 37 °C. Medium containing 5% serum was added, and the cells were pelleted at 400*g* for 5 min. The supernatant was discarded and the cell clusters resuspended in 500 µl of infection medium (see above). Cell clusters were combined with 500 µl of viral suspension and transferred into 4 wells of a 48-well culture plate. The plate was centrifuged at 600*g* at 32 °C for 60 min, and placed for another 6 h in an incubator at 37 °C. After this time, the cells were collected, transferred into 1.5 ml Eppendorf tube and spun them down at 400*g* for 5 min. The supernatant was discarded, and the pellet was resuspended in 100 µl Matrigel (BD Biosciences) and distributed to two wells of a 24-well culture plate. 500 µl of infection medium without polybrene was added per well. Two days after infection, the medium was refreshed and puromycin (2 µg ml^{-1}) was added. Organoids were maintained in Sto culture conditions and passaged every week. Marker dsRed expression was scored and Cdx2 protein expression assayed by immunofluorescence.

4

References

Barker, N., Huch, M., Kujala, P., van de Wetering, M., Snippert, H.J., van Es, J.H., Sato, T., Stange, D.E., Begthel, H., van den Born, M.*, et al.* (2010). Lgr5(+ve) stem cells drive self-renewal in the stomach and build long-lived gastric units in vitro. Cell stem cell *6*, 25-36.

Barker, N., van Es, J.H., Kuipers, J., Kujala, P., van den Born, M., Cozijnsen, M., Haegebarth, A., Korving, J., Begthel, H., Peters, P.J.*, et al.* (2007). Identification of stem cells in small intestine and colon by marker gene Lgr5. Nature *449*, 1003-1007.

Beck, F., Chawengsaksophak, K., Luckett, J., Giblett, S., Tucci, J., Brown, J., Poulsom, R., Jeffery, R., and Wright, N.A. (2003). A study of regional gut endoderm potency by analysis of Cdx2 null mutant chimaeric mice. Developmental biology *255*, 399-406.

Chawengsaksophak, K., James, R., Hammond, V.E., Kontgen, F., and Beck, F. (1997). Homeosis and intestinal tumours in Cdx2 mutant mice. Nature *386*, 84-87.

Coskun, M., Troelsen, J.T., and Nielsen, O.H. (2011). The role of CDX2 in intestinal homeostasis and inflammation. Biochimica et biophysica acta *1812*, 283-289.

Hashimshony, T., Wagner, F., Sher, N., and Yanai, I. (2012). CEL-Seq: single-cell RNA-Seq by multiplexed linear amplification. Cell reports *2*, 666-673.

Hinoi, T., Lucas, P.C., Kuick, R., Hanash, S., Cho, K.R., and Fearon, E.R. (2002). CDX2 regulates liver intestine-cadherin expression in normal and malignant colon epithelium and intestinal metaplasia. Gastroenterology *123*, 1565-1577.

Hryniuk, A., Grainger, S., Savory, J.G., and Lohnes, D. (2012). Cdx function is required for maintenance of intestinal identity in the adult. Developmental biology *363*, 426-437.

Ikeda, H., Sasaki, M., Ishikawa, A., Sato, Y., Harada, K., Zen, Y., Kazumori, H., and Nakanuma, Y. (2007). Interaction of Toll-like receptors with bacterial

components induces expression of CDX2 and MUC2 in rat biliary epithelium in vivo and in culture. Laboratory investigation; a journal of technical methods and pathology *87*, 559-571.

Koo, B.K., Stange, D.E., Sato, T., Karthaus, W., Farin, H.F., Huch, M., van Es, J.H., and Clevers, H. (2012). Controlled gene expression in primary Lgr5 organoid cultures. Nature methods *9*, 81-83.

Lee, H.S., Lee, H.K., Kim, H.S., Yang, H.K., Kim, Y.I., and Kim, W.H. (2001). MUC1, MUC2, MUC5AC, and MUC6 expressions in gastric carcinomas: their roles as prognostic indicators. Cancer *92*, 1427-1434.

Leung, W.K., Yu, J., Chan, F.K., To, K.F., Chan, M.W., Ebert, M.P., Ng, E.K., Chung, S.C., Malfertheiner, P., and Sung, J.J. (2002). Expression of trefoil peptides (TFF1, TFF2, and TFF3) in gastric carcinomas, intestinal metaplasia, and non-neoplastic gastric tissues. The Journal of pathology *197*, 582-588.

Li, H., and Durbin, R. (2010). Fast and accurate long-read alignment with Burrows-Wheeler transform. Bioinformatics *26*, 589-595.

Mari, L., Milano, F., Parikh, K., Straub, D., Everts, V., Hoeben, K.K., Fockens, P., Buttar, N.S., and Krishnadath, K.K. (2014). A pSMAD/CDX2 Complex Is Essential for the Intestinalization of Epithelial Metaplasia. Cell reports *7*, 1197-1210.

Maunoury, R., Robine, S., Pringault, E., Leonard, N., Gaillard, J.A., and Louvard, D. (1992). Developmental regulation of villin gene expression in the epithelial cell lineages of mouse digestive and urogenital tracts. Development *115*, 717-728.

Mesquita, P., Jonckheere, N., Almeida, R., Ducourouble, M.P., Serpa, J., Silva, E., Pigny, P., Silva, F.S., Reis, C., Silberg, D.*, et al.* (2003). Human MUC2 mucin gene is transcriptionally regulated by Cdx homeodomain proteins in gastrointestinal carcinoma cell lines. The Journal of biological chemistry *278*, 51549-51556.

Meyer, L.R., Zweig, A.S., Hinrichs, A.S., Karolchik, D., Kuhn, R.M., Wong, M., Sloan, C.A., Rosenbloom, K.R., Roe, G., Rhead, B.*, et al.* (2013). The UCSC Genome Browser database: extensions and updates 2013. Nucleic

4

acids research *41*, D64-69.

Munoz, J., Stange, D.E., Schepers, A.G., van de Wetering, M., Koo, B.K., Itzkovitz, S., Volckmann, R., Kung, K.S., Koster, J., Radulescu, S.*, et al.* (2012). The Lgr5 intestinal stem cell signature: robust expression of proposed quiescent '+4' cell markers. The EMBO journal *31*, 3079-3091.

Mutoh, H., Hakamata, Y., Sato, K., Eda, A., Yanaka, I., Honda, S., Osawa, H., Kaneko, Y., and Sugano, K. (2002). Conversion of gastric mucosa to intestinal metaplasia in Cdx2-expressing transgenic mice. Biochemical and biophysical research communications *294*, 470-479.

Naito, Y., Oue, N., Hinoi, T., Sakamoto, N., Sentani, K., Ohdan, H., Yanagihara, K., Sasaki, H., and Yasui, W. (2012). Reg IV is a direct target of intestinal transcriptional factor CDX2 in gastric cancer. PloS one *7*, e47545.

Sato, T., van Es, J.H., Snippert, H.J., Stange, D.E., Vries, R.G., van den Born, M., Barker, N., Shroyer, N.F., van de Wetering, M., and Clevers, H. (2011). Paneth cells constitute the niche for Lgr5 stem cells in intestinal crypts. Nature *469*, 415-418.

Sato, T., Vries, R.G., Snippert, H.J., van de Wetering, M., Barker, N., Stange, D.E., van Es, J.H., Abo, A., Kujala, P., Peters, P.J.*, et al.* (2009). Single Lgr5 stem cells build crypt-villus structures in vitro without a mesenchymal niche. Nature *459*, 262-265.

Sheng, Y.H., Triyana, S., Wang, R., Das, I., Gerloff, K., Florin, T.H., Sutton, P., and McGuckin, M.A. (2013). MUC1 and MUC13 differentially regulate epithelial inflammation in response to inflammatory and infectious stimuli. Mucosal immunology *6*, 557-568.

Silberg, D.G., Sullivan, J., Kang, E., Swain, G.P., Moffett, J., Sund, N.J., Sackett, S.D., and Kaestner, K.H. (2002). Cdx2 ectopic expression induces gastric intestinal metaplasia in transgenic mice. Gastroenterology *122*, 689-696.

Silberg, D.G., Swain, G.P., Suh, E.R., and Traber, P.G. (2000). Cdx1 and cdx2 expression during intestinal development. Gastroenterology *119*, 961-971.

Stange, D.E., Koo, B.K., Huch, M., Sibbel, G., Basak, O., Lyubimova, A., Kujala, P., Bartfeld, S., Koster, J., Geahlen, J.H.*, et al.* (2013). Differentiated Troy+ chief cells act as reserve stem cells to generate all lineages of the stomach epithelium. Cell *155*, 357-368.

Stringer, E.J., Duluc, I., Saandi, T., Davidson, I., Bialecka, M., Sato, T., Barker, N., Clevers, H., Pritchard, C.A., Winton, D.J.*, et al.* (2012). Cdx2 determines the fate of postnatal intestinal endoderm. Development *139*, 465-474.

van der Flier, L.G., Haegebarth, A., Stange, D.E., van de Wetering, M., and Clevers, H. (2009). OLFM4 is a robust marker for stem cells in human intestine and marks a subset of colorectal cancer cells. Gastroenterology *137*, 15-17.

Verzi, M.P., Shin, H., He, H.H., Sulahian, R., Meyer, C.A., Montgomery, R.K., Fleet, J.C., Brown, M., Liu, X.S., and Shivdasani, R.A. (2010). Differentiation-specific histone modifications reveal dynamic chromatin interactions and partners for the intestinal transcription factor CDX2. Dev Cell *19*, 713-726.

Verzi, M.P., Shin, H., Ho, L.L., Liu, X.S., and Shivdasani, R.A. (2011). Essential and redundant functions of caudal family proteins in activating adult intestinal genes. Molecular and cellular biology *31*, 2026-2039.

Xu, Y., Watanabe, T., Tanigawa, T., Machida, H., Okazaki, H., Yamagami, H., Watanabe, K., Tominaga, K., Fujiwara, Y., Oshitani, N.*, et al.* (2010). Bile acids induce cdx2 expression through the farnesoid x receptor in gastric epithelial cells. Journal of clinical biochemistry and nutrition *46*, 81-86.

Yamamoto, H., Bai, Y.Q., and Yuasa, Y. (2003). Homeodomain protein CDX2 regulates goblet-specific MUC2 gene expression. Biochemical and biophysical research communications *300*, 813-818.

4

Supplementary Materials

4
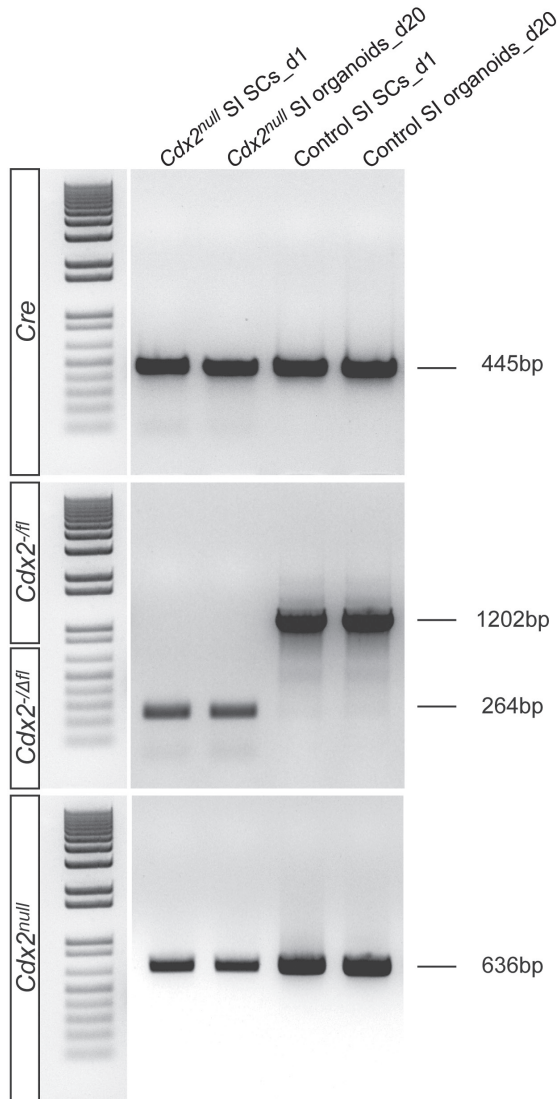
Supplementary Fig. 1. Genotyping of *Cdx2^{null}* and control SI SCs at different time points of the cultures. Shown here are the diagnostic PCR results for FACS-sorted *Cdx2^{-fl}/Lgr5-EGFP-Ires-CreERT2* SI SC samples after treatment with 4-hydroxytamoxifen (*Cdx2^{null}*) or untreated (control). The *Cre* allele and one *Cdx2^{null}* allele are present everywhere, the *Cdx2^{fl}* allele is present solely in the absence of 4-hydroxytamoxifen (control), and the inactivated *Cdx2^{Δfl}* allele is present solely in the presence of 4-hydroxytamoxifen (*Cdx2^{null}*). Genotyping was performed on samples of clonal cultures one day after 4-hydroxytamoxifen treatment and repeated after two passages to verify homogeneity of the *Cdx2^{null}* organoids.

a

b

c
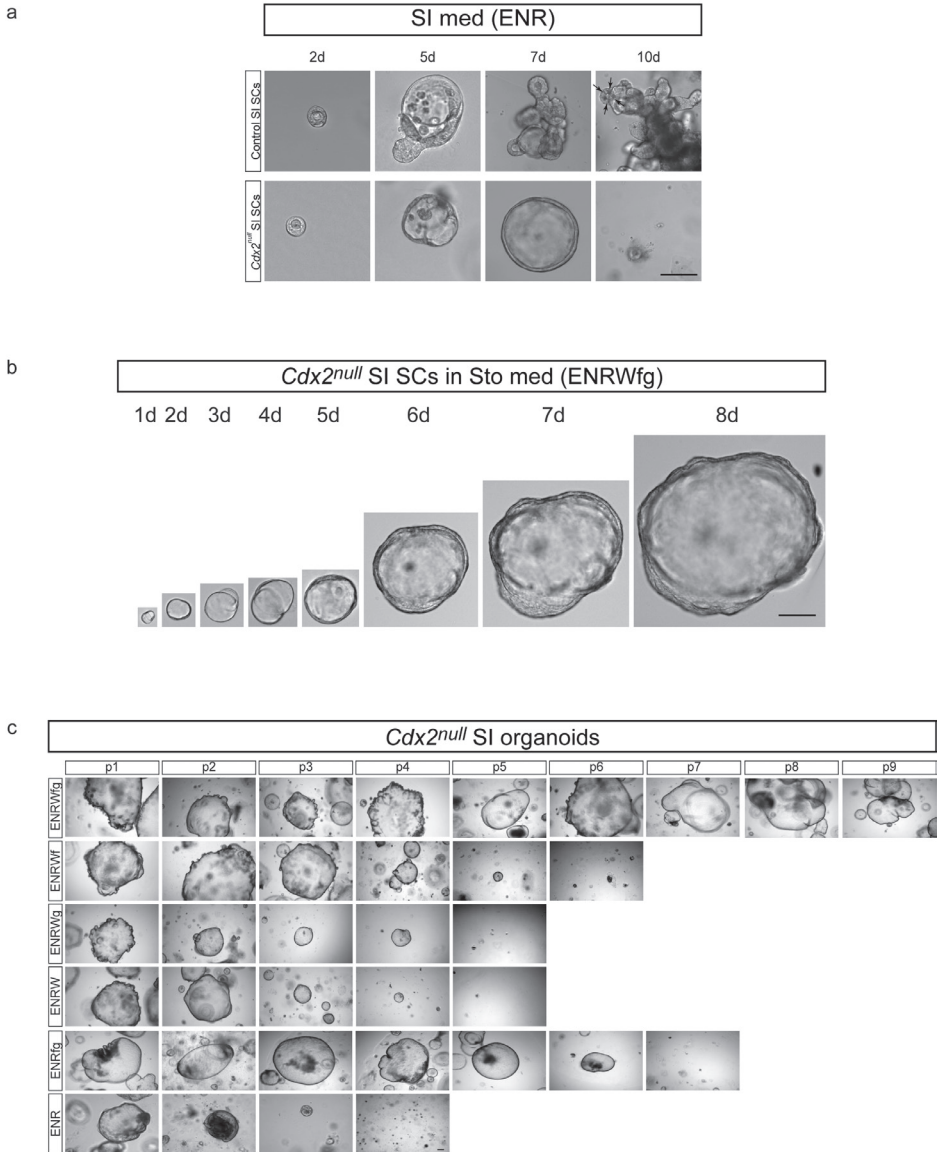
Supplementary Fig. 2. *Cdx2null* SI SCs require stomach growth conditions and generate stomach organoids. a. *Cdx2null* SI SCs fail to generate buds and instead become cystic and die in intestinal medium ENR, whereas their control counterpart grow, generate numerous buds and can be passaged indefinitely. Arrows indicate Paneth cells. **b.** Isolated *Cdx2null* SI SCs grow as gastric organoids in stomach medium, ENRWfg, containing ENR supplemented with Wnt3a (W), Fgf10 (f) and Gastrin (g). **c.** *Cdx2null* small intestinal organoids totally depend on the stomach-specific organoid conditions to grow. Views of a growing culture of SC-derived *Cdx2null* SI organoids, in stomach medium ENRWfg (first row); the first 9 of a large number of passages are shown. The following rows show the evolution of such cultures when deprived of, respectively Gastrin (second row), Fgf10 (third row), Fgf10 and Gastrin (fourth row), Wnt3a (fifth row), and Wnt3a, Fgf10 and Gastrin (last row). The latter condition (ENR or SI medium) does not allow the culture to be passaged more than once or twice. Bar, 150 µm. med, medium.
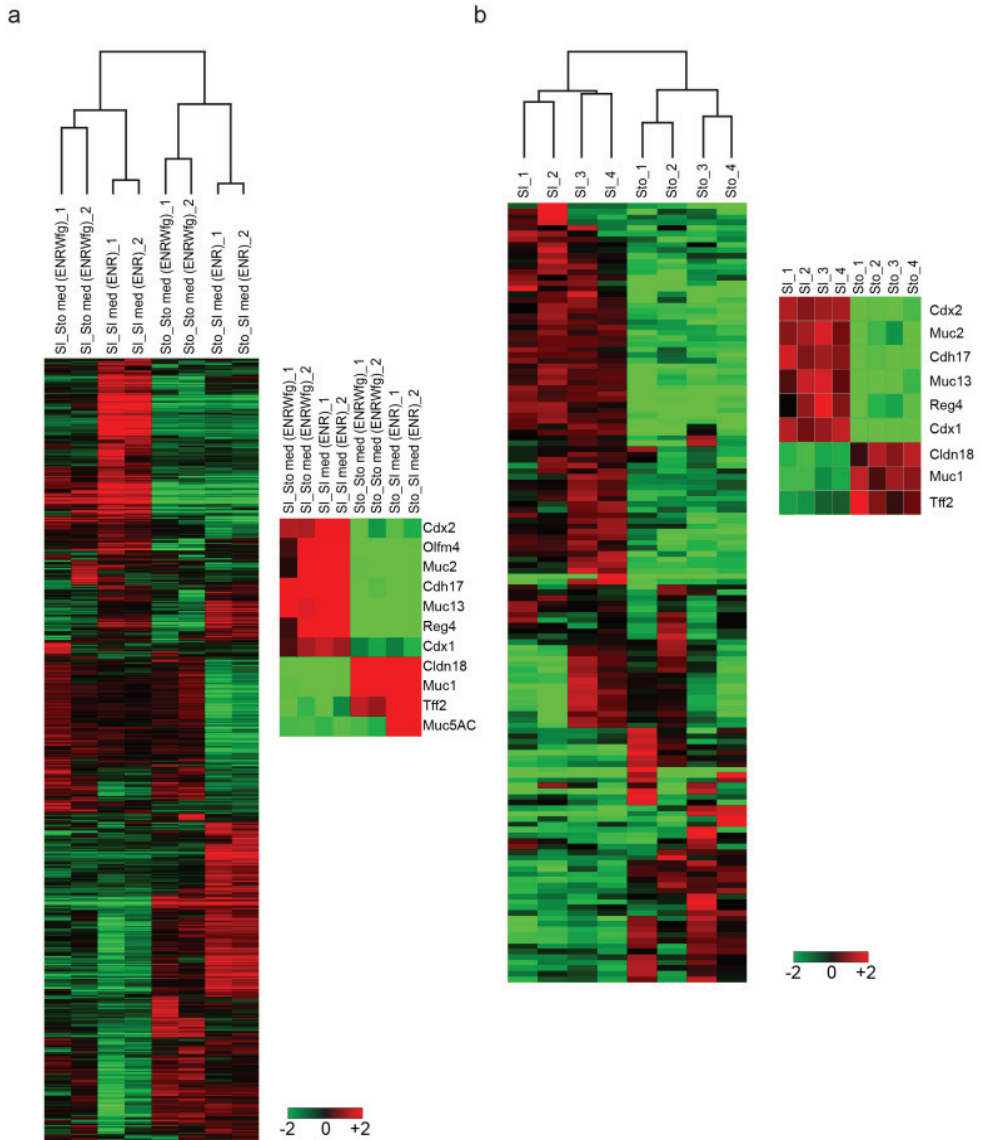
Supplementary Fig. 3. Organoids express an organ-specific signature independently of the culture conditions. a. Comparison of the transcriptional profiles by microarray analysis of two independent replicates of SI and Sto samples cultured in either SI or Sto conditions. Hierarchical clustering shows that the SI samples separate from Sto samples no matter in which medium they are cultured. Heatmap with specific markers on the right shows the expression of intestinal and gastric markers relevant for SCs identity and confirms that the culture conditions do not alter the intestinal or gastric signature of these SCs. Intestinal markers, *Cdx2, Olfm4, Muc2, Cdh17, Muc13, Reg4* and *Cdx1*; gastric markers, *Cldn18, Muc1, Tff2* and *Muc5AC*. **b.** mRNA sequencing data showing Log_2 fold changes in gene expression in Sto and SI organoids grown in the same stomach medium (4 independent samples), compared to the mean across all samples in the analysis. Genes with at least a two-fold change compared to the mean are included in the heatmap. For scaling purposes genes that have more than four-fold change are depicted as four-fold change. Inset on the right shows a selection of marker genes for intestine (*Cdx2, Muc2, Cdh17, Muc13, Reg4* and *Cdx1*) or stomach (*Cldn18, Muc1* and *Tff2*). med, medium.
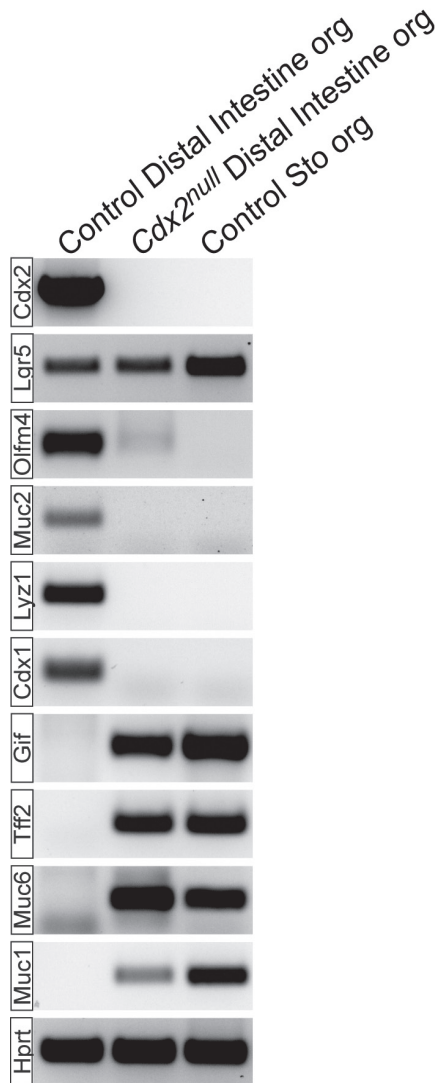
Supplementary Fig. 4. SCs from the distal small intestine also convert to Sto SCs in the absence of Cdx2. RT PCR experiments using RNA from SC-derived control distal intestinal organoids (first column), *Cdx2null* distal intestinal organoids (second column) and control Sto organoids (third column), all grown in gastric conditions; intestinal markers *Olfm4, Muc2, Lyz1,* and *Cdx1,* are expressed in control distal intestinal organoids and fail to be expressed in *Cdx2null* distal intestinal organoids; gastric markers *Gif, Tff2, Muc6,* and *Muc1* are not expressed in distal intestinal organoids but strongly upregulated in *Cdx2null* distal intestinal organoids. This experiment was performed three times using independently generated samples. org, organoids.

4

131
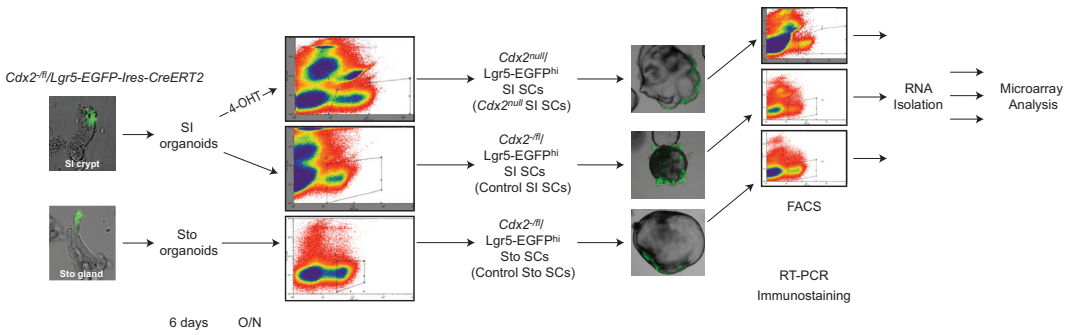
Supplementary Fig. 5. Structure of the experiments to characterize single clones of *Cdx2^null* SI SCs versus controls. Each step of the protocol is described in the Methods section (Generating organoids from intestinal crypts and stomach glands, Single cell sorting and organoid culture, and Cell sorting and RNA isolation for microarray analysis).

4
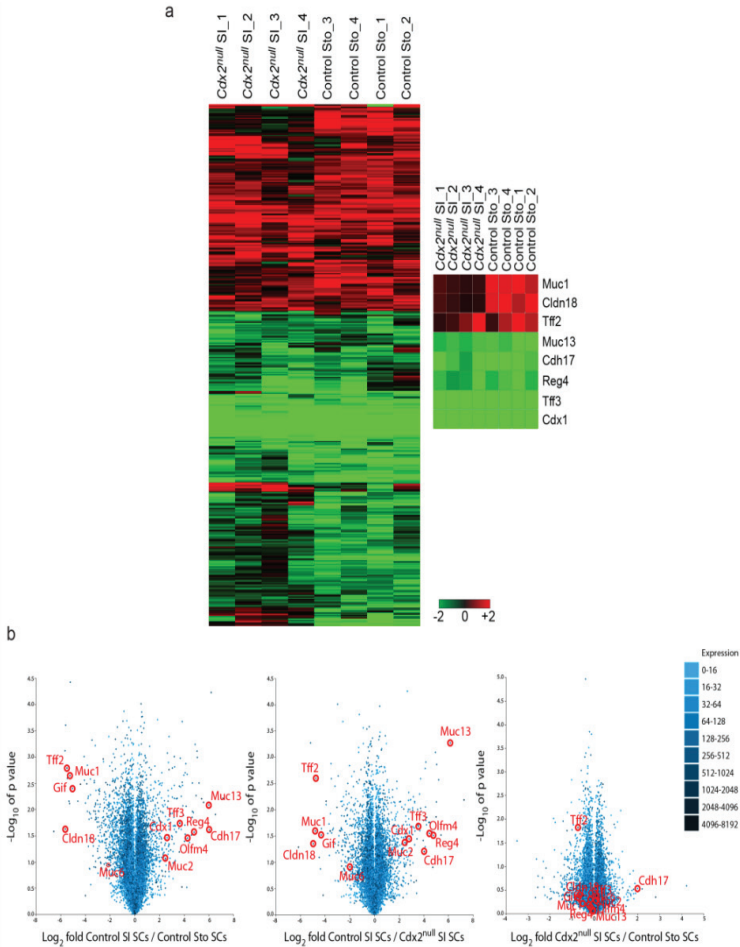
Supplementary Fig. 6. a. Transcription profile of additional SC-derived *Cdx2^null* SI versus Sto control organoids. mRNA sequencing data comparing Log$_2$ fold changes in SC-derived *Cdx2^null* SI and

control Sto organoids (4 independent samples of each), each relatively to control SI organoids (mean of 4 independent samples). Genes with at least an average of two-fold change compared to the control SI organoids are included in the heatmap. For scaling purposes genes that have a more than four-fold change are depicted as four-fold change. Extraction of data corresponding to stomach markers (*Muc1, Cldn18* and *Tff2*) intestinal (*Muc13, Cdh17*, *Reg4*, *Tff3* and *Cdx1*) and is shown on the right. The comparison stresses the similarity between *Cdx2null* SI and control Sto organoids. **b. Quantitative statistical analysis of the transcription changes measured by microarray between *Cdx2null* SI SCs and controls.** Pairwise volcano plot analysis of the microarray data shown in Fig. 3a (two independent samples of each type of SCs) shows the differences, using pair-wise comparisons, between *Cdx2null* SI SCs, control Sto SCs and control SI SCs. Each gene present on the Affimetrix array used is represented by a dot in the graphs, with darker color meaning higher expression level. In each graph, genes projecting on the x value zero do not show change in expression in the two samples compared. Per graph, genes indicated in red projecting on negative values on the x axis are decreased in expression in the first sample of the comparison versus the second, and genes indicated in red projecting on positive values of the x axis are increased in expression in the first sample of that comparison. Projections on the y axis indicate statistical significance ($-\text{Log}_{10}$ of p value). The genes highlighted in red are the same markers as highlighted in the heatmap of Fig. 3a, and this marker gene series overlaps with the gene series studied by independent direct quantitative RNA analysis (Fig. 4 and Supplementary Fig. 7).
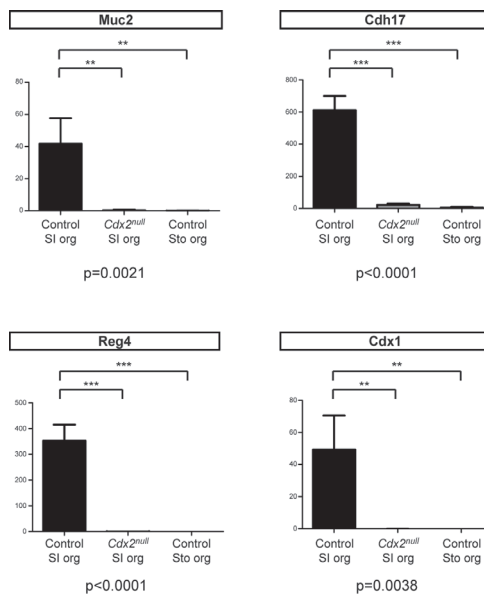
Supplementary Fig. 7. Assessment of the down regulation of Cdx2 targets in independent samples of *Cdx2null* SI versus controls. Direct Cdx2 targets normally expressed in control SI SCs such as *Muc2, Cdh17*, *Reg4* and *Cdx1* were considerably downregulated in the *Cdx2null* SI organoids compared with control SI organoids. These markers are lowly and similarly expressed in *Cdx2null* SI and in control Sto organoids. Quantitative RT PCR analysis was performed on three independent samples of each type of material. Values along the y axis are relative amounts of RNA normalized for *Gapdh* expression. Error bars are standard deviations. For each marker, one way analysis of variance according to the ANOVA test is indicated by the p value underneath the graph. p<0.05 indicates that the differences are significant. Tuckey's test for multiple comparison was run for pair-wise comparison of the means of the samples, with

*** meaning highly significant difference, ** very significant difference and * significant difference. See Methods for more details about statistical analysis. org, organoids.

Supplementary Fig. 8. Lentiviral expression construct used to force Cdx2 expression in Sto organoids. Full-length *Cdx2* cDNA was cloned behind the PGK promoter into Sal1 and Xho1 restriction sites of the pLV_pGK_2A_dsRED_IRES-Puro plasmid.
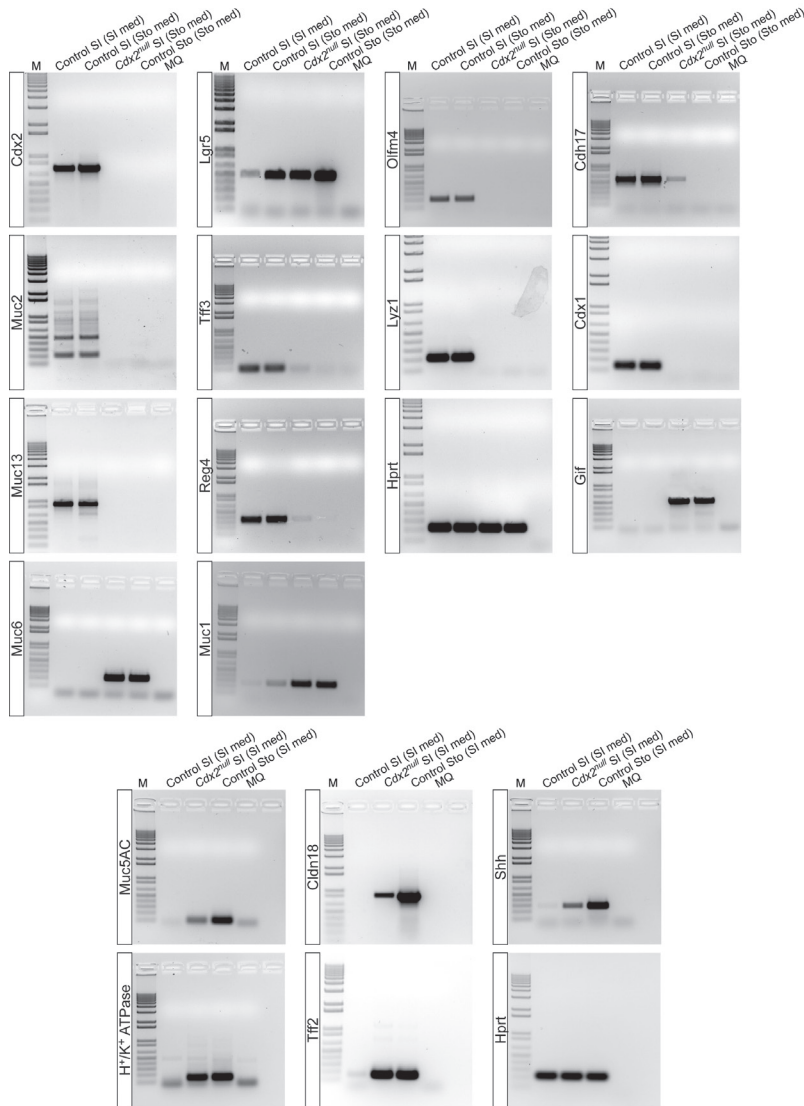
Supplementary Fig. 9. Full gels corresponding to the data shown in Fig. 2c and f.
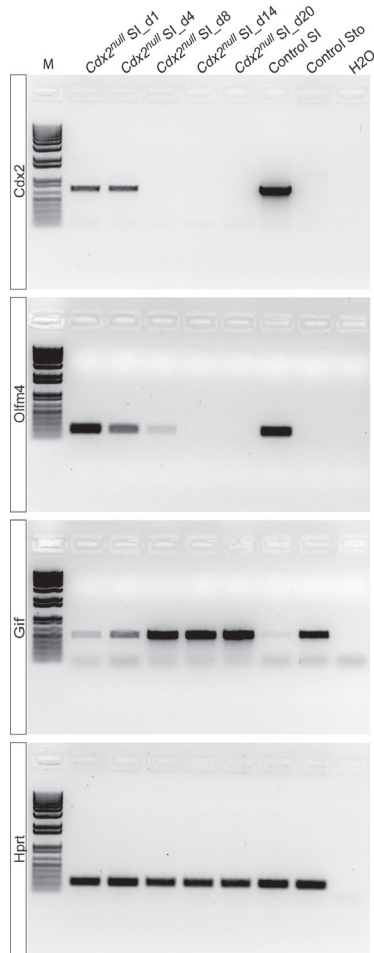
Supplementary Fig. 10. Full gels corresponding to the data shown in Fig. 4c left panel.

Supplementary Methods

Primers for genotyping

Primer	Sequence
Cre-For	CCGGGCTGCCACGACCAA
Cre-Rev	GGCGCGGCAACACCATTTTT
Cdx2^{fl}-For	TGGGGCAATCTTAATGGGTA
Cdx2^{fl}-Rev	TGTAGCCTCGACTTGGCTTT
Cdx2$^{\Delta fl}$-For	ACGCGTTCCAAGTGAAAGGA

Cdx2$^{\Delta fl}$-Rev	CGCTCTTTCTCTGTCCAAGTG
Cdx2^{null}-For	ATATTGCTGAAGAGCTTGGCGGC
Cdx2^{null}-For	TAAAAGTCAACTGTGTTCGGATCC

Primers for RT-PCR

Primer	Sequence
Cdx2-For	GTACACAGACCATCAGCGGC
Cdx2-Rev	CCACCCCATCCAGTCTCACT
Lgr5-For	TGCCATCTGCTTACCAGTGTTGT
Lgr5-Rev	ATTCCGTCTTCCCACCACGC
Olfm4-For	GCCACTTTCCAATTTCAC
Olfm4-Rev	GAGCCTCTTCTCATACAC
Cdh17-For	CAAGTCTGTGCACCAAGCAC
Cdh17-Rev	TGCCATAGCCAAGTTGGAGG
Muc2-For	GAACGGGGCCATGGTCAGCA
Muc2-Rev	CATAATTGGTCTGCATGCC
Lyz1-For	GAGAACCGAAGCACCGACTATG
Lyz1-Rev	CGGTTTTGACATTGTGTTCGC
Cdx1-For	GCTCACAGAGCGGCAGGTAA
Cdx1-Rev	GGTGTGGGAGTGCCATCCAG
Muc13-For	AAAACTCCAGGCAGCGAAGG
Muc13-Rev	AATGTCCCCAGGGAATGTCG
Reg4-For	GCCTTGCACAAACTCTTCCC
Reg4-Rev	TGGTTTGACAGAGACGCAGT
Tff3-For	TTGCTGGGTCCTCTGGGATA
Tff3-Rev	GACATTTGCCGGCACCATAC
Gif-For	TGAATCCTCGGCCTTCTATG
Gif-Rev	CAGTTAAAGTTGGTGGCACTT
Muc6-For	TGCATGCTCAATGGTATGGT
Muc6-Rev	TGTGGGCTCTGGAGAAGAGT
Tff2-For	ACCCGGGCATCAGTCCCGA
Tff2-Rev	GCAGCTCCCAGGGAACGGGT
Muc1-For	AGTACCAAGCGTAGCCCCTA

Muc1-Rev	AAGGGCATGAACAGCCTACC
Muc5AC-For	CATGACCTGTTATAGCTCCGA
Muc5AC-Rev	CTCAGTAACAACACAGCCTC
Cldn18-For	GCCTGTCTCTTGTCCTCTCC
Cldn18-Rev	CAGGTTGGCGGGTCTTAGAGC
Shh-For	TGATCCTTGCTTCCTCGCTG
Shh-Rev	CACCTCTGAGTCATCAGCCG
H+/K+ ATPase-For	GTTCCAGTGGTGGCTGGT
H+/K+ ATPase-Rev	GCTGATAGTGGATGGAGAGATG
Hprt-For	TCCTCAGACCGCTTTTTGCC
Hprt-Rev	GTGATGGCCTCCCATCTCCT

Primers for real time quantitative PCR

Primer	Sequence
Cdx2-For	TCCCTAGGAAGCCAAGTGAAA
Cdx2-Rev	AGTGAAACTCCTTCTCCAGCTC
Olfm4-For	GCCACTTTCCAATTTCAC
Olfm4-Rev	GAGCCTCTTCTCATACAC
Dach1-For	TTGAGACAAAACGCCGTGAG
Dach1-Rev	CGGTCAGCTTCTATCTCAGGG
Clca4-For	CCTGGAGGCTGAGTTTATAGGTG
Clca4-Rev	GAGCCAGAGAATGCCCACTC
Smoc2-For	ACAAGTCCATCACCGTGCAG
Smoc2-Rev	CAGCCGTTCATCCTTGTTTCC
Cdca7-For	GGAGTCCTGGTGTATCTGGC
Cdca7-Rev	ACGTCGAGAACAAGAGAGCC
Msi1-For	GGTTTCGGCCACAGTCTTG
Msi1-Rev	CTGGCTCAGTCTGGTCCTC
Gif-For	CCTGGGGCCTTATTGTCTCTTC
Gif-Rev	TGAAGTTGGCTGTGATGTGC
Col11a2-For	GATGAGCTGAGCCCTGAGAC
Col11a2-Rev	CTGCTCCAGTACAGGCGTG
Pgc-For	TGCCTACCCTCACTTTTGTCC

4

Pgc-Rev	CACTCTCAGCGTTCAGGGAG
Muc2-For	GAACGGGGCCATGGTCAGCA
Muc2-Rev	CATAATTGGTCTGCATGCC
Cdh17-For	CAAGTCTGTGCACCAAGCAC
Cdh17-Rev	TGCCATAGCCAAGTTGGAGG
Reg4-For	GCCTTGCACAAACTCTTCCC
Reg4-Rev	TGGTTTGACAGAGACGCAGT
Cdx1-For	GCTCACAGAGCGGCAGGTAA
Cdx1-Rev	GGTGTGGGAGTGCCATCCAG
Muc6-For	TGCATGCTCAATGGTATGGT
Muc6-Rev	TGTGGGCTCTGGAGAAGAGT
Tff2-For	ACCCGGGCATCAGTCCCGA
Tff2-Rev	GCAGCTCCCAGGGAACGGGT
Cldn18-For	GCCTGTCTCTTGTCCTCTCC
Cldn18-Rev	CAGGTTGGCGGGTCTTAGAGC
Gapdh-For	TTCACCACCATGGAGAAGGC
Gapdh-Rev	GGCATGGACTGTGGTCATGA

4

Chapter 5
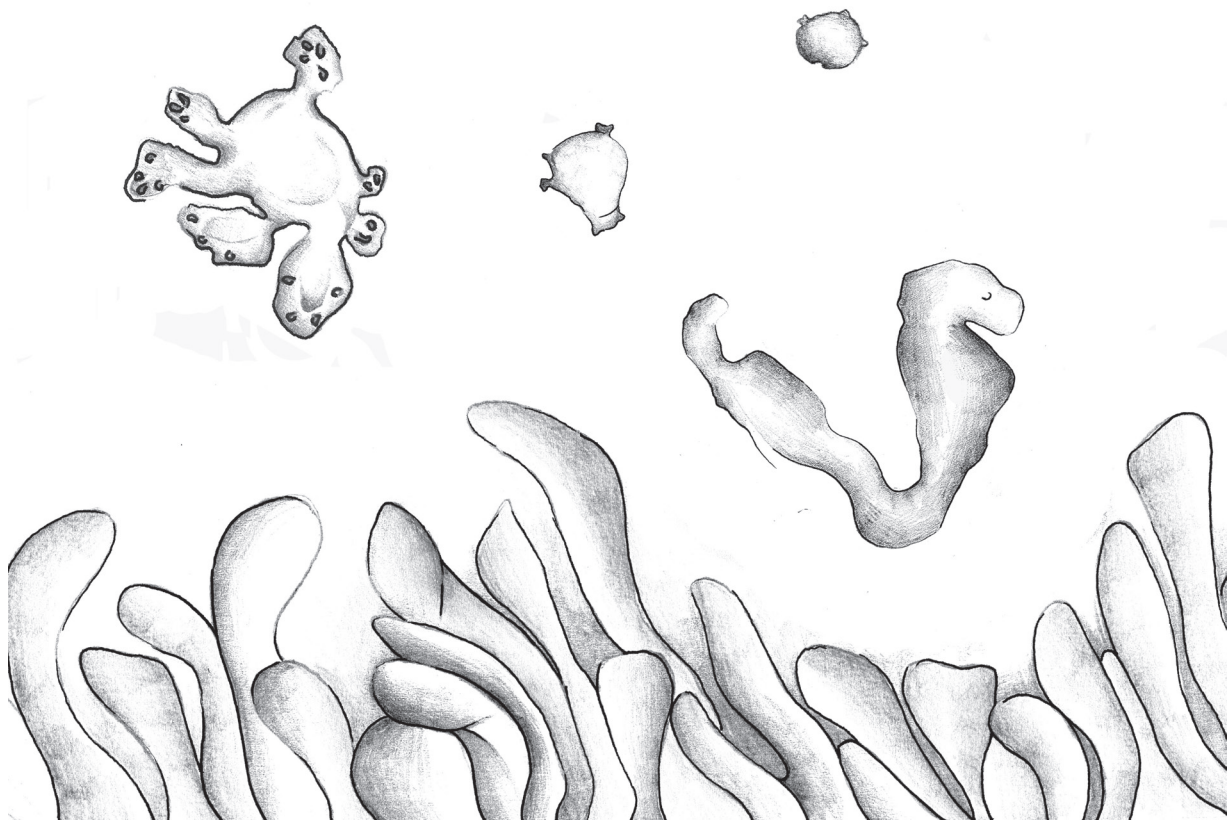
General Discussion
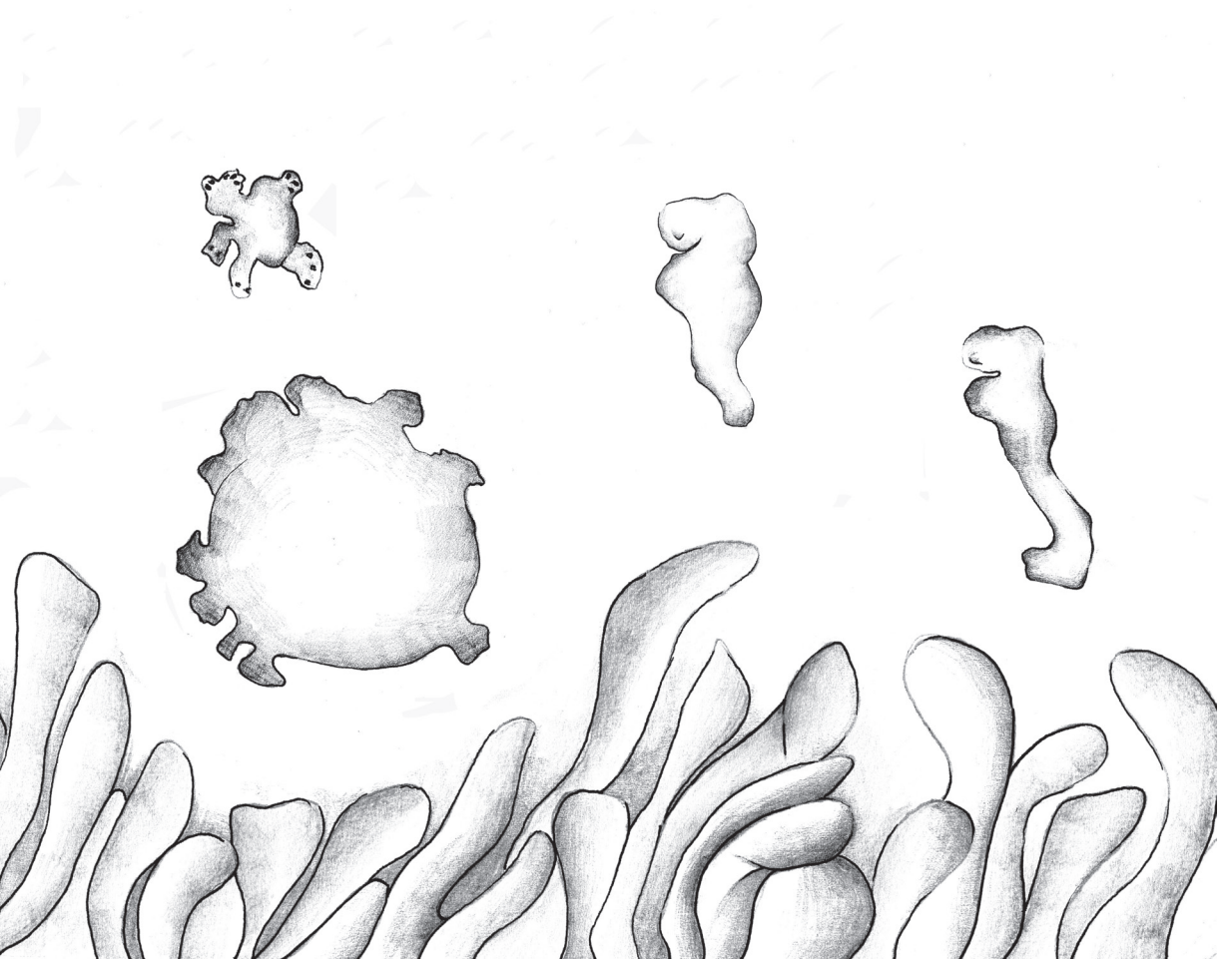
Cdx are evolutionary highly conserved genes that regulate formation and antero-posterior (AP) patterning of axial primordia during embryo development. In this thesis we demonstrated that the three mouse Cdx genes are essential during embryonic axial elongation to give rise to all post-occipital trunk and tail tissues (Chapter 2). We showed that *Cdx2* is required to the same extent as the well-known *T Brachyury* for tissue generation along the AP axis (Chapter 3). Furthermore, we characterized the fundamental role played by *Cdx2* in specifying identity and functions of the small intestinal stem cells (Chapter4). Our results indicate that Cdx genes play crucial roles in tissues of the three embryonic germ layers and adult mice.

Ancestral function of Cdx in AP axial elongation

Generation and characterization of triple Cdx mutant mouse embryos allowed us to reveal the extent of the role played by these three genes in the formation and patterning of all post-occipital primordia (see Chapter 2). The three mouse Cdx genes seem to have conserved most of the original function of their ancestor *caudal* (*cad*). *cad* plays crucial roles in tissue segmentation along the AP body axis and in mid/hindgut development in early *Drosophila* embryos. The maternally derived caudal protein is distributed in a posterior to anterior gradient and is involved in controlling the generation of the eighth abdominal segment. Subsequently a zygotic *cad* expression persists posteriorly, sustaining mid/hindgut development. *cad* mutants, lacking both maternal and zygotic contribution, show alteration of abdominal segments and loss of posterior terminalia (Macdonald and Struhl, 1986). Therefore it would seem reasonable to suggest that *cad* expression and function has been evolutionary conserved between fly fruit and mouse. However, the body of *Drosophila* is not generated by an axial elongation process. The fruit fly belongs to the long-germband arthropods in which all the body segments are laid down during the blastoderm stage. Therefore trunk and tail structures of the animal are not generated by posterior addition of tissues. In short-germband (this term includes also the intermediate-germband) arthropods species like *Gryllus Bimaculatus* (Shinmyo et al., 2005), *Artemia franciscana* and *Tribolium castaneum* (Copf et al., 2004), the most anterior segments are laid down in the blastoderm whereas more posterior segments are generated

sequentially from a posteriorly located presegmental zone, usually referred to as "growth zone" (Davis and Patel, 2002; Patel et al., 1989). It has been shown that disruption of *cad* expression in short-germband arthropods causes complete agenesis of post-occipital structures (Copf et al., 2004; Shinmyo et al., 2005). Interestingly, the truncation phenotype of Cdx^{null} mutant embryos, that we describe in Chapter 2, resembles the defects observed in short-germband arthropods, more than the phenotype observed in *Drosophila cad* mutants. In vertebrates and short-germband arthropods axial structures are generated sequentially from a self-renewing posteriorly located population of cells (Davis and Patel, 2002; Patel et al., 1989; Wilson et al., 2009). Caudal/Cdx genes support this process and specify the identities of the structures formed from the posterior growth zone during axial elongation. This seems to be an ancestral function of *caudal*, which has been lost in long-germband arthropods like *Drosophila melanogaster*.

Cdx and *T Brachyury* regulate distinct processes with different mechanisms

Previous evidence (Chawengsaksophak et al., 2004; Chawengsaksophak et al., 1997; Savory et al., 2009; Savory et al., 2011; van de Ven et al., 2011; van den Akker et al., 2002; van Nes et al., 2006; Young et al., 2009) together with our results reported in Chapter 2 (van Rooijen et al., 2012) indicate that Cdx genes participate in controlling axial elongation in a dosage dependent manner. In Chapter 4 we show that Cdx genes are also active in adult mice playing a crucial role in maintaining intestinal epithelium identity and functions throughout life. These observations raise the question whether Cdx genes regulate embryonic axial elongation and maintenance of the adult intestinal epithelium with the same mechanism.

Regarding the function of Cdx in embryonic axial elongation, Bialecka and colleagues (Bialecka et al., 2010) showed that these genes play an essential role in maintaining a signaling-dependent niche for the posterior axial progenitors. They transplanted GFP labeled-$Cdx2^{+/-}Cdx4^{null}$ mutant and wild-type-control axial progenitors into the node-streak border (NSB) region of unlabeled wild-type recipient mouse embryos. After a period of *in vitro* embryo culture they observed that mutant and wild-type GFP labeled progenitors contribute to the same extent to descendants in the elongating axis and in the posterior growth zone. This indicated that Cdx are non-cell-

autonomously required for axial progenitors activity during mouse embryonic trunk and tail formation. In the NSB/CNH of the posterior growth zone Cdx genes cooperate with signaling pathways to generate a unique niche for the progenitor cells to remain undifferentiated, to self-renew and to actively contribute descendants to the primordia of the axial structures for long periods of time (Bialecka et al., 2010). In the adult intestine, Cdx genes function in a cell-autonomous manner (Chapter 4). Cdx2 ablation, in *in vitro* cultured small intestinal stem cells (SI SCs), directly affected their self-renewal capability and their differentiation potential. Analysis of *Cdx2* mutant stem cells and SC-derived organoids which are endoderm epithelial devoid mesenchyme, allowed to demonstrate that *Cdx2* is cell-autonomously required in SI SCs for keeping them self-renewing and to maintain their intestinal identity. *Cdx2* is therefore at work in embryonic axial progenitors and in adult endoderm stem cells with a different mechanism. In both cases, more work will be required to elucidate the molecular mechanism involved.

The T-box protein-encoding gene, *T Brachyury*, shares part of its functions with *Cdx2* and, like *Cdx2*, it also plays multiple roles in embryos involving different mechanisms.

5

T Brachyury is an evolutionary highly conserved gene coding for a DNA-binding protein. In mouse, as well as in zebrafish, mutations in *T Brachyury* strongly affect notochord development and primitive streak maintenance. The phenotype of *T Brachyury*^{null} mouse embryos is also characterized by a significantly shorter allantois compared to the wild-type embryos. Generation of mouse chimeras from wild-type and *T Brachyury*^{null} ES cells (Rashbass et al., 1991) allowed to test to which extent *T Brachyury*^{null} embryonic defects could be rescued in the presence of wild-type cells. Rashbass and colleagues showed that only the allantois phenotype could be rescued suggesting that *T Brachyury* cell-autonomously controls notochord development and primitive streak activity, whereas it is required for allantois formation via regulating signaling pathways (Inman and Downs, 2006a, b; Rashbass et al., 1991).

The function of *T Brachyury* is conserved in axial elongation between mouse and zebrafish. Martin and colleagues have shown that *ntl*$^-$ or *ntl*$^-$/*bra*$^-$ cells from embryonic tailbud (zebrafish has two Brachyury genes) transplanted into wild-type embryos contribute to somites formation but not to notochord development indicating that zebrafish *T Brachyury*, cell-autonomously

controls notochord development, while regulating axial elongation in a non-cell-autonomous manner (Martin and Kimelman, 2008), like shown in the mouse (Bialecka et al., 2010). Moreover, it has been shown that Wnt and Fgf are intermediate factors downstream of Brachyury in axial elongation in both mouse and zebrafish (Martin and Kimelman, 2008; Yamaguchi et al., 1999).

In conclusion, although Cdx and *T Brachyury* genes encode transcription factors, thus acting in the cell that produces them, they also regulate processes in a non-cell-autonomous manner by controlling signaling pathways.

Cdx genes pattern posterior endoderm both in embryos and adult mice: an evolutionary conserved function?

Similarly to mesoderm and neuroectoderm, endoderm of the digestive tract is generated sequentially from anterior (foregut) to posterior (hindgut) during embryogenesis (see Introduction Fig.3). It is known that, when mutated, Cdx genes cause a variety of homeotic transformations that involve vertebral elements at different levels of the mouse AP axis (Subramanian et al., 1995; van den Akker et al., 2002; van Nes et al., 2006). Similarly, *Cdx2* loss in the endoderm leads to anteriorization of the identity of the hindgut epithelium both at embryonic stages and in adult mice (Beck et al., 1999; Chawengsaksophak et al., 1997; Gao et al., 2009; Grainger et al., 2010; Hryniuk et al., 2012; Stringer et al., 2012; Verzi et al., 2010). *Cdx2^{null}* SI SCs and organoids show a global downregulation of intestinal markers and a significant upregulation of several stomach specific genes (Chapter 4). This, together with the potential exhibited by *Cdx2^{null}* SI SCs to support generation of all stomach cell types, suggests that *Cdx2* in the intestine acts as suppressor of foregut differentiation program (Verzi et al., 2010). ChIP-Seq experiments performed on villi fractions of adult intestinal tissues showed the direct involvement of Cdx2 in controlling intestinal gene expression. No direct binding has been detected on stomach specific genes, even though stomach markers were upregulated in *Cdx2^{null}* mouse mutant intestine (Verzi et al., 2010). These results indicated that Cdx2 directly controls intestinal specific genes while it indirectly suppresses foregut gene expression. However, the rapidity of the transcriptional response of stomach genes to Cdx2 inactivation, observed in our experiments (see Chapter 4), could also indicate a primary involvement of Cdx2 in inhibiting foregut genes in the SI SCs of the crypts.

Therefore, in order to definitely complete the functional characterization of Cdx2 in the endoderm epithelium of the adult mouse it will be necessary to reveal its direct targets by ChIP-Seq analysis in stem cells of the intestine.

We mentioned earlier in this section that *caudal* also plays an important role during mid/hindgut development in *Drosophila*. Disruption of normal *cad* expression in the fruit fly affects the correct formation of the posterior segments including the hindgut. Induction of cad mutations at larval stages led to failure of hindgut development and homeotic transformation of the analia epithelium into male genitalia (normally more anteriorly formed) in adults (Moreno and Morata, 1999). This suggests that in *Drosophila*, as in vertebrates (Sherwood et al., 2009), *cad* is also required for hindgut development. While the crucial role played by *Cdx2* in the adult mouse intestinal stem cells has been largely described (Chapter 4), little is known about *cad* functions in the gut of the adult fruit fly. Interestingly, *Drosophila* adult intestinal epithelium also harbors stem cells that ensure function and renewal of the tissue throughout adult life (Micchelli and Perrimon, 2006; Ohlstein and Spradling, 2006). Therefore, given the high conservation of *cad* during evolution, it would be interesting to test whether the role of Cdx2 in the adult intestinal stem cells represents another evolutionary conserved mechanism.

T Brachyury and its evolutionary conserved functions: involvement in endoderm before mesoderm?

In vertebrates, *T Brachyury* is initially expressed in all nascent mesodermal cells. As development proceeds, *T Brachyury* expression becomes restricted to the notochord and tailbud (Kispert and Herrmann, 1994; Knezevic et al., 1997; Wilkinson et al., 1990) and is necessary for AP axial elongation (Wilson and Beddington, 1997). Because mollusc larval *Brachyury* shows an expression pattern similar to that in vertebrates, it has been speculated that the role of T Brachyury in controlling AP patterning might be conserved among all bilaterians (Kispert et al., 1994). However, the *T Brachyury* otholog of arthropods, *brachyenteron* (*byn*), is exclusively expressed in the posterior terminal region where it is required for endoderm descendants in hindgut and anal pads (Kispert et al., 1994).

Interestingly, *T Brachyury* might also play a role in endoderm development of the mouse. It is expressed in the mesoendodermal cell populations (Singer et al., 1996) emerged from the anterior part of primitive streak (Rodaway et

al., 1999) and later in part of the hindgut endoderm (unpublished data from S.S. and J.D.). The involvement of T Brachyury in endoderm development has also been suggested by Kubo and colleagues who demonstrated that a *T Brachyury* expressing ES cells population displays the potential to produce endoderm beside mesoderm (Kubo et al., 2004). Recently, ChIP-Seq experiments on ES cells cultured *in vitro* and differentiated into primitive streak-like cells, revealed T Brachyury binding sites on genes involved in endoderm formation (Lolas et al., 2014). Furthermore, direct T Brachyury binding (Lolas et al., 2014) was found on the endoderm transcriptional regulators *Foxa2* and *Sox17* (Drukker et al., 2012).

All these observations suggest that the involvement of T Brachyury in mouse endoderm development could correspond to ancestral function in endoderm generation and patterning. Possibly, it is only more recently in evolution that T Brachyury gained a function in controlling mesoderm specification and notochord development. This could have occurred when the midline structure in arthropods (the gut) became backed by a rod like mesodermal structure that later on would be included in the vertebral column, the notochord. Although notochord (of chordates) and gut (of arthropods) differentiate from different germ layers (from mesoderm and from endoderm respectively), they share a similar longitudinal features and position in the midline of the embryo. These observations lead to the speculation that chordate notochord derived from a hindgut-like structure in insects (Kispert et al., 1994). This would imply a common evolutionary origin for the hindgut of insects and the notochord of chordates, and a crucial function of *T Brachyury* in both.

5

Cdx2: from extension and patterning of the embryonic endoderm, to identity specification of adult intestinal stem cells

Sherwood and colleagues (Sherwood et al., 2009) proposed a model for endoderm development (see Introduction Fig. 3). During gastrulation, Nodal signaling, anteriorly, and Wnt and Fgf signaling, posteriorly, initiate AP patterning defining two mutually exclusive and molecularly distinct domains. These domains are characterized by the anterior expression of *Sox2* and the posterior expression of *Cdx2* (Sherwood et al., 2009). Later on, *Cdx2* plays a crucial role as master regulator of extension and patterning of the

hindgut (see Introduction Fig.3). Loss of function of *Cdx2* before E8.5 blocks the extension of the axis affecting all three germ layers, among which the endoderm (Chawengsaksophak et al., 2004; Savory et al., 2009; Young et al., 2009). *Cdx2* ablation at later stages, E9.5 (Gao et al., 2009) and E13.5 (Grainger et al., 2010), affects the patterning of the hindgut leading to homeotic transformation of the epithelium into esophagus (Gao et al., 2009) or stomach (Grainger et al., 2010), respectively. Several other studies focused on elucidating the function of Cdx2 in the intestinal epithelium, but mainly in adults (Beck et al., 1999; Chawengsaksophak et al., 1997; Hryniuk et al., 2012; Stringer et al., 2012; Verzi et al., 2010; Verzi et al., 2011). In particular the study of Stringer and colleagues (Stringer et al., 2012), and our Chapter 4, revealed the fundamental role played by *Cdx2* in maintaining the identity and supporting the functions of the adult intestinal stem cells. Despite all these studies on Cdx2 in the adult intestine, little is still known about whether Cdx2 is involved in the initial specification of the Lgr5-positive adult intestinal stem cells in the fetus, and whether it plays a role or not in crypts/villi formation (villogenesis).

The first Lgr5 expression in the gut endoderm can be detected in the fetal intestine at E15 (Garcia et al., 2009). At this stage the hindgut epithelium undergoes villogenesis with the definition of crypts and villi structures characteristic of the adult intestine. Mustata and colleagues (Mustata et al., 2013) demonstrated that before (E14) and during the complete period of specification of the Lgr5-positive adult stem cells (from E15 until P5) other progenitor cells are responsible for the generation of the fetal intestinal epithelium. These progenitors are characterized by the expression of the *Trop2* and *Cnx43* markers and give rise to spheroids when cultured *in vitro*. Analysis of the gene expression profile of intestinal spheroids showed higher expression of gastric and esophageal markers compared to the profile of the adult intestinal organoids. Recent generation of stomach fetal spheroids *in vitro*, allowed Fernandez-Vallone V. and colleagues to analyze their transcriptional profile and to compare it with the profile of intestinal spheroids (personal communication from Fernandez-Vallone V. at the EMBO Conference Stem Cells in Cancer and Regenerative Medicine-October 2014). They found high similarities between the two profiles suggesting that intestine and stomach are not very different from one another before villogenesis. They share the expression of many markers among which *Trop2* and *Cnx43*.

The high similarity between stomach and intestine at fetal stages was already described by Li and colleagues (Li et al., 2009). They investigated the dynamic gene expression patterns in the fetal stomach and intestine between E14.5 and E16.5. They showed that the global expression profiles of these two tissues are quite similar to one another at E14.5. They found that *Sox2* (stomach – foregut marker) and *Cdx2* (intestinal – hindgut marker) were co-expressed in the pylorus. Only after villogenesis, at E16.5, stomach and intestinal profiles dramatically changed (Li et al., 2009). This suggested that, differently from what Sherwood and colleagues proposed (Sherwood et al., 2009), the boundary formed by *Sox2* and *Cdx2* at early developmental stages is rather diffuse within stomach, pylorus and duodenum until E15 (Li et al., 2009). At this time a burst of transcription occurs in the intestinal epithelium leading to a distinct compartimentalization of the gene expression in the duodenum (Li et al., 2009). This compartimentalization has been defined as intestinalization and corresponds to the global vertical maturation of the intestinal epithelium by which crypts/villi functional units are formed (Li et al., 2009). Therefore, it seems that intestinalization sharpens the foregut/hindgut and *Sox2/Cdx2* boundary allowing the differentiation of the intestinal and stomach specific cell types to occur very close to one another.

Indications that *Cdx2* plays an important role during villogenesis arise from the high similarities between fetal intestinal spheroids (Mustata et al., 2013) and adult *Cdx1/Cdx2* knockout intestine transcriptional profiles (Verzi et al., 2011): they both exhibit high expression of gastric markers (Mustata et al., 2013). This observation, together with the abnormal morphogenesis of the intestinal epithelium, upon loss of *Cdx2* at E13.5, and the severe subsequent defects in villogenesis observed at E18.5 by Grainger and colleagues (Grainger et al., 2010) suggests that intestinalization and villogenesis are dependent on *Cdx2* expression in the fetal hindgut.

All these arguments invite to a revision of the current model (Sherwood et al., 2009) that describes the patterning of the endoderm. At early stages of development, *Sox2* and *Cdx2* would establish a boundary defining the regions wherefrom the distinct organs will develop in the gut tube (Li et al., 2009). This boundary would be diffuse, rather than sharp, defining a region of overlap between the developing stomach and intestinal epithelia that express common markers until fetal stages (Li et al., 2009). Two of these markers, *Trop2* and *Cnx43*, acknowledge the presence of common progenitors in both

5

epithelia (Mustata et al., 2013) (personal communication from Fernandez-Vallone V. at the EMBO Conference Stem Cells in Cancer and Regenerative Medicine-October 2014). Around E15, intestinalization, together with villogenesis, would finally sharpen the boundary between stomach and intestine leading to the final development of the two adult organs (Li et al., 2009; Mustata et al., 2013).

As briefly mentioned above, Lgr5-positive adult stem cells are detected during villogenesis in the intestinal epithelium at E15. However, in adult mice Lgr5-positive stem cells reside both at the bottom of the adult pyloric glands and of the intestinal crypts (Barker et al., 2010; Sato et al., 2009) (see also Chapter 4). This raises several questions about the origin of the Lgr5-positive stem cells in the two organs. One possibility is that Lgr5-positive stem cells would be specified de novo in epithelial cells of the pyloric glands and the intestinal crypts. Another, more likely possibility is that the *Trop2/Cnx43* expressing stomach and intestinal common progenitors would have the potential to independently give rise to Lgr5-positive stem cells in each adult compartment. This has been already documented for the intestinal progenitors (Mustata et al., 2013), but it still needs to be investigated for the stomach progenitors.

The fact that stomach and intestinal Lgr5-positive adult stem cells support distinct differentiation programs in adults (see Fig.S1 of Chapter 4) might be related to the boundary established by Sox2 and Cdx2 proteins during the fetal intestinalization process. Considering the results showed in Chapter 4 it seems reasonable to speculate that *Cdx2* in the intestine specifies the identity of the Lgr5-positive adult intestinal stem cells, converting them from their early common stomach/intestinal state in the fetal duodenum. Regarding the adult Lgr5-positive stomach stem cells, it is still unknown which factor would specify their identity. It is unlikely to be Sox2 given the fact that Sox2-positive and Lgr5-positive stem cells constitute two different pools of stem cells in the adult stomach epithelium (Arnold et al., 2011; Barker et al., 2010).

References

Arnold, K., Sarkar, A., Yram, M.A., Polo, J.M., Bronson, R., Sengupta, S., Seandel, M., Geijsen, N., and Hochedlinger, K. (2011). Sox2(+) adult stem

and progenitor cells are important for tissue regeneration and survival of mice. Cell stem cell *9*, 317-329.

Barker, N., Huch, M., Kujala, P., van de Wetering, M., Snippert, H.J., van Es, J.H., Sato, T., Stange, D.E., Begthel, H., van den Born, M*., et al.* (2010). Lgr5(+ve) stem cells drive self-renewal in the stomach and build long-lived gastric units in vitro. Cell stem cell *6*, 25-36.

Beck, F., Chawengsaksophak, K., Waring, P., Playford, R.J., and Furness, J.B. (1999). Reprogramming of intestinal differentiation and intercalary regeneration in Cdx2 mutant mice. Proceedings of the National Academy of Sciences of the United States of America *96*, 7318-7323.

Bialecka, M., Wilson, V., and Deschamps, J. (2010). Cdx mutant axial progenitor cells are rescued by grafting to a wild type environment. Developmental biology *347*, 228-234.

Chawengsaksophak, K., de Graaff, W., Rossant, J., Deschamps, J., and Beck, F. (2004). Cdx2 is essential for axial elongation in mouse development. Proceedings of the National Academy of Sciences of the United States of America *101*, 7641-7645.

Chawengsaksophak, K., James, R., Hammond, V.E., Kontgen, F., and Beck, F. (1997). Homeosis and intestinal tumours in Cdx2 mutant mice. Nature *386*, 84-87.

Copf, T., Schroder, R., and Averof, M. (2004). Ancestral role of caudal genes in axis elongation and segmentation. Proceedings of the National Academy of Sciences of the United States of America *101*, 17711-17715.

Davis, G.K., and Patel, N.H. (2002). Short, long, and beyond: molecular and embryological approaches to insect segmentation. Annual review of entomology *47*, 669-699.

Drukker, M., Tang, C., Ardehali, R., Rinkevich, Y., Seita, J., Lee, A.S., Mosley, A.R., Weissman, I.L., and Soen, Y. (2012). Isolation of primitive endoderm, mesoderm, vascular endothelial and trophoblast progenitors from human pluripotent stem cells. Nature biotechnology *30*, 531-542.

Gao, N., White, P., and Kaestner, K.H. (2009). Establishment of intestinal

5

identity and epithelial-mesenchymal signaling by Cdx2. Developmental cell *16*, 588-599.

Garcia, M.I., Ghiani, M., Lefort, A., Libert, F., Strollo, S., and Vassart, G. (2009). LGR5 deficiency deregulates Wnt signaling and leads to precocious Paneth cell differentiation in the fetal intestine. Developmental biology *331*, 58-67.

Grainger, S., Savory, J.G., and Lohnes, D. (2010). Cdx2 regulates patterning of the intestinal epithelium. Developmental biology *339*, 155-165.

Hryniuk, A., Grainger, S., Savory, J.G., and Lohnes, D. (2012). Cdx function is required for maintenance of intestinal identity in the adult. Developmental biology *363*, 426-437.

Inman, K.E., and Downs, K.M. (2006a). Brachyury is required for elongation and vasculogenesis in the murine allantois. Development *133*, 2947-2959.

Inman, K.E., and Downs, K.M. (2006b). Localization of Brachyury (T) in embryonic and extraembryonic tissues during mouse gastrulation. Gene expression patterns : GEP *6*, 783-793.

Kispert, A., and Herrmann, B.G. (1994). Immunohistochemical analysis of the Brachyury protein in wild-type and mutant mouse embryos. Developmental biology *161*, 179-193.

Kispert, A., Herrmann, B.G., Leptin, M., and Reuter, R. (1994). Homologs of the mouse Brachyury gene are involved in the specification of posterior terminal structures in Drosophila, Tribolium, and Locusta. Genes & development *8*, 2137-2150.

Knezevic, V., De Santo, R., and Mackem, S. (1997). Two novel chick T-box genes related to mouse Brachyury are expressed in different, non-overlapping mesodermal domains during gastrulation. Development *124*, 411-419.

Kubo, A., Shinozaki, K., Shannon, J.M., Kouskoff, V., Kennedy, M., Woo, S., Fehling, H.J., and Keller, G. (2004). Development of definitive endoderm from embryonic stem cells in culture. Development *131*, 1651-1662.

Li, X., Udager, A.M., Hu, C., Qiao, X.T., Richards, N., and Gumucio, D.L.

5

(2009). Dynamic patterning at the pylorus: formation of an epithelial intestine-stomach boundary in late fetal life. Developmental dynamics : an official publication of the American Association of Anatomists *238*, 3205-3217.

Lolas, M., Valenzuela, P.D., Tjian, R., and Liu, Z. (2014). Charting Brachyury-mediated developmental pathways during early mouse embryogenesis. Proceedings of the National Academy of Sciences of the United States of America *111*, 4478-4483.

Macdonald, P.M., and Struhl, G. (1986). A molecular gradient in early Drosophila embryos and its role in specifying the body pattern. Nature *324*, 537-545.

Martin, B.L., and Kimelman, D. (2008). Regulation of canonical Wnt signaling by Brachyury is essential for posterior mesoderm formation. Developmental cell *15*, 121-133.

Micchelli, C.A., and Perrimon, N. (2006). Evidence that stem cells reside in the adult Drosophila midgut epithelium. Nature *439*, 475-479.

Moreno, E., and Morata, G. (1999). Caudal is the Hox gene that specifies the most posterior Drosophile segment. Nature *400*, 873-877.

Mustata, R.C., Vasile, G., Fernandez-Vallone, V., Strollo, S., Lefort, A., Libert, F., Monteyne, D., Perez-Morga, D., Vassart, G., and Garcia, M.I. (2013). Identification of Lgr5-independent spheroid-generating progenitors of the mouse fetal intestinal epithelium. Cell reports *5*, 421-432.

Ohlstein, B., and Spradling, A. (2006). The adult Drosophila posterior midgut is maintained by pluripotent stem cells. Nature *439*, 470-474.

Patel, N.H., Kornberg, T.B., and Goodman, C.S. (1989). Expression of engrailed during segmentation in grasshopper and crayfish. Development *107*, 201-212.

Rashbass, P., Cooke, L.A., Herrmann, B.G., and Beddington, R.S. (1991). A cell autonomous function of Brachyury in T/T embryonic stem cell chimaeras. Nature *353*, 348-351.

Rodaway, A., Takeda, H., Koshida, S., Broadbent, J., Price, B., Smith,

5

J.C., Patient, R., and Holder, N. (1999). Induction of the mesendoderm in the zebrafish germ ring by yolk cell-derived TGF-beta family signals and discrimination of mesoderm and endoderm by FGF. Development *126*, 3067-3078.

Sato, T., Vries, R.G., Snippert, H.J., van de Wetering, M., Barker, N., Stange, D.E., van Es, J.H., Abo, A., Kujala, P., Peters, P.J.*, et al.* (2009). Single Lgr5 stem cells build crypt-villus structures in vitro without a mesenchymal niche. Nature *459*, 262-265.

Savory, J.G., Bouchard, N., Pierre, V., Rijli, F.M., De Repentigny, Y., Kothary, R., and Lohnes, D. (2009). Cdx2 regulation of posterior development through non-Hox targets. Development *136*, 4099-4110.

Savory, J.G., Mansfield, M., Rijli, F.M., and Lohnes, D. (2011). Cdx mediates neural tube closure through transcriptional regulation of the planar cell polarity gene Ptk7. Development *138*, 1361-1370.

Sherwood, R.I., Chen, T.Y., and Melton, D.A. (2009). Transcriptional dynamics of endodermal organ formation. Developmental dynamics : an official publication of the American Association of Anatomists *238*, 29-42.

Shinmyo, Y., Mito, T., Matsushita, T., Sarashina, I., Miyawaki, K., Ohuchi, H., and Noji, S. (2005). caudal is required for gnathal and thoracic patterning and for posterior elongation in the intermediate-germband cricket Gryllus bimaculatus. Mechanisms of development *122*, 231-239.

Singer, J.B., Harbecke, R., Kusch, T., Reuter, R., and Lengyel, J.A. (1996). Drosophila brachyenteron regulates gene activity and morphogenesis in the gut. Development *122*, 3707-3718.

Stringer, E.J., Duluc, I., Saandi, T., Davidson, I., Bialecka, M., Sato, T., Barker, N., Clevers, H., Pritchard, C.A., Winton, D.J.*, et al.* (2012). Cdx2 determines the fate of postnatal intestinal endoderm. Development *139*, 465-474.

Subramanian, V., Meyer, B.I., and Gruss, P. (1995). Disruption of the murine homeobox gene Cdx1 affects axial skeletal identities by altering the mesodermal expression domains of Hox genes. Cell *83*, 641-653.

van de Ven, C., Bialecka, M., Neijts, R., Young, T., Rowland, J.E., Stringer, E.J.,

Van Rooijen, C., Meijlink, F., Novoa, A., Freund, J.N*., et al.* (2011). Concerted involvement of Cdx/Hox genes and Wnt signaling in morphogenesis of the caudal neural tube and cloacal derivatives from the posterior growth zone. Development *138*, 3451-3462.

van den Akker, E., Forlani, S., Chawengsaksophak, K., de Graaff, W., Beck, F., Meyer, B.I., and Deschamps, J. (2002). Cdx1 and Cdx2 have overlapping functions in anteroposterior patterning and posterior axis elongation. Development *129*, 2181-2193.

van Nes, J., de Graaff, W., Lebrin, F., Gerhard, M., Beck, F., and Deschamps, J. (2006). The Cdx4 mutation affects axial development and reveals an essential role of Cdx genes in the ontogenesis of the placental labyrinth in mice. Development *133*, 419-428.

van Rooijen, C., Simmini, S., Bialecka, M., Neijts, R., van de Ven, C., Beck, F., and Deschamps, J. (2012). Evolutionarily conserved requirement of Cdx for post-occipital tissue emergence. Development *139*, 2576-2583.

Verzi, M.P., Shin, H., He, H.H., Sulahian, R., Meyer, C.A., Montgomery, R.K., Fleet, J.C., Brown, M., Liu, X.S., and Shivdasani, R.A. (2010). Differentiation-specific histone modifications reveal dynamic chromatin interactions and partners for the intestinal transcription factor CDX2. Developmental cell *19*, 713-726.

Verzi, M.P., Shin, H., Ho, L.L., Liu, X.S., and Shivdasani, R.A. (2011). Essential and redundant functions of caudal family proteins in activating adult intestinal genes. Molecular and cellular biology *31*, 2026-2039.

Wilkinson, D.G., Bhatt, S., and Herrmann, B.G. (1990). Expression pattern of the mouse T gene and its role in mesoderm formation. Nature *343*, 657-659.

Wilson, V., and Beddington, R. (1997). Expression of T protein in the primitive streak is necessary and sufficient for posterior mesoderm movement and somite differentiation. Developmental biology *192*, 45-58.

Wilson, V., Olivera-Martinez, I., and Storey, K.G. (2009). Stem cells, signals and vertebrate body axis extension. Development *136*, 1591-1604.

Yamaguchi, T.P., Takada, S., Yoshikawa, Y., Wu, N., and McMahon, A.P.

5

(1999). T (Brachyury) is a direct target of Wnt3a during paraxial mesoderm specification. Genes & development *13*, 3185-3190.

Young, T., Rowland, J.E., van de Ven, C., Bialecka, M., Novoa, A., Carapuco, M., van Nes, J., de Graaff, W., Duluc, I., Freund, J.N.*, et al.* (2009). Cdx and Hox genes differentially regulate posterior axial growth in mammalian embryos. Developmental cell *17*, 516-526.

5

Addendum

Nederlandse samenvatting

Riassunto della tesi

Abbreviations

List of pubblications

Curriculum Vitae

Nederlandse samenvatting

Voorlopercellen gelegen langs de primitiefstreep en in de staartknop deponeren tijdens de ontwikkeling van de muis nakomelingen die op hun beurt primordiale cellen van alle weefsels van romp en staart genereren. Sommige van deze cellen hebben stamceleigenschappen en dragen tijdens de groei van de lichaamsas bij aan neurale en mesodermale weefsels. Deze cellen worden "Neuro-Mesodermal axial progenitors" (Neuromesodermale voorlopers) genoemd, en samen met het epiblast langs de primitiefstreep vormen ze de posterieure groeizone van het embryo. Dat wordt in de introductie beschreven (Hoofdstuk 1).

De drie Cdx genen van de muis coderen voor transcriptiefactoren die betrokken zijn bij morfogenese van de embryonale lichaamsas. Ze komen in de posterieure groeizone tot expressie. Om de rol van deze genen tijdens het aanleggen van de romp en staart aan te tonen, hebben we embryo's bestudeerd die alle drie Cdx-genen tegelijk missen (Hoofdstuk 2). Deze mutanten verliezen de activiteit van hun groeizone, en hun lichaamsas wordt niet verlengd na het niveau van de nek. Onze resultaten tonen aan dat Cdx-genen essentieel zijn voor het aanleggen van posterieure embryonale structuren en dat ze dat doen door het activeren van Wnt- en Fgf-signalering.

Vergelijking tussen fenotypen van Cdx-mutanten maakte duidelijk dat van de drie Cdx-genen Cdx2 het meest bijdraagt aan de groei van de lichaamsas. Een andere transcriptiefactor, T Brachyury, komt ook in de groeizone tot expressie en is onmisbaar voor de groei van de lichaamsas. Ondanks het feit dat Cdx en T Brachyury beide via een positieve regulatie van Wnt- en Fgf-signalering werken, is het niet duidelijk of ze via andere mechanismen ook betrokken zijn. Om beter te begrijpen hoe Cdx en T Brachyury interageren bij het reguleren van de groei van de lichaamsas, hebben we mutanten gegenereerd die beide transcriptiefactoren missen (Hoofdstuk 3). We tonen aan dat het simultane verlies van Cdx en T Brachyury de posterieure groei veel meer aantast dan elke individuele nulmutatie. We bespreken de mogelijkheid dat Cdx en T Brachyury posterieure weefselgroei tijdens embryonale ontwikkeling bevorderen via parallelle maar verbonden paden.

Maagklieren en darmcrypten zijn functionele eenheden in het epitheel van respectievelijk maag en darm. Zij bevatten actief delende, Lgr5 ex-

presserende stamcellen die voor het vernieuwen van het epitheel zorgen. Geïsoleerde Lgr5-positieve stamcellen van maag en darm kunnen in vitro driedimensionale structuren vormen waarvan het epitheel de eigenschappen vertoont van de oorspronkelijke organen. Dat wordt in de introductie beschreven (Hoofdstuk 1). Gebruikmakend van dit "organoïd" kweeksysteem hebben wij gevonden dat de expressie van Cdx2 strikt noodzakelijk is voor het behouden van de identiteit van de volwassen darm-stamcellen (Hoofdstuk 4). *Cdx2^{null}* darm stamcellen vertonen een maag- in plaats van darmidentiteit, zowel qua genexpressie als wat betreft het fenotype van afgeleide organoïden. Onze resultaten tonen aan dat Cdx2 op een cel-autonome manier onmisbaar is in de volwassen darmstamcellen, om hun vermogen tot zelfvernieuwing en hun differentiatieprogramma in stand te houden. We laten zien dat volwassen darm-stamcellen plastisch zijn, en dat hun darmidentiteit in maagidentiteit verandert na de inactivatie van een enkele transcriptiefactor, Cdx2.

Hoofdstuk 5 bevat een algemene discussie van onze bevindingen.

6

Riassunto in italiano

Durante lo sviluppo embrionale, cellule "progenitrici" (progenitors), presenti lungo la linea primitiva (primitive streak) e la nascente coda, producono cellule "discententi" che generano tutti i tessuti primordiali che contribuiscono alla formazione del tronco e della coda dell'embrione. Un gruppo di cellule "progenitrici", con proprietà simili a cellule staminali, contribuisce alla formazione del neuroectoderma e del mesoderma durante l'allungamento del tronco e della coda lungo l'asse antero-posteriore dell'embrione. Queste cellule definite come cellule staminali "progenitrici" bipotenti Neuro-Mesodermiche (long-term bipotent Neuro-Mesodermal axial progenitors), insieme alle cellule dell'epiblasto che risiedono intorno alla linea primitiva (caudal lateral epiblast), formano la regione posteriore di crescita embrionale (embryonic posterior growth zone). Questo è descritto nell'Introduzione (Capitolo 1).

I tre geni Cdx di topo codificano per fattori di trascrizione coinvolti nell'allungamento e nel modellamento (patterning) delle strutture dell'asse antero-posteriore dell'embrione. Questi geni sono espressi nella regione posteriore di crescita embrionale. Allo scopo di scoprire fino a che punto i tre geni Cdx sono importanti per la formazione dei tessuti primordiali di tronco e coda, abbiamo generato e caratterizzato tripli embrioni mutanti per i geni *Cdx* (*Cdx^{null}*) (Capitolo 2). La regione posteriore di crescita embrionale di questi mutanti risulta non essere più funzionale e questo incide fortemente sulla formazione dei tessuti che si localizzano in posizioni più posteriori rispetto alle strutture occipitali. I nostri dati indicano che i geni Cdx sono cruciali per la generazione del tronco e dei tessuti posteriori perché regolano, a valle, le cascate di segnale di Fgf e Wnt nella regione di crescita embrionale.

La comparazione dei fenotipi manifestati dagli embrioni mutanti per i geni Cdx ha reso possibile riconoscere *Cdx2* come il gene che contribuisce in maggior misura all'allungamento degli assi. Un altro fattore di trascrizione, *T Brachyury*, é espresso nella regione di crescita embrionale ed é cruciale per l'allungamento posteriore dell'asse embrionale. *Cdx2* e *T Brachyury* supportano questo processo regolando positivamente le cascate di segnale di Fgf e Wnt. Tuttavia, non é ancora del tutto chiara quale tipo di interazione intercorre tra questi due fattori di trascrizione durante lo sviluppo embrionale di topo. Per saperne di più sul ruolo svolto da *Cdx2* e *T Brachyury* durante

6

l'allungamento degli assi, abbiamo generato doppi embrioni mutanti per *Cdx2* e *T Brachyury* (*Cdx2^{null}/T Brachyury^{null}*) (Capitolo 3). Abbiamo dimostrato che la perdita di funzione simultanea di questi due geni incide negativamente sull'allungamento dell'asse antero-posteriore in un modo ancora più severo rispetto a ciascuna singola mutazione. Noi proponiamo un modello che supporta la cooperazione di *Cdx2* e *T Brachyury* nella regolazione di cascate di segnale parallele durante lo sviluppo embrionale. Inoltre, forniamo le prime evidenze che indicano come queste cascate di segnale potrebbero interagire durante la generazione del tronco e della coda dell'embrione.

L'epitelio dello stomaco/piloro e quello dell'intestino tenue contengono unità funzionali chiamate ghiandole dello stomaco e cripte/villi intestinali. Esse contengono cellule staminali costantemente attive che esprimono Lgr5 e che sono responsabili del rinnovamento dei due epiteli per tutta la durata della vita dell'organismo. Le cellule staminali intestinali e dello stomaco, positive al marker Lgr5, possono essere isolate *in vitro* e possono generare strutture tridimensionali epiteliali che assomigliano al corrispettivo organo di origine. Questo è descritto nell'Introduzione (Capitolo 1). Utilizzando questo sistema di coltura *in vitro*, definito organoide, abbiamo dimostrato che l'espressione di *Cdx2* è assolutamente necessaria per mantenere l'identità delle cellule staminali intestinali adulte (Capitolo 4). Le cellule staminali intestinali mutanti per *Cdx2* presentano un'espressione genica caratteristica dello stomaco più che dell'intestino e danno origine ad organoidi che assomigliano ad organoidi dello stomaco ed esprimono marcatori dello stomaco/piloro. I nostri dati indicano che *Cdx2* è richiesto nelle cellule staminali intestinali adulte per regolarne l'auto-rigenerazione e per mantenere il loro programma di differenziamento intestinale. Per la prima volta abbiamo fornito la prova della plasticità delle cellule staminali adulte la cui identità può essere convertita da intestinale a gastrica tramite l'inattivazione del singolo fattore di trascrizione Cdx2.

Il Capitolo 5 contiene una discussione generale dei dati descritti nei capitoli precedenti.

6

Abbreviations

3D = Three Dimensional

All = Allantois

AP = Antero-Posterior

AVE = Anterior Visceral Endoderm

cad = Drosophila caudal

CBC = Crypt-Base Columnar

ChIP-Seq = Chromatin Immunoprecipitation-Sequencing

CLE = Caudal Lateral Epiblast

CNH = Cordo-Neural Hinge

DE = Definitive Endoderm

DVE = Distal Visceral Endoderm

E = Embryonic day

EGF = Epidermal Growth Factor

EMT = Epithelial-Mesenchymal Transition

ENR = Egf, Noggin, Rspondin1

ENRWfg = Egf, Noggin, Rspondin1, Wnt3a, fgf10, gastrin

ExE = Extraembryonic Ectoderm

FGF = Fibroblast Growth Factor

GI = Gastro-Intestinal

ICM = Inner Cell Mass

6

LT NM = Long-Term NeuroMesodermal

N = Node

NM = NeuroMesodermal

NSB = Node Streak Border

PS= Primitive Streak

PSM = Presomitic Mesoderm

RA = Retinoic Acid

T Bra = T Brachyury

TA = Transit Amplifying

TE = Trophectoderm

VE = Visceral Endoderm

wt = wild-type

6

List of pubblications

Transformation of intestinal stem cells into gastric stem cells on loss of transcription factor Cdx2. **Salvatore Simmini***, Monika Bialecka*, Meritxell Huch, Lennart Kester, Marc van de Wetering, Toshiro Sato, Felix Beck, Alexander van Oudenaarden, Hans Clevers and Jacqueline Deschamps.
Nature Communications; 5:5728. doi:10.1038/ncomms6728.
December 11, 2014

Region-specific regulation of posterior axial elongation during vertebrate embryogenesis. Roel Neijts, **Salvatore Simmini**, Fabrizio Giuliani, Carina van Rooijen, Jacqueline Deschamps.
Developmental Dynamics; 243(1):88-98. September 6, 2013

Evolutionarily conserved requirement of Cdx for post-occipital tissue emergence. van Rooijen C, **Salvatore Simmini***, Monika Bialecka*, Roel Neijts*, Cesca van de Ven, Felix Beck, Jacqueline Deschamps.
Development; 139(14):2576-83. June 6, 2012

The miR-144/451 locus is required for erythroid homeostasis. Rasmussen KD, **Salvatore Simmini**, Abreu-Goodger C, Bartonicek N, Monica Di Giacomo, Bilbao-Cortes D, Horos R, Von Lindern M, Enright AJ, Donal O'Carroll.
J Exp Med.; 207(7):1351-8. May 31, 2010

6

Curriculm Vitae

Salvatore Simmini was born on 2nd of Februari 1985 in Copertino (Lecce), Italy. From 1999 until 2004 he attended the "Banzi Bazoli Liceum" in Lecce where he obtained his highschool diploma. Then he enrolled as a student at the faculty of Biology of Alma Mater Studiorum - Bologna University, where he obtained his machelor degree in Biotechnologies in 2007 and his master degree in Molecular Biotechnologies in 2010. During his studies, Salvatore completed internships in the group of Dr. Patrizia Brigidi at the Pharmaceutical and Biotechnologies Department of Bologna University and in the group of Dr. Donal O'Carroll at the European Molecular Biology Laboratory (EMBL), Monterotondo, Rome. In Dr. Patrizia Brigidi's laboratory he collaborated with Dr. Ciro Pugliese, at that time post-doc fellow in the laboratory, in characterizing the effects of prebiotics on human gastrointestinal microbiota. In the laboratory of Dr. Donal O'Carroll he worked with Dr. Kasper Rasmussen, at that time PhD fellow in the laboratory, in characterizing the function of the micro-RNA cluster 144/451 in hematopoiesis. During the last internship at the EMBL he worked a lot on mouse embryos and this determined his future direction and interests. In September 2010 he started his PhD studies at the research group of Dr. Jacqueline Deschamps at the Hubrecht Institute in Utrecht within the frame of Cancer, Stem Cells and Developmetal Biology PhD program. As described in this thesis, Salvatore has been involved in research projects focused on mouse development and stem cell biology of the adult intestine and stomach. In the future he is planning to continue his research in science as post-doc fellow focusing on stem cells and cancer biology.

6